DISS. ETH No. 23426

Advanced sensing and quantification strategies using DNA and living cell based materials

A thesis submitted to attain the degree of

DOCTOR OF SCIENCES of ETH Zurich

(Dr. sc. ETH Zurich)

presented by

CARLOS ANDREA MORA

MSc ETH Biology

born on 27.07.1987

citizen of Zurich (ZH) and Capriasca (TI),
Switzerland

accepted on the recommendation of

Prof. Dr. Wendelin J. Stark, examiner
Prof. Dr. Andrew J. deMello, co-examiner

2016

Imagination is more important than knowledge.
For knowledge is limited, whereas imagination encircles the world.

Albert Einstein, 1929

Acknowledgments

My PhD studies at the *Functional Materials Lab* were a great experience and I have never regretted to have joined this amazing and unique research group.

I would like to express my deepest gratitude to Prof. Wendelin Stark for giving me the valuable opportunity as a student from a 'foreign' and non-chemical scientific discipline (biology) to do my PhD thesis in his research group. I have always very appreciated his helpful and motivating support for my ideas and projects, which was in every case adequate to give me guidance when I needed it, but also let me enough freedom to independently pursue my projects, fail in my experiments and learn from my own mistakes. Because of that, I could develop my own experience-based scientific and project management skills. Additionally, besides scientific knowledge and experience, I have also learned a lot about engineering and problem solving, especially by applying the concepts of straightforward tinkering and out-of-the-box thinking.

Special thanks go to my co-examiner Prof. Andrew de Mello for being my co-referee and for his interest in my work.

From the beginning, I was fascinated by the interdisciplinary, creative and enthusiastic atmosphere predominating at the FML and created by all members of the research group. First, I would like to thank Dr. Robert Grass, for his always very helpful inputs and discussions regarding my own research. Many thanks go also to all the other people with whom I had the opportunity to closely work with or share the office space in my time at the FML, especially Daniela Paunescu-Bluhm, my main co-worker, good friend, and consultant for life (romance!) and business (CV!), Renzo Raso, our group philosopher and discussion partner about god and the world, Vladimir Zlateski, with whom I actually wanted to realize many ideas (MEPCo!), Gadas Mikutis, a dedicated scientist and qPCR crack, Antoine Herzog, who already had visionary ideas as master student, Jonas Halter, who shared my fascination for mealworms (also from a culinary point of view) and gave me the opportunity to publish one of his projects, Corinne Hofer, who introduced me to the world of cobalt nanoparticles, Michela Puddu, a co-worker on the never-ending project of DNA extraction with magnetic nanoparticles, Anne Engmann (Brain Research Institute) and Marco Zahner (Institute of Electromagnetic Fields), with whom I spent many interesting hours in front of the microscope, Philipp Stössel and Robert Stettler, with whom I did funny microbiological experiments with toast and CaO, Hans-Jakob Schärer and Dr. Thomas Oberhänsli (FiBL), for giving me the chance to do real field experiments, and Aline Rotzetter, who enabled me to be on a scientific paper for the first time. For their support during my time here at the FML, I would also like to express my sincere

gratitude to Dirk Mohn, Tino Zeltner, Christoph Kellenberger, Michael Loepfe, Elia Schneider, Mario Stucki, Lukas Langenegger, Xavier Kohll, Christoph Schumacher, Alex Stepuk, Nora Hild, Roland Fuhrer, Stephanie Bubenhofer, Inge Herrmann, and Mirjam Giacomin. Finally, I would also like the thank the undergraduate students that contributed and inspired my research, namely Madeleine Bloch, Antoine Herzog, Célia Mignan, Andri Mani, and Olivier Gröninger.

I would like to express my deepest and heartfelt gratitude towards my family, especially my parents Pia and Gianni, my sister Virginia, and my grandparents Oskar and Marianne. Without their unconditional love and support, I would never be, where I am now.

Finally, and most importantly, I want to thank Sarah for her love. With you at my side, I feel complete, happy and strong enough to face any challenge in life.

Contents

Zusammenfassung

Die hier vorliegende Doktorarbeit beschreibt die Entwicklung, Untersuchung und Anwendung von neuen Quantifizierungs- und Sensorwerkzeugen basierend auf biologisch inspirierten Materialien. Das Ziel dieser Arbeit ist es zu zeigen, dass diese Werkzeuge effiziente Quantifizierungsstrategien in wissenschaftlichen Disziplinen wie Ökologie, Umwelt- und Gesundheitswissenschaften darstellen und das Potential haben, existierende Techniken zu ersetzten, welche teurer, arbeits- und zeitaufwändiger sind und/oder grosses technisches Knowhow und Laborinfrastruktur voraussetzen.

Kapitel 1 führt in das Thema der Quantitativen Analyse ein und gibt einen kurzen Überblick über quantitative analytische Prozesse, Methoden und Strategien, gefolgt von einer Beschreibung, wie bestimmte Erkenntnisse der biologischen Wissenschaftsdisziplinen die Quantitative Analyse in verschiedenen Bereichen revolutioniert hat. Zum Beispiel hat die Anwendung von Biomolekülen wie Enzymen, Immunglobulinen, Nukleinsäuren sowie lebendigen Zellen zur Entwicklung von besseren analytischen Werkzeugen geführt, besonders im Hinblick auf die Messung von bioaktiven Substanzen. Zwei unterschiedliche Anwendungen und ihre zugrundeliegenden Konzepte werden im Detail erläutert: (1) Die Einkapselung von Nukleinsäuren in amorphem Siliziumdioxid (Silica), was zu vielseitig verwendbaren Markierungsmaterialen, den sogenannten ‘silica particles with encapsulated DNA’, abgekürzt SPED, geführt hat. (2) Das Einbetten von lebendigen Zellen in flache Polymerfolien, wodurch lebendige Hybrid-Materialen geschaffen werden, welche unter anderem zur Quantifizierung von chemischen Analyten verwendet werden können.

In **Kapitel 2** wird gezeigt, wie man SPED als quantitatives Werkzeug für die Untersuchung und Beobachtung ökologischer Netzwerke wie z.B. Nahrungsketten verwenden kann. Ökologische Netzwerke sind extrem komplex, können jedoch wichtige Information über die Belastbarkeit und momentanen Zustand eines Ökosystems liefern. In vielen Fällen ist es nicht möglich trophische Interaktionen, das heisst Interaktionen zwischen Räuber und Beute, direkt zu beobachten und es ist mit den heute verfügbaren Methoden schwierig, diese Interaktionen zu quantifizieren. Die Studie ergab, dass man mit SPED Nahrungsquellen sowie Lebewesen spezifisch markieren kann und dass es möglich ist, den Mengentransfer zwischen Nahrungsquelle und Tier und/oder zwischen Tieren (Beute und Räuber) über mehr als eine trophische Stufe zu quantifizieren. SPED waren vom Anfang bis zum Ende einer zweistufigen Arthropoden-Nahrungskette transferier- und quantifizierbar, wurden in das Verdauungssystem der untersuchten Tiere aufgenommen und konnten in den markierten Tieren über mehrere Tage

nachgewiesen werden. Wenn unterschiedlich markierte SPED in vordefinierten Mengenverhältnissen verwendet wurden, konnte festgestellt werden, dass diese Information über trophische Stufen und über die Zeit in den Tieren erhalten blieb. SPED wurden auch für die Untersuchung der Blütenpräferenz von Fliegen verwendet und erwiesen sich als schnelle und genaue Analysemethode für diese Art von Untersuchungen.

Neben Tierinteraktionen können SPED auch verwendet werden, um chemische Substanzen wie z.B. Pestizide oder andere anthropogene Substanzen in der Umwelt zu verfolgen, um deren Ursprung zu finden oder deren exakte Konzentration zu ermitteln. Das Aufkommen von landwirtschaftlichen Technologien mit geringerer Pestizidanwendung, wie z.B. der biologische Landbau, machen es notwendig, dass quantitative Werkzeuge entwickelt werden, welche die Pestizidabdrift bei tiefen Konzentrationen messen können und kosteneffektive Multiplex-Experimente erlauben. In **Kapitel 3** wird gezeigt, dass SPED stabil in organische und anorganische Pestizide eingebracht und wieder zurückgewonnen werden können. In Feldexperimenten konnten sehr tiefe Pestizidkonzentrationen bis zu 1 Nanoliter pro Quadratzentimeter quantifiziert werden, nachdem ein hindernisfreies Feld sowie eine Apfelbaumplantage mit einer mit 5.8 Milligramm pro Liter SPED-markierten Testflüssigkeit besprüht worden war. Windmuster und die Beschaffenheit des untersuchten Feldes bzw. Plantage waren durch die Analyse der SPED-Verteilung klar nachvollziehbar.

In **Kapitel 4** wird ein neuartiges Sensormaterial präsentiert, welches bioaktive Moleküle von flüssigen Proben quantifizieren kann. Das Ziel war es ein günstiges und einfach zu bedienendes Werkzeug zu schaffen, welches krankheitsrelevante Moleküle messen kann. Der sogenannte ‘living material-based analytical sensor’, abgekürzt LiMBAS, beinhaltet lebende, genetisch-modifizierte Bakterien der Spezies *Escherichia coli* zwischen einer nanoporösen Deckmembran und einer nicht-porösen Bodenmembran. Er kann die krankheitsrelevanten Oligosaccharide Laktose (Milchzucker) und Galaktose quantifizieren. Nachdem man einen Tropfen mit einem Volumen von 1 - 10 Mikroliter einer zu untersuchenden Probe auf die poröse Sensoroberfläche platziert hat, reagieren die im Sensor eingeschlossenen Mikroorganismen mit der Expression von fluoreszierenden Proteinen. Dadurch visualisieren sie das Diffusionsverhalten des zu messenden Moleküls, wovon dessen Konzentration abgeleitet werden kann. Nach Inkubation bei Raumtemperatur wird das flache, halb-transparente Sensormaterial über eine blaue Lichtquelle gehalten und damit die fluoreszierenden Flächen sichtbar gemacht. LiMBAS konnte die Konzentrationen von Laktose oder Galaktose in unverdünnten Nahrungsmittelproben genau bestimmen und war fähig die Konzentration dieser Moleküle in

einem Bereich zwischen 1 – 1000 Millimol pro Liter zu messen, was dem relevanten Konzentrationsbereich z.B. bei krankheitsbedingten Nahrungsmittelintoleranz entspricht. Das Sensormaterial konnte bei Kühlschranktemperaturen über mindestens sieben Tage gebrauchsbereit gelagert werden ohne an Funktionalität einzubüssen.

In **Kapitel 5** wird die Bedeutung der Ergebnisse der vorherigen Kapitel nochmals kurz rekapituliert und ein Ausblick auf Verbesserungsmöglichkeiten und denkbare Anwendungen von SPED und LiMBAS gegeben.

Summary

The present thesis describes the development, investigation and application of novel analytical quantification and sensing tools based on bioinspired materials. The overall goal of this dissertation is to demonstrate that these tools represent efficient quantification strategies in fields such as ecology, environmental and health sciences, and have the potential to substitute existing techniques that are costlier, more laborious, and more time-intensive, and/or require a high level of technical skills and laboratory infrastructure.

Chapter 1 introduces the topic of quantitative analysis by providing a brief overview of quantitative analytical processes, methods and strategies followed by a description of how certain findings from biological disciplines revolutionized quantitative analysis in many aspects. The application of biomolecules such as enzymes, immunoglobulins or nucleic acids, as well as living cells in quantitative analysis have led to the development of better analytical tools, especially for the measurement of bioactive substances. Two different applications and their underlying concepts are elucidated in detail: (1) The encapsulation of nucleic acids in amorphous silicon dioxide (silica) resulting in versatile quantitative tracers, the so called ‘silica particles with encapsulated DNA’ (SPED). (2) The embedding of living cells in flat polymer sheets creating living hybrid-materials able to quantify chemical analytes.

In **Chapter 2**, the concept of using SPED as quantitative tool for investigating and monitoring ecological networks such as food webs is demonstrated. Ecological networks are extremely complex and can provide important information about the robustness and present condition of an ecosystem. In most cases it is not feasible to directly observe trophic interactions, i.e., interactions between predators and prey, and with the currently available methods it is difficult to quantify the connections between them. With SPED, specific food source as well as organism labeling and quantification of food-to-animal and animal-to-animal transfer over more than one trophic level are possible. SPED were readily transferable and quantifiable from the bottom to the top of a two-level food chain of arthropods, were taken up in the gut system of the investigated animals, and remained persistent in the labeled animals over several days. When differently labeled SPED were applied at predefined mass ratios it was found that information about their relative abundance was reliably conserved after trophic level transfer and over time. SPED were also applied to investigate the flower preference of fly pollinators and proved to be a fast and accurate analysis method.

Besides animal interactions, SPED could be also used to trace chemical substances in the environment such as pesticides or other anthropogenic substances in order to find their original

source or to evaluate their exact concentrations. The rise of agricultural techniques with reduced pesticide usage, such as organic farming, makes it necessary to develop tools that efficiently assess pesticide drift at low concentrations and allow cost-effective multiplexing experiments. **Chapter 3** shows that SPED can be stably incorporated and recovered from inorganic and organic pesticides. In field experiments, very low pesticide deposits down to 1 nanoliter per square centimeter could be quantified after spraying a SPED-labeled test liquid containing 5.8 milligrams per liter SPED on an obstacle-free field and an apple orchard. Based on the analysis of the SPED distribution, wind and field-related patterns were clearly traceable.

Chapter 4 presents a novel sensor material to quantify bioactive molecules from liquid samples with the aim to provide an easy-to-handle and inexpensive quantitative tool to detect disease-relevant molecules. The so-called living material-based analytical sensor (LiMBAS) contains living genetically-modified *Escherichia coli* bacteria between a nanoporous and a support polymer foil for a facile quantification of disease-relevant oligosaccharides lactose and galactose. After putting a droplet with a volume of 1 – 10 microliters of a sample onto the porous sensor surface, the enclosed microorganisms react by expressing fluorescent proteins thereby visualizing the diffusion behavior of the molecule of interest. From that, the original concentration of the analyte can be deduced. After incubation at ambient environmental conditions, the fluorescent diffusion zones were made visible by holding the half-transparent material over a blue-light source. LiMBAS could accurately quantify concentrations of lactose or galactose in undiluted food samples and was able to measure food intolerance relevant concentrations from 1 - 1000 millimol per liter. At fridge temperatures, the ready-to-use sensing material was storable for at least seven days without losing functionality.

Chapter 5 concludes the preceding chapters and gives an outlook on the further improvements and applications of SPED as well as LiMBAS.

1. Quantitative analysis: How biological findings inspire the development of powerful analytical tools

1.1 Overview of quantitative analytical methods

1.1.1 Definition

The following definition for quantitative analysis was given by the International Union of Pure and Applied Chemistry (IUPAC):[1]

> "The general expression Qualitative Analysis (...) refers to analyses in which substances are identified or classified on the basis of their chemical or physical properties, such as chemical reactivity, solubility, molecular weight, melting point, radiative properties (emission, absorption), mass spectra, nuclear half-life, etc. Quantitative Analysis refers to analyses in which the amount or concentration of an analyte may be determined (estimated) and expressed as a numerical value in appropriate units. Qualitative Analysis may take place with Quantitative Analysis, but Quantitative Analysis requires the identification (qualification) of the analyte for which numerical estimates are given."

Thus, qualitative methods, which are procedures that identify the analyte are preceding or intrinsically combined with quantitative methods.

1.1.2 Selection of a suitable quantitative method

There are numerous ways how to analyze compounds quantitatively. In many cases, one can choose from a variety of different quantification methods to assess a certain compound, which usually range from so-called 'semi-quantitative', i.e., simple, but less precise methods (e.g., diagnostic dipsticks) to more complex and exact methods (e.g., liquid chromatography coupled mass spectrometry).[2] Choosing a suitable method for the quantification of a certain substance is dependent on numerical criteria, which include precision, bias, sensitivity, detection limit, dynamic range, selectivity, and further aspects such as speed of analysis, ease and convenience of operation, skill required by the operator, cost and availability of equipment as well as per-sample-cost.[3]

1.1.3 Process of quantitative analysis

Basically, the process of quantitative analysis from sample collection to data analysis can be divided into four, partially overlapping parts: i) sample collection, ii) preparation and/or selection, iii) quantitative measurement or respectively, transduction of non-electrical to electrical information (or the converse), and iv) data processing and analysis. **Figure 1.1**

explains schematically, how this process is organized. In correspondence to the definition of quantitative analysis, this process includes always also qualitative aspects.

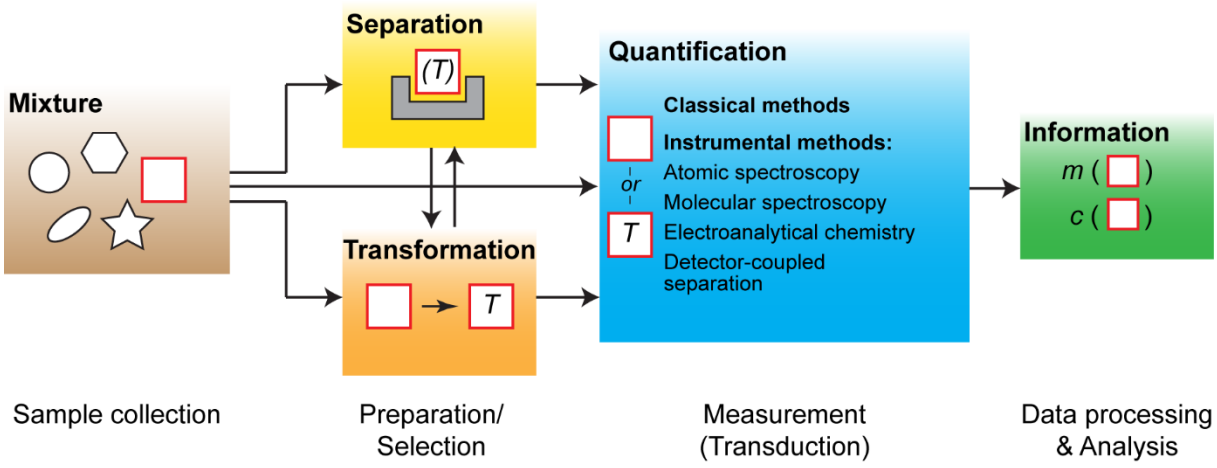

Figure 1.1. *Description of the process of quantitative analysis.* Sample collection: *A sample is collected, which may be a mixture of different compounds containing the analyte.* Preparation/Selection: *The sample may have to be prepared a) by selectively separating the analyte from other components present in the sample and/or b) by performing some kind of physical or chemical transformation before the actual quantification of the analyte can be performed (Symbol 'T').* Measurement (Transduction): *The quantitative methods yield analytical information which are transduced, e.g., to digital information.* Data processing & Analysis: *The obtained data are processed leading to comparable quantitative numerical values such as mass and concentration of the analyte.*

At the beginning of the process the analyte to be quantified is defined and a sample is collected. The sample can be of, e.g., environmental or human origin, and represents usually a homo- or heterogenous mixture. Depending on the characteristics of the sample, analyte, and the chosen quantification method, different preparative and/or selective steps may be necessary before the actual quantitative measurement can be performed. These steps include separative and transformative processes. Separative processes can be of physical, chemical or physico-chemical nature and aim to selectively purify the analyte from the sample which may also contain other substances that can impair the quantitative measurement. See **Table 1.1** for an (non-exclusive) overview of possible separative procedures. Transformative processes change the physical or chemical characteristics of the analyte to enable its quantification, and can be of physical (e.g., phase transition by vaporization, sublimation, ionization), or chemical nature, i.e., by reacting the analyte to a readily quantifiable compound. An example for chemical transformation would be chromogenic reactions such as the well-known Griess test,[4] where nitrite (NO_2^-) is reacted to a red-colored azo dye for spectrophotometric quantification in the

visible light range. Without a chromogenic transformation, the colorless nitrite would not be quantifiable by UV/Vis spectrophotometry. Sometimes, the target substance itself is not transformed, but acts as a catalyst or is selectively linked to a catalyst, that enables the transformation of another compound that can then be quantified. An example would be the enzyme-linked immunosorbent assay (ELISA),[5] see also Chapters 1.2.1 and 1.2.2. Furthermore, transformative procedures can also be used to enable separative procedures and vice versa. For example, it is necessary to physically transform substances to the gas phase before doing separation by gas chromatography.[6] On the other hand, it may be necessary to split mixtures into their components before applying transformative procedures.

Table 1.1. *Method types to separate hetero- or homogenous mixtures.*

Type	Subtype	Examples
physical	thermal	Distillation
		Drying
	mechanical	Filtration
		Sedimentation
		Magnetic separation
chemical		Precipitation
		Extraction
physicochemical		Electrolysis
		Electrophoresis
		Chromatography
		Field-flow fractionation

After the preparative steps, the actual quantitative measurement follows. Quantitative analytical methods can be divided into classical or sometimes called wet-chemical methods and instrumental techniques.[3] Quantification with classical methods is either performed gravimetrically by measuring the mass of an analyte or analyte transformation product, or volumetrically by measuring the volume or mass of a standard solution required to react completely with the analyte. The determination of the concentration of acids or bases by titration with a neutralizing base or acid (respectively) and a pH-indicator is a well-known example of a classical method. In contrast to classical methods, instrumental methods usually provide some sort of stimulus from an energy source (e.g., electromagnetic, electrical, mechanical), which elicits a response from the system under study caused by the interaction between stimulus and analyte giving qualitative and quantitative information about the analyte. To get a meaningful readout, several components may need to be installed in the analytical instrument to transduce and process the analytical information. For a photometer this could be

a light filter (information sorter), a photodiode (input transducer), an amplifier and digitizer (signal processor), and a LED display (readout). In **Figure 1.1**, four example subgroups of instrumental methods are listed: atomic spectroscopy, molecular spectroscopy, electroanalytical chemistry, and detector-coupled separation techniques. **Table 1.2** provides some example methods for each subgroup. In the following, the basic mechanism of the four subgroups are briefly explained: The first two subgroups comprise spectrometric methods, which are based on the interactions of various types of energy forms with matter and the measurement of the resulting intensity of the energy output. Those energy forms range from electromagnetic radiation to acoustic waves and beams of particles (e.g., ions, and electrons). *Atomic* spectroscopy elucidates the elemental composition and *molecular* spectroscopy the molecular composition of an analyte. Electroanalytical chemistry methods are based on the electrical properties of a solution of the analyte as part of an electrochemical cell. Finally, detector-coupled separation methods usually combine an instrumental separation technique (e.g., liquid chromatography) with an instrumental detector system (e.g., mass spectrometry).[3]

Table 1.2. *An overview of instrumental quantitative analytical methods.*

Subgroup	Methods (examples)
Atomic spectroscopy	Atomic absorption spectrometry
	Atomic emission spectrometry
	Atomic mass spectrometry
Molecular spectroscopy	UV/Vis molecular absorption spectrometry
	Molecular luminescence spectrometry
	Infrared spectrometry
	Molecular mass spectrometry
Electroanalytical chemistry	Potentiometry
	Coulometry
	Voltammetry
Detector-coupled separation	Gas chromatography
	Liquid chromatography
	Capillary electrophoresis
	Field-flow fractionation

1.1.4 Quantitative chemical analysis outside of a laboratory environment

To quantitatively determine chemical substances in real-world applications outside of a well-equipped chemical laboratory, analytical devices that integrate the whole process of quantitative analysis into a single compact device need to be designed. This enables their usage without requiring extensive training and know-how, and allows an automated monitoring of the analyte. Analytical devices capable of continuously and reversibly monitoring specific

chemical species are called ‘chemical sensors’. In general, they consist of a chemically selective recognition phase (e.g., a selective polymer) conjugated to a transducer element (e.g., a piezoelectric quartz crystal). If biomolecules are involved in molecular recognition, the device is generally called ‘biosensor’.[3]

In contrast to the above stated definition of a sensor, the recognition phase of biosensors and some chemical sensors cannot always be used reversibly and continuously, at least not over a longer time period, due to several reasons: i) the components of the recognition phase are instable over time, which is the case for many hydrated biomolecules (see also Chapter 1.3) or for cells; ii) the analyte binds irreversibly to the recognition phase, for example in immunoassays; iii) the sample cannot be sufficiently washed away from the molecular phase without damaging it. One prominent example for a commercially available, single-use biosensor is the point-of-care blood glucose meter (glucometer) employed for assessing blood glucose levels of Diabetes patients. Such glucometers usually consist of two components: A disposable strip (recognition phase) coated with enzymes that transform glucose to a quantifiable signal, and a non-disposable readout device with an electrochemical or spectrophotometric transducer element. After applying the blood sample, the strip is inserted into a reader device and the glucose concentration is determined.[7]

In the following subchapters, it will be further explained how biological findings have led to the development of new quantitative analytical methods and sensors.

1.2 Findings from biology and their benefits for quantitative analysis

With the increase in knowledge about molecular processes and reactions in biological systems over the past century, certain findings have contributed to optimize quantitative methods or have even led to completely new methods especially in the area of medical diagnostics. Three biomolecule classes have proven especially helpful, namely enzymes, the protein catalysts in biological systems, immunoglobulins, highly versatile proteins involved in immune response against pathogens, and nucleic acids, the carrier molecules for biological information. Additionally, living cells have been increasingly used as part of analytical methods.

1.2.1 Enzymes: Versatile catalysts under mild reaction conditions

Enzymes have been employed in many analytical assays to selectively catalyze reactions enabling the quantification of analytes. Because enzymes have been adapted to their function via evolutionary processes over millions of years, they usually achieve a much higher catalytic activity and reaction specificity resulting in less side products than corresponding organic or inorganic chemical catalysts. In contrast to many chemical catalysts, enzymes work at mild reaction conditions, usually below 100 °C, at atmospheric pressure, and in aqueous solutions at nearly neutral pH. Additionally, their activity can be in many cases tightly regulated. Enzymes catalyze a reaction in the same way chemical catalysts do, i.e., by stabilizing the transition state of the catalyzed reaction thereby reducing the free energy of the transition state.[8] They can catalyze a wide variety of different reactions enabling the biosynthesis of all necessary molecules of a living organism. A specific enzyme catalyzes usually only one designated reaction *in vivo* and has one designated substrate. However, some enzymes are more permissive in their geometric specificity, and thus they can accept a variety of different structurally similar molecules as substrate. For example, the oxidoreductase 'NAD^+-dependent yeast alcohol dehydrogenase' (EC 1.1.1.1) can accept various primary alcohols (e.g., ethanol, propanol) or secondary alcohols (e.g., isopropanol, benzyl alcohol).[9] However, the catalytic efficiencies differ significantly between the different possible substrates. Consequently, certain enzymes can be employed in assays to quantify analytes that do not exist in nature. Additionally, it is nowadays possible to engineer enzymes, e.g., by directed evolution, so that they accept an artificial substrate. Reactions can be designed to create and/or amplify a specific quantitative signal, e.g., a fluorescent molecule.[10] This is especially useful, if the analyte is not readily quantifiable (e.g., absorbs light only outside of the UV/Vis range) and/or present in small quantities. See also the example of ELISA described in Chapter 1.2.2. In the field of quantitative analysis, enzymes have been employed in molecular spectroscopy (colorimetric, fluorometric,

and bioluminescence assays), as well as in electrochemical and radiochemical analytical methods.[11] Enzymes thus play an important role in the preparative/selective steps of the quantitative analytical process enabling highly selective, versatile and fast transformation reactions under mild reaction conditions. For example, the colorimetric quantification of nitrite by the Griess test described in Chapter 1.1.3 could now be extended to the analysis of nitrate employing the enzyme 'nitrate reductase' that converts nitrate to nitrite, which proved to be a faster, less tedious and more reliable method for nitrate analysis in urine samples than other methods.[12]

1.2.2 Immunoglobulins: High affinity molecules for selection

Immunoglobulins, also known as antibodies, form a diverse group of proteins and bind to foreign macromolecules, so called antigens, as part of the acquired humoral immune response in vertebrate animals.[13] From a structural point of view, all immunoglobulins consist of at least four subunits: two light (~23 kD) and two heavy chains (53-75 kD). The subunits are connected by disulfide bonds as well as noncovalent interactions and form Y-shaped bisymmetric molecules. Methods have been developed to make antibodies specific against macromolecules of any kind and to produce antibodies in large quantities, such as the hybridoma technique for the production of monoclonal antibodies.[14] As a consequence of that, immunoglobulins have been integrated into many quantitative analytical methods as highly specific and versatile binding molecules for macromolecular analytes. In order to obtain a quantifiable signal, immunoglobulins are either tagged (e.g., with enzymes, or fluorophores) or the antigen-immunoglobulin interaction is directly measured by label-free methods, such as surface plasmon resonance (SPR) techniques.[15] One of the most prominent and applied quantitative immunoassay is the enzyme-linked immunosorbent assay (ELISA).[5] Different variations of this assay exist. In general, either the antigen or antigen-specific antibody is immobilized on a microtiter plate surface. After letting the antigen bind to the antibody, the interaction between them is quantified by adding a second, enzyme-conjugated antibody specific for either the antigen or the primary antibody. After subsequent washing steps, the conjugated enzyme catalyzes a colorigenic or fluorogenic reaction, which can be assessed by spectrophotometry giving quantitative information about the analyte.[15]

1.2.3 Nucleic acids: Useful for recognition and tagging

In every organism, the fundamental source of biological information is encoded in nucleic acids. Nucleic acids are single- or double stranded polymeric molecules consisting of four

building blocks called nucleotides containing a phosphate residue coupled to a pentose sugar (ribose in ribonucleic acid [RNA], deoxyribose in deoxyribonucleid acid [DNA]) and one of four nucleobases (i.e., adenine, guanine, cytosine, thymine [DNA]/uracil [RNA]). In most biological systems (except some viruses), the ultimate genetic information is encoded in DNA, whereas RNA has a broader range of functions, e.g., as messenger for protein synthesis, as structural element, as regulator or as catalyst. DNA (and also RNA) can form double stranded molecules which are connected by non-covalent hydrogen bonds formed between the corresponding bases on each nucleic acid strand. A purine base binds to a pyrimidine base forming either two (adenine with thymine) or three (guanine with cytosine) hydrogen bonds between them. As a consequence of that, only two nucleic acid molecules with reverse complementary nucleotide sequences can bind (hybridize) to each other forming a double-helical structure (see **Figure 1.2**).[8]

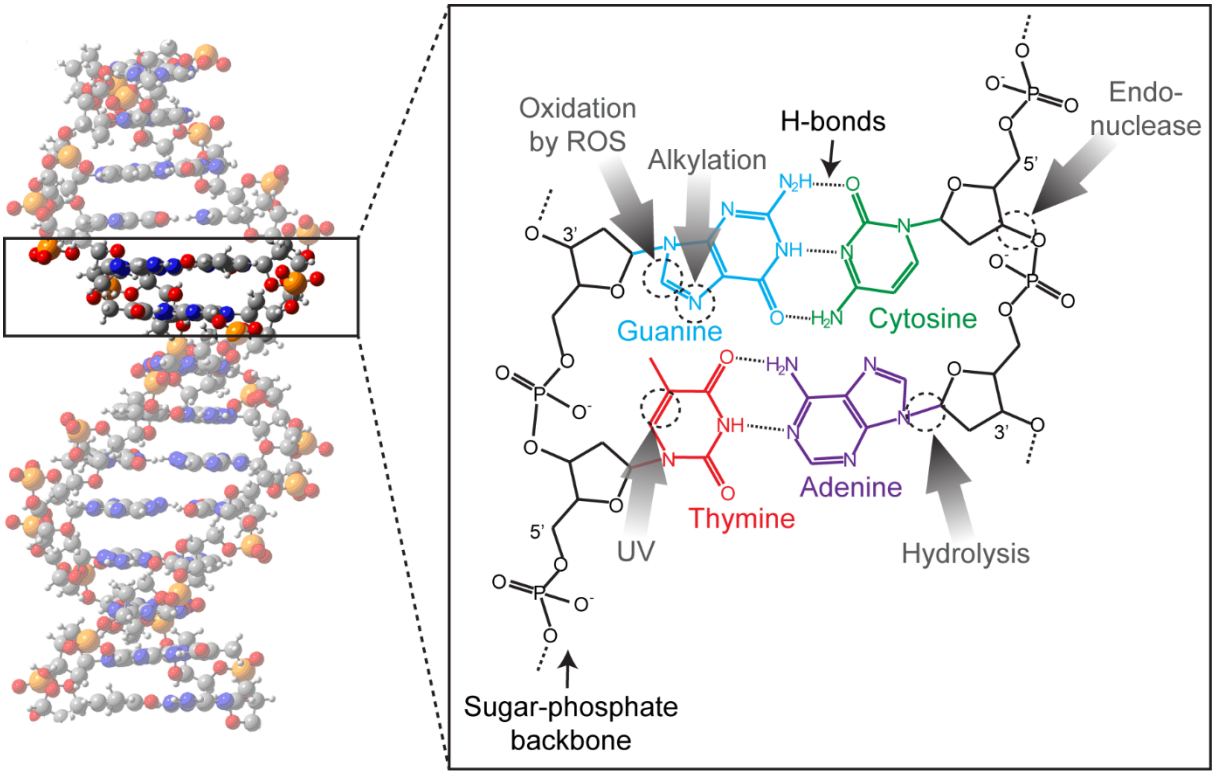

Figure 1.2. *The double helical and molecular structure of double stranded DNA is shown with its four different building blocks containing each a different nucleobase. Two kind of base pairs can be formed, guanine – cytosine with three hydrogen bonds and adenine – thymine with two hydrogen bonds (H-bonds). The nucleobases are connected to a sugar-phosphate backbone which is negatively charged under physiological conditions (pH ~7). Possible attacking points for hydrolysis, oxidation, alkylation, ultra-violet (UV) radiation or DNA-degrading enzymes (nucleases) are indicated.*

Nucleic acids itself can be quantified either unspecifically by UV/VIS absorption spectrometry at a wavelength of 260 nm or by using some kind of tagging molecule that binds nucleic acids, for example, a nucleic acid intercalating fluorescent dye, such as ethidium bromide, or SYBR Green. If a specific nucleic acid with a certain nucleotide sequence needs to be detected and quantified, another, single stranded labeled nucleic acid molecule (a so called 'probe') with a complementary nucleotide sequence can be added, which then hybridizes to the target nucleic acid. The thereby specifically labeled target nucleotide can then be quantified. This method is employed to quantitatively assess the amount of a certain nucleic acid molecule present e.g., in specific tissues or cells. Examples of methods that use labeled DNA probes are Northern blotting[16] (for RNA), Southern blotting[17] (for DNA), and DNA microarrays.[18] To increase the sensitivity of the quantification method, the target nucleic acids can be amplified, e.g., by polymerase chain reaction (PCR). For PCR, the enzyme 'DNA polymerase' has to be added, as well as primers, i.e., complimentary single stranded DNA oligonucleotides that bind to the beginning and end of the target DNA sequence, single nucleotides, and buffer solution. For quantitative real-time PCR (qPCR), e.g., sequence-unspecific DNA-binding dyes (e.g., the fluorescent dsDNA intercalating SYBR Green) or fluorescence resonance energy transfer (FRET) probes (e.g., a hydrolysis-based 'Taqman' probe) can be added. The increase in fluorescence which correlates to an increase in DNA molecules is monitored in real-time during PCR. From the fluorescence data, the relative amount of DNA molecules present in the sample can be determined. **Figure 1.3** schematically explains the principle behind quantitative real-time PCR with a DNA-binding dye to determine the sample DNA concentration.

Nowadays, nucleic acids cannot only be readily analyzed in regard of their sequence or quantity, but also designed *in silico*, as well as chemically assembled and modified *in vitro* in order to serve different purposes. Nucleic acids as tools in quantitative analysis can be for example used as highly specific recognition molecule for other complementary nucleic acid molecules. By creating DNA origami molecules, i.e., by specifically engineering the DNA three-dimensional structure and by adding additional chemical functionalizations, nucleic acids can be applied as recognition/sensing tools in quantitative analytical methods for a broad spectrum of molecules, similar to enzymes or immunoglobulins. For example, it was shown that DNA origami structures can be used for pH sensing[19] or for sensing of biomolecules.[20]

Instead of using DNA as a mean to recognize other molecules, it can also be employed as versatile tagging agent, e.g., in DNA-encoded chemical libraries, where DNA oligomers are used as tags in screening applications for pharmaceutically relevant molecules.[21] DNA is

especially suited for such a task, due to its relatively low production cost, high chemical stability, and combinatorial coding properties.[22] Already a sequence of five nucleotides allows the generation of $4^5 = 1024$ different codes.

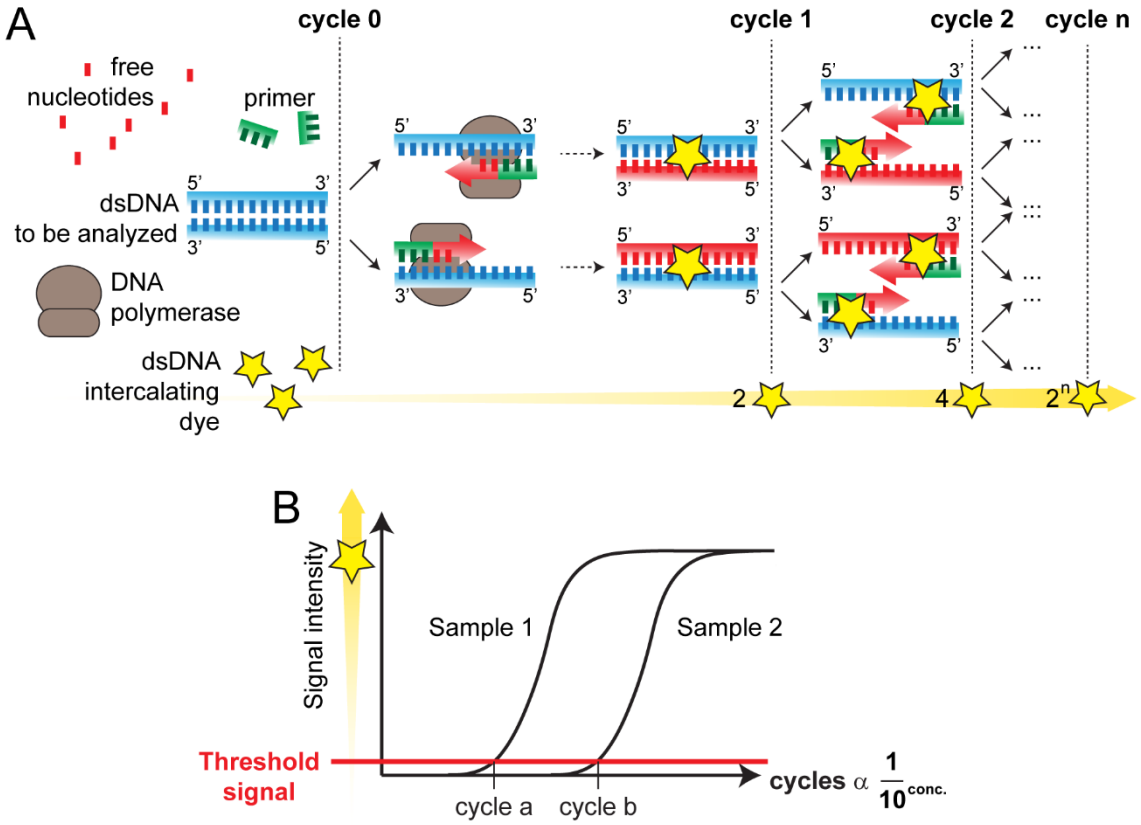

Figure 1.3. *Scheme of quantitative real-time polymerase chain reaction (qPCR). (A) Several components need to be added to a sample of which the amount of a certain DNA sequence needs to be determined. To perform qPCR using, e.g., the dye-intercalating method, sequence-specific single-stranded DNA primers (~20 bases long), free nucleotides (ATP, CTP, GTP, and TTP), a fluorescent double-stranded DNA-intercalating dye (e.g., SYBR Green), as well as a heat-resistant DNA polymerase, ions and buffers have to be added to the sample. The DNA in the sample is then exponentially amplified in cycles, whereas in each cycle, the double-stranded DNA is melted at high temperatures (95 °C), and replicated once at lower temperatures (~72 °C). Thus, the amount of DNA doubles after each cycle. At the end of each cycle the signal intensity of the DNA-bound fluorescent dye correlating to the amount of DNA is measured in 'real-time'. (B) The cycle number where the signal intensity function crosses the threshold intensity, which is significantly different from the background intensity, is determined for each sample. The DNA concentration is inversely proportional to the threshold cycle number and can be calculated from a standard curve generated with known concentrations of DNA.*

Synthetic DNA has also been used as tracer tag to quantitatively evaluate, for example, hydrological flowpaths,[23, 24] and the biodistribution of nanoparticles.[25] Quantitative analysis of the DNA tracer molecules is usually done by qPCR. One of the main advantages of using synthetic DNA as tag is the almost unlimited number of different tracers that can be artificially designed, which makes multiplexing experiments with many tracers in parallel possible and further allows the use of DNA tags as biochemical 'barcodes' for labeling and tracing, e.g., valuable products, or living organisms.

Another advantage is the high sensitivity and specificity of the employed quantification method (qPCR), allowing to evaluate samples with less than one hundred DNA molecules per microliter under optimal conditions. However, depending on the application, the use of unprotected DNA has some major drawbacks, such as loss of DNA by degradation in aqueous solution, unspecific binding, as well as lack of efficient purification methods from a sample and thus a lowered sensitivity due to matrix related effects that disturb qPCR.[26, 27]

To protect a DNA tag from degradation and to purify it more conveniently from other, disturbing constituents of a sample, the DNA tag could be shielded from its surrounding environment by encapsulation, e.g., in a robust, but chemically inert nanomaterial. The rationale of using encapsulated DNA tags will be further elaborated in Chapter 1.3.

1.2.4 Living cells: Programmable self-reproducing sensors

In the previous sections, biomolecules were discussed that are themselves components of a biological system, i.e., a bioorganism. In the past decades, biologists have developed tools enabling the manipulation and engineering of bioorganisms or isolated cells in order to create new biological functions, e.g., to produce highly complex organic molecules such as pharmaceuticals, fuels, and food additives, that would be otherwise costly and/or tedious to synthesize by just pure synthetic chemistry means. But bioorganisms can also be engineered to have other functions, and it may not be surprising, that (microbial) cells have been employed to serve as quantitative analytical tool, as part of so called 'whole-cell sensing systems'. In contrast to, e.g., enzymatic assays, microbial cells reproduce and provide the necessary sensing constituents such as enzymes, cofactors, and coenzymes themselves. Additionally, they cannot only exert one, but a series of reactions between the molecular recognition of an analyte and generation of a quantifiable signal. The interesting part is that most of these reactions are potentially programmable by manipulating the genetic information of the cells. Thus, cells could be programmed as sensing platforms for a broad spectrum of molecules and

quantification methods, e.g., by implementing reporter gene systems for different compounds.[28] **Figure 1.4** illustrates a reporter gene-system based sensing system.

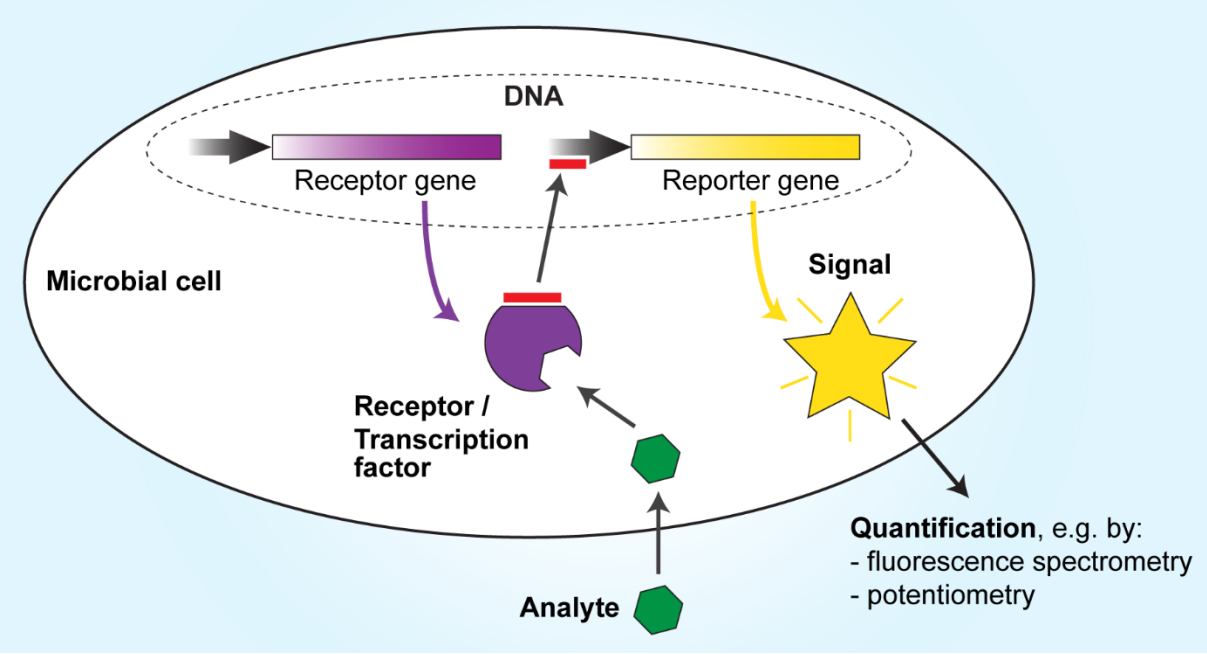

Figure 1.4. *Reporter gene-system based whole-cell sensing system. An analyte is recognized by a cellular receptor which can activate a transcription factor (a molecule that influences the transcription of specific genes) or is itself a transcription factor. The receptor/transcription factor is either already naturally present in the cell or introduced to the cell by genetic engineering. After binding to the analyte through a lock-and-key mechanism, the receptor/transcription factor undergoes a conformational change enabling it to bind to a specific DNA sequence (indicated by a red line) causing the expression of the reporter gene. The reporter gene product leads to or is itself a quantifiable molecule (e.g., a fluorescent protein) by various methods.*

Besides that, (microbial) living organisms can be very useful for the quantitative assessment of global parameters such as stress conditions or toxicity levels, especially in cases where the stress or toxic agent is unknown. However, it is usually not possible to determine which compound exactly was measured. A commercially available example is the use of the naturally bioluminescent bacterium *Vibrio fischeri* as part of a whole-cell sensing system for water toxicity assessments. Compounds interfering with the metabolism of this bacterium will have a direct effect on the amount of bioluminescence produced, which can be quantitatively monitored with a luminometer.[29] A similar approach has been followed for assessing herbicides that interfere with the chlorophyll metabolism. Microalgae (*Chlorella vulgaris*) were immobilized on an optical quartz microfiber placed in a membrane-confined flow cell. The

amount of herbicides present was monitored by measuring the chlorophyll fluorescence.[30] Other whole-cell sensing systems use cells of bacterial or fungal (e.g., yeast) origin, and quantification methods that are usually spectrophotometric (e.g., fluorescence, bioluminescence) or electrochemical (e.g., amperometric, potentiometric), and are engineered to sense inorganic and/or organic molecules, as well as physical parameters (e.g., UV light).[31]

A great potential of whole-cell sensing systems lies in their programmability. However, genetically modified organisms can usually not be used outside of a laboratory environment for biosafety reasons. Thus, ways have to be found to design intrinsically safe programmable whole-cell sensing systems. This will be discussed in detail in Chapter 1.4.

1.3 Creating a versatile quantification tool by fossilizing DNA in silica

As discussed in Chapter 1.2.3, DNA has a great potential for usage as quantifiable, highly versatile tagging agent and tracer. However, three main issues have to be addressed: 1) The stability of DNA in aqueous solutions against chemically inherent and environmental factors, 2) unspecific binding of DNA, and 3) efficient sample recovery of the DNA tag. Concerning the stability, unprotected DNA is – in contrast to RNA – reasonably stable in aqueous solution and under physiological conditions, due to the lack of the 2'-hydroxyl residue at the sugar backbone (2-*deoxy*ribose) which strengthens the phosphodiester bond. However, unprotected and in aqueous solution dissolved DNA can still degrade significantly already after several days at ambient temperature (25 °C). Several mechanisms contribute to *in vitro* instability of DNA in an aqueous solution. The most important ones are listed and explained below, see also **Figure 1.2**:

1) Acid-catalyzed hydrolysis of the N-glycosidic bond, i.e., the chemical bond between the sugar and nucleobase. The purine bases guanine and adenine are much more affected than the pyrimidine bases cytosine and thymine. Subsequently to the cleavage of the N-glycosidic bond, a base-catalyzed β-elimination results in the cleavage of the DNA backbone, i.e., the sugar 3'- phosphoester, leading to DNA chain break.[32-34]
2) Oxidation of DNA bases and sugar by free reactive oxygen species (ROS), e.g., hydroxyl radicals, generated in the presence of catalyzing impurities such as transition metal ions (e.g., Fe^{2+}, Cu^{2+}) or lipids. DNA oxidation can lead to the production of oxidized nucleobases (e.g., 8-oxoguanine) and to strand breaks.[33, 34]

Degradation mechanisms 1) and 2) can be slowed down considerably by storing DNA highly purified at optimal conditions, i.e., at low temperature ≤ 4 °C, nearly-neutral pH (i.e., pH 7 - 8), and in the presence of ROS-scavengers (e.g., mannitol).[34] But conditions in the environment where DNA would be applied as tracer are usually suboptimal. Additionally, there exist other degradation mechanisms in the environment:

3) Enzymatically catalyzed degradation by DNA nucleases (DNase), produced by, e.g., bacteria as extracellular virulence factor, can lead to rapid DNA degradation at ambient temperatures.[26, 35]
4) The presence of chemicals such as nitrous acid (HNO_2) or alkylating agents (e.g., used for cancer treatment) lead to formation of purine nucleotide derivatives, increasing the rate of depurination (hydrolysis of purines, see point 1) up to 10^6 fold.[36, 37]

5) Photochemical reactions in DNA, for example pyrimidine dimerization, are caused by electromagnetic radiation with wavelengths around the absorption maximum of DNA (~260 nm) such as UVB and UVC radiation. Also light with longer wavelengths such as UVA can cause indirect damage by the production of ROS. UVA and UVB radiation are both components of sunlight that reach the earth's surface.[38]

Because most of the here mentioned decomposing mechanisms (1 – 4) strongly depend on the presence of water molecules, dehydration of DNA molecules is a way to lower the degradation rate. Some microbial organisms such as the bacterium *Bacillus subtilis* undergo sporulation under unfavorable conditions, which also includes the partial dehydration of their DNA to increase its stability.[39] The use of dry (lyophilized) DNA or other non-aqueous solvents may have a use for storage purposes in laboratory applications, but less so for tagging applications in the environment at ambient conditions.

To keep DNA in a highly dehydrated, solid-state form, and to address also the remaining two issues, avoidance of unspecific binding and efficient recovery from an environmental sample, a relatively obvious strategy would be the enclosing of the DNA tag into a material that i) excludes water, ROS, enzymes and other damaging factors, ii) is chemically inert, and iii) can be readily separated from a sample to recover the incorporated DNA. Ideally, the capsules containing the DNA should have identical physical as well as chemical properties, and a very small size so that the capsules are stably dispersible in all kinds of matrices and do not disturb the matrix properties, at least not at lower capsule concentrations.

Silica (silicon dioxide, SiO_2) is a chemically and thermally highly inert material having excellent barrier properties, low solubility in water at ambient conditions, and is widely used in the chemical and food industry. Silica is not affected by most chemical reactants, only hydrofluoric acid (HF) readily dissolves it. Monodisperse amorphous silica spheres in the nano- to micrometer range can be readily synthesized at room temperature by the so called 'Stöber process', i.e., the polycondensation of tetraethyl orthosilicate.[40] In 2013, Paunescu *et al.* – inspired by the recovery of 'ancient' DNA from hundred thousand years old fossilized bones or amber – encapsulated DNA oligomers in amorphous silica particles. To synthesize these 'fossilized' DNA particles, the DNA was first immobilized on the surface of positively charged silica particles (Ø 100 - 200 nm), onto which a dense layer of silica was deposited. The DNA tagged particles were then applied as 'barcode' labels for polymers and showed high stability towards ROS and elevated temperatures. The encapsulated DNA was recovered from the particles by adding a highly diluted buffered fluoride-containing solution which dissolved the

silica, but left the DNA unharmed. Afterwards, the label was quantified by qPCR (see **Figure 1.5**).[41, 42] Other studies investigated the application of the so called silica particles with encapsulated DNA (SPED), for example, as quantitative tracers and sensors in the environment,[43] food,[44] or microorganisms.[45] Additionally, SPED with magnetic[46] or UV-shielding[47] properties were produced. The long-term stability of DNA in SPED was also assessed in detail.[48]

In this doctoral thesis, the applications of SPED as quantitative labels in ecological networks and as pesticide taggant were investigated. These studies are shown in detail in Chapter 2 and Chapter 3.

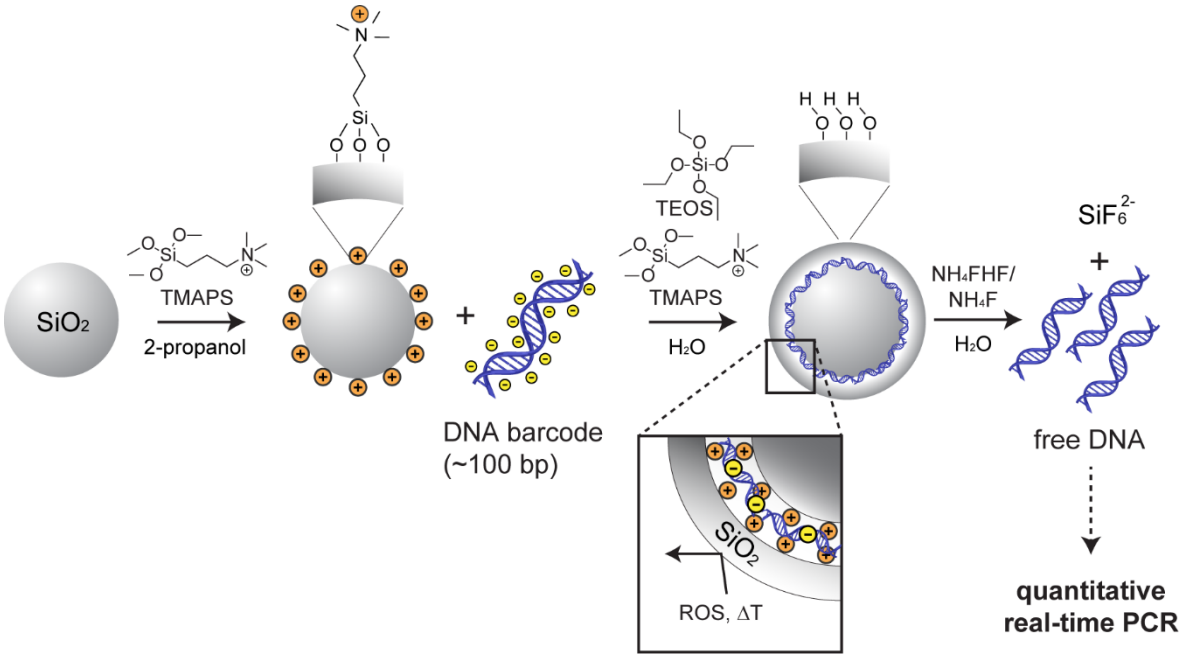

Figure 1.5. *Synthesis of silica particles with encapsulated DNA after Paunescu et al. (2013).*[41, 42] *First, amorphous silica particles (Ø 100 - 250 nm) are functionalized with a positively charged silane, N-trimethoxysilylpropyl-N,N,N-trimethylammonium chloride (TMAPS). Free negatively charged double-stranded DNA oligomers (~100 bp) in aqueous solution at pH 7 are then added to the ammonium-functionalized silica particles, and bind to the positively charged particle surface via electrostatic interactions. Subsequently, the bound DNA molecules are covered by a layer of TMAPS molecules and a protecting layer of silica (12 – 15 nm) is added by a sol-gel process using tetraethyl orthosilicate (TEOS). The encapsulated DNA resists chemical or physical treatments such as reactive oxygen species (ROS) or elevated temperatures (ΔT). For analysis, the DNA can be recovered by dissolving the silica particles in an aqueous buffered fluoride-containing solution and quantified by quantitative real-time PCR.*

1.4 Living materials: A niche for analytical applications with living cells

As mentioned in Chapter 1.2.4., (microbial) living cells can be broadly applied as relatively cost-effective parts for recognition and quantitative signal generation in analytical systems. Genetic programming would allow the creation of cells capable of sensing a wide variety of different compounds. However, the use of genetically modified microorganisms is usually restricted to an enclosed, laboratory environment with biosafety measures in place. For their applications as part of biosensors outside of a microbiologist laboratory, new ways have to be found to safely contain cells within a sensor system. Another important challenge when using living organisms for sensor applications is their need for a specially designed, regulated environment suiting their species-dependent requirements in terms of availability of specific nutrients, temperature, pH, osmotic pressure, and removal of waste products to optimally fulfill their designated function. The mentioned challenges limit the use of genetically modified sensing cells for applications outside of a specialized analytical laboratory, such as for diagnostic point-of-care tests.

When designing a new out-of-lab whole-cell sensing system, it is first of all crucial to determine the type of cell culturing. Several culturing types of whole-cell sensor systems have been developed, including freshly suspended, freeze-dried or immobilized cell methods. The setup and prolonged maintenance of a suspended cell culture requires significant skills and instruments, and is not well suited for an out-of-lab application. Freeze-dried cells are easy to bring to a suspended culture, but to continuously culture them requires the same skills than for cultures from fresh cells. Immobilized cells ideally require much less attention for preparation and maintenance. An example for an immobilized whole-cell sensor assay has been showed by Lynberg *et al.* (1999): They immobilized genetically modified bacteria (*Escherichia coli*) in latex and applied them for the sensitive, qualitative detection of mercury Hg(II) in liquids.[49] However, in this sensing system, the bacteria were – although entrapped in latex – able to leak out of the latex to the sample liquid, which poses a biosafety risk. A second important criterion would therefore be the ability of the immobilizing matrix to retain the incorporated cells.

In 2012, Gerber *et al.* have designed a so called ‘living material’ containing fungi, i.e., the molds *Penicillium camemberti* and *Pencillium chrysogenum,* in a flat hydrogel layer between a layer of a non-porous and a layer of a porous membrane. The material was inspired by natural living surfaces such as lichens, and bacterial or fungal biofilms. The porous membrane would allow the exchange between the inner ‘living’ layer with the outside world and vice versa, but would confine the microorganism to the designed niche within the material. It was shown that

those living materials can react in response to stimuli such as food or pathogens that come into contact with the porous top membrane, e.g., by producing antibiotics.[50, 51]

Incorporating genetically modified sensor cells into the ‘living material’ could result in the creation of a whole-cell sensing platform, applicable to quantify different chemical analytes. Potentially, quantification could be done by measuring the intensity of the produced reporter signal, e.g., fluorescence, bioluminescence, in response to the analyte. However, gene expression is usually regulated in a binary rather than gradual fashion, i.e., expression is either switched ‘on’ or ‘off’ above or below a certain threshold concentration of the analyte. Thus, sophisticated gene regulatory mechanisms would have to be implemented to achieve a gradual expression correlating to the concentration of the analyte, at least in a certain concentration range. Additionally, in order to achieve reproducible and comparable intensity measurements, the immobilized cells would need to be homogenously distributed throughout the material and different sensors would need a similar cell density. Also the analyte would need to be applied homogenously to the sensor surface, which can be difficult especially with low-volume samples.

To avoid these pitfalls, another quantitative approach for immobilized whole-cell sensing systems employing ‘diffusion’ as main analytical parameter instead of ‘intensity’ is described in this doctoral thesis in Chapter 4.

2. Silica particles with encapsulated DNA as trophic tracers

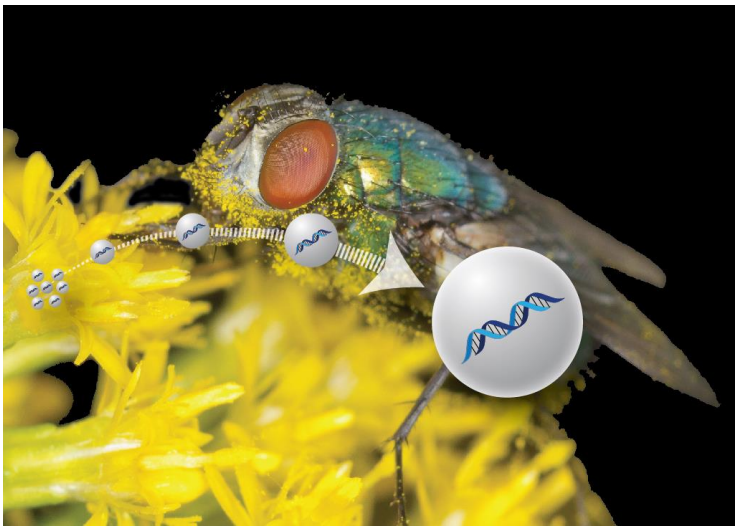

Published in parts as:

Carlos A. Mora, Daniela Paunescu, Robert N. Grass and Wendelin J. Stark,

Molecular Ecology Resources **2015**, 15, 231-241.

2.1 Introduction

The analysis of food webs gives information about the robustness and productivity of an ecosystem.[52] It is, therefore, crucial to have a detailed overview of interactions and dependencies between different species in an ecosystem and to quickly detect when these interactions start to change in order to be able to take measures against negative trends. In many cases, it is not possible to observe trophic interactions between predator and prey directly[53] and it is difficult to identify strong and weak interactions between predator and prey.[54] Most of the methods used for empirical investigation of food webs employ intrinsic tracers that are naturally present in an organism's diet. Examples of such tracers are DNA,[55-57] antigens,[58] fatty acids,[59] or isotopes.[60-62] Stable isotope analysis can also provide information about the trophic position of an organism in a food web.[63, 64] Food sources may also be labeled extrinsically with isotopes to reveal the structure of a food web.[65] Other extrinsic ecological tracers such as dyes, fluorescent plastic beads and fluorescently labeled bacteria have been employed to investigate the predator-prey interaction between protists and bacteria.[66, 67]

The usage of degradable intrinsic markers such as DNA, fatty acids or antigens is limited by the fact that these molecules are usually not transferable over more than one trophic level. While techniques for diet analysis such as DNA barcoding can assess food webs even in a multiplex format, there are many potential biases concerning the quantitative evaluation of the results.[57] Extrinsic tracers such as fluorescent dyes, beads and microorganisms are degradable, can be bleached due to light exposure and are difficult to detect at low concentrations or when incorporated in biological tissue. Stable isotopes of carbon (^{13}C), nitrogen (^{15}N) or sulfur (^{34}S) can only provide information about the relative contribution of different potential food sources if the diet sources have sufficiently different stable isotope ratios. For instance this is the case between aquatic and terrestrial diet sources or C3 and C4 plants,[60] but often isotope ratios overlap in potential prey.[68] Additionally, the diet of an organism may vary depending on season or availability. The time that the isotopic composition of ^{13}C, ^{15}N or ^{34}S in an organism needs to adapt to the dietary shift is a function of an organism's metabolic turnover and growth rate. A complete isotope adaption could take years for slow-growing organisms.[69, 70] Additional experiments are thus necessary to determine the specific isotopic exchange rates of the investigated organisms based on their growth and metabolic turnover rate prior to quantitative analysis of their food habits and habitats.[71]

One of the main advantages of extrinsic compared to intrinsic tracers is the fact that they are traceable back to their origin or entry-point into a food web. An extrinsic tracer that is capable

of monitoring interaction strengths from the bottom to the top of a food web and shows flexibility to dietary shifts would be a useful quantitative tool in food web analysis. To design such an extrinsic tracer that is superior to the already applied ecological tools, many aspects need to be considered. First, environmental safety including chemical and biological inertness as well as low toxicity has to be ensured. For accurate tracking of multiple organisms and food sources the tracer needs a unique, highly variable label, has to be non-degradable in a biological setting, must show an adequate but limited persistence in bioorganisms and be transferable to other trophic levels. Finally, the tracer should enable a qualitative and quantitative analysis at an ultra-low concentration level in a biological setting. Recently, SiO_2 Particles with Encapsulated DNA (SPED) have been developed.[41, 42, 46] These studies showed that DNA oligomers embedded in SiO_2 are difficult to degrade even under harsh radical and heat treatments. Standard biological liquids (e.g. digestive fluids) do not significantly damage the encapsulated DNA,[41, 42] which makes this system suitable to trace interactions over several trophic levels in biological organisms. SPED are submicron-sized in the range of 100 - 150 nm.[21, 22] The short DNA sequences are randomly generated with a length of ~100 - 120 bp and can be recovered from the particles under appropriate chemical conditions. The DNA labels can only be amplified with a matching primer pair and are quantifiable by real-time PCR (qPCR), a widely-used technique for DNA analysis.[72] Nano-scale silica colloids are considered non-toxic and are widely used in different industries such as the metal, paper and food industry as binders, desiccants and fillers.[73-75]

In the present study, we used silica particles with encapsulated DNA (SPED) as an extrinsic food-web tracer (**Figure 2.1**). We developed an efficient extraction and quantitation method of SPED from animals and investigated the uptake and transfer of particle tracers using a two-level arthropod food web within a laboratory. Additionally, we applied SPED to a more realistic field situation by investigating the flower color preference of fly pollinators. We showed that it is feasible to use SPED as detection and quantification tool in ecological applications and propose their use in examining and monitoring food webs in ecosystems.

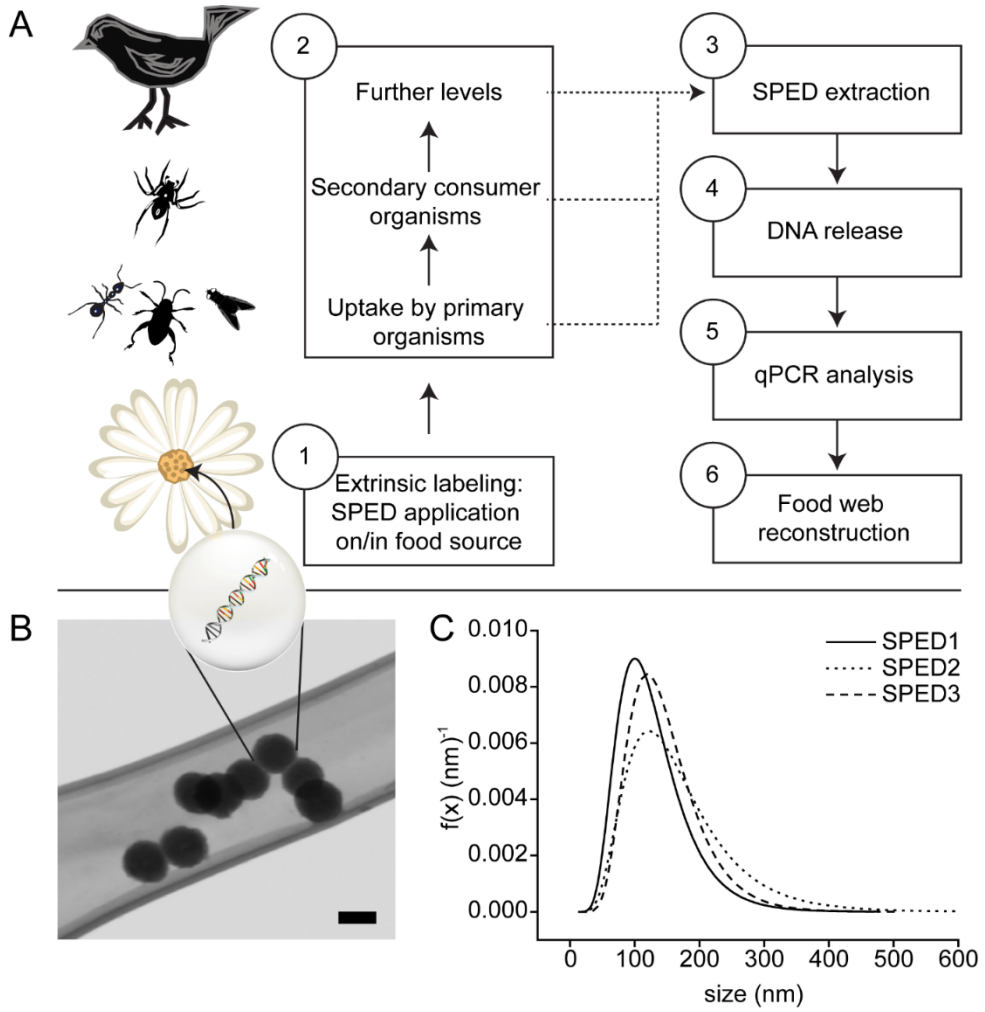

Figure 2.1. *Illustration of the application of SPED to a food web and an overview of the experimental procedure and SPED characteristics.* ***(A)*** *(1) Food sources are extrinsically labeled with SPED and enter (2) the food web by uptake and subsequent transfer to higher trophic levels. (3) Samples are taken from different animals in the food web and the SPED are extracted and concentrated. (4) The encapsulated DNA label is subsequently released by chemical etching. (5) Finally the resulting free DNA is quantified via qPCR and (6) the food web connections reconstructed.* ***(B)*** *Scanning-transmission electron microscopy (STEM) image of SPED3. Scale bar, 100 nm.* ***(C)*** *Fitted log-normal size distribution determined by sedimentation analysis and confirmed by scanning-transmission electron microscopy image analysis.*

2.2 Experimental

2.2.1 Animal cultures

Drosophila melanogaster imagos, *Tenebrio molitor* larvae and *Lucilia caesar* larvae were all bought from Reptile-Food GmbH, Switzerland. We used a vestigial wing mutant of *D. melanogaster* flies which is unable to fly. *D. melanogaster* flies were cultured on the following medium (per liter): 100 g grounded corn kernels, 70 g sucrose, 12 g agar (AppliChem), 25 g dry yeast, filled to 1 L with H_2O. The flies were kept in 1 L glass beakers filled with 300 mL medium each and covered by nylon fabric at constant room temperature (22 ± 2 °C), humidity (40 ± 10 %) and light conditions (12 h / 12 h light/dark cycle). Transfer to new medium occurred every three weeks. *Tenebrio molitor* larvae and imagos were cultured separately at room temperature (22 ± 2 °C) in semi-darkness on a mix of wheat bran and flour (3:1 ratio) and fed with 1-2 apple slices per week. Transfer to new medium occurred every 2 months. *Lucilia caesar* larvae were let mature to adults in a 1 L glass beaker at constant room temperature, humidity (40 ± 10 %) and light conditions (12 h / 12 h light/dark cycle). The adult flies were fed with a 1:1 mixture of honey and water. *Pholcus phalangioides* individuals were collected in house basements in the area of Zurich, Switzerland between May – July 2013. They were kept separately in closed plastic beakers with porous lids around 2-3 weeks before an experiment at room temperature (22 ± 2 °C) in semi-darkness and fed once per week with 4 – 6 unlabeled fruit flies. Before an experiment, the spiders were starved for one week.

2.2.2 SPED synthesis and characterization

For the synthesis of the particle batches SPED2 and SPED3, non-fluorescent silica particles were used (SiO_2 research particles, 142 nm, Micro Particles GmbH, Germany). For SPED1, silica particles containing a fluorescent rhodamine-derivative (Ex: 569 nm, Em: 585 nm) were purchased (sicastar®-redF, 100 nm, Micromod Partikeltechnologie GmbH, Germany) to verify the presence of particles by fluorescence microscopy in histological sections of *Drosophila* in parallel to qPCR analysis (see section 2.2.6 and **Figure A.1.1,** Appendix). DNA was encapsulated according to the method of Paunescu et al.:[42] 50 mg silica particles in 1 mL ethanol were functionalized with 10 µL *N*-trimethoxylsilylpropyl-*N*,*N*,*N*-trimethylammonium chloride (TMAPS; 50% in MeOH, ABCR GmBH) overnight. 35 µL TMAPS-functionalized particles were mixed with 1 mL dH_2O and 20 µL of respective pre-annealed dsDNA (25 µM, Microsynth AG, Switzerland). To remove excess DNA molecules, the particles were washed 3 times with dH_2O and resuspended in 0.5 mL dH_2O. After stirring with 0.6 µL TMAPS and 0.6 µL tetraethyl orthosilicate (TEOS, ≥ 99 %, Sigma-Aldrich) for 4 h at RT, additional 4 µL TEOS

were added and the mixture stirred for 4 days at RT. Afterwards the DNA-containing particles were washed 3 times with dH_2O and resuspended in 10 mL dH_2O for subsequent ball milling with 10 g zirconium oxide beads (0.1 mm, YTZ Grinding medium, Tosoh Corp.) at 500 rpm for 4 min (Planetary Micro Mill Pulverisette 7, Fritsch, Germany). The milled particles were centrifuged at 10'000xg for 15 min and resuspended in 200 µL dH_2O. Nanoparticle size was determined by scanning transmission electron microscopy (STEM, Nova NanoSEM 450, FEI) and volume-weighted sedimentation analysis (ρ = 2.2 g·cm^{-3}, Lumisizer, LUM GmbH). The particle concentration was determined by dry mass measurement of the particles. The particle DNA load was determined by fluorometric quantitation (Qubit, dsDNA HS assay, Life Technologies Corp.) after dissolving a known amount of particles in buffered oxide etch (BOE) containing 2.3 wt% ammonium hydrogen difluoride (NH_4FHF, pure, Merck) and 1.9 wt% ammonium fluoride (NH_4F, puriss., Sigma-Aldrich) in dH_2O. Typically about 50 µg SPED in 5 µL dH_2O and 20 µL BOE were mixed together and DNA was measured. The approximate DNA load per particle was calculated by assuming a spherical shape of the particles and a density of 2.2 g·cm^{-3} (**Table 2.1**).

2.2.3 SPED uptake for *D. melanogaster*

SPED particles dispersed in a volume of 100 µl ultra-pure water were evenly applied to the solidified *Drosophila* medium surface and let dry for 1 hour at room temperature. Medium had been filled up to the 5 mL mark in a 50 mL tube, resulting in a medium surface area of A = 491 mm^2. One experimental unit consisted of a tube containing 20 flies. The flies had been randomly chosen from a maximally 7-day old stock culture (approx. balanced male/female ratio). To take samples, the tubes were placed in a freezer at -20 °C for 15 min. In general, at least three independent replicas per experimental condition were implemented. To assess particle uptake on SPED1-labeled medium, the medium surface was labeled with 50 µg (5· 10^7 particles per mm^2) SPED1 particles. Animal samples were taken after exposure to the medium at different time points (0.5, 2, 3, 4.5, 6, 24 and 48 h). To investigate the particle loss on a SPED1-free medium the flies were exposed to medium labeled with 0.6 mg (7 ·10^8 particles per mm^2) for 4 hours and transferred to tubes containing non-labeled medium (total inner tube surface area = 80.5 cm^2). Flies were sampled after 0, 1, 2, 4 and 7 days on SPED1-free medium. Usually 15 flies of each tube were allocated for qPCR analysis and the remaining 5 flies were prepared for microscopic examination (see section 2.2.5). For the analysis of the persistence of differently labeled SPED particles, 20 flies per tube were exposed for 3 hours to medium

labeled with both SPED1 and SPED2 in a 1:1, 1:5 or 5:1 ratio totaling to 0.6 mg particles per tube.

Table 2.1. *Mean particle sizes and calculation of the approximate DNA load per SPED in nmol per mg.*

SPED#	Mean particle size[A] ± SEM, nm	Molar mass of DNA kDa (μg·nmol^{-1})	Particle concentration[B] particles·mg^{-1}	DNA load per SPED[C] ± SEM μg·mg^{-1}	nmol·mg^{-1}
1	116 ± 2	69.9	$5.6 \cdot 10^{11}$	2.2 ± 0.1	$5.6 \cdot 10^{-14}$
2	132 ± 2	62.4	$3.8 \cdot 10^{11}$	0.33 ± 0.02	$1.4 \cdot 10^{-14}$
3	121 ± 3	66.8	$4.9 \cdot 10^{11}$	0.2 ± 0.02	$6.7 \cdot 10^{-15}$

[A] Mean particle size was determined by sedimentation analysis from four independent samples (n = 4).
[B] Approximate particle concentration was derived from mean particle size with ρ = 2.2 g·cm^{-3} assuming a spherical particle shape.
[C] DNA load was determined from three independent samples (n = 3).

2.2.4 SPED uptake for *T. molitor* larvae

Vacuum-dried SPED (SPED1) (Concentrator plus 5305, Eppendorf), particles were thoroughly mixed (SpeedMixer DAC 150, Hausschild Engineering) with commercially available white wheat flour at a concentration of 0.1 mg/g ($6 \cdot 10^{10}$ particles per g). 10 g of SPED1-labeled flour was added to a plastic beaker (A = 28 cm^2). All larvae had a weight of 60 – 100 mg. 5 single larvae were analyzed per experimental condition. To investigate SPED uptake, 20 *T. molitor* larvae were added to a beaker containing labeled medium and sampled at different time points (1, 3, 6 and 24 hours). To investigate the particle loss over time, the larvae were cultured on a SPED-free medium for 4 days after exposing them to SPED1-labeled medium (0.1 mg/g) for 1 day. Samples were taken after 1 and 5 days. The sampled larvae were weighed and subsequently killed by freezing at -20 °C for 30 min. The outer surface of the dead larvae was then washed with 1 mL 100x diluted buffered oxide etch (BOE, see section 'SPED extraction') by pipetting up and down for 10 seconds to remove surface bound SPED particles. The washing solution was removed and stored for further analysis. For neutralization of residual hydrofluoric acid, the larvae were washed with 1 mL 0.1 M $CaCl_2$.

2.2.5 Histological sections of *D. melanogaster*

5 flies were placed together in a paraffin embedding cartridge (Bio-Net, Biosystems AG, Switzerland) and subsequently fixed in 4 % paraformaldehyde overnight. The flies were washed once with water and dehydrated by increasing the concentration of ethanol (≥ 99.8 %, Fluka) stepwise (20 %, 40 %, 70 %, 90 %, 95 % to 100 %) for 1 hour each. The dehydrated flies were then treated with xylenes (≥ 97%, Fluka) for 1 hour and subsequently infiltrated with liquid

paraffin overnight (Tissue Processor 15 Duo, Medite AG, Switzerland). Single flies were embedded in paraffin (Tissue Embedding Station, Medite AG, Switzerland) and paraffin sections were cut into 12 µm thin sections with a rotary microtome (HM 355 S, Microm Intern. GmbH, Germany). The cut sections were mounted on microscope slides (Polysine slides, Thermo Scientific), de-paraffinized in xylenes and rehydrated 95%, 90%, 70% and H_2O for 5 min each. The sections were fixed with a non-fluorescing mounting medium (Shandon Immu-Mount, Thermo Scientific) and stored at 4 °C.

2.2.6 Confocal fluorescence microscopy

For fluorescence imaging an inverse filter-free confocal scanning system was used (Leica DMIRE2, Leica Microsystems) equipped with an argon laser as well as a 20X and 63X oil immersion objective (HC/HCX PL Apo, Leica Microsystems). Fluorescence of SPED and surrounding tissues of the flies was recorded at two different excitation wavelengths simultaneously by z-stacking. Tissue auto-fluorescence was excited at 405 nm and recorded at 415 - 479 nm. Fluorescent SPED (SPED1) containing a rhodamine-derivative were excited at 561 nm and recorded at 574-637 nm. Images were recorded with the Leica Confocal Software (LCS, Leica Microsystems) and z-stacks rendered with the image analysis software Imaris (Version 7.4.0, Bitplane AG, Switzerland).

2.2.7 SPED transfer from *D. melanogaster* to *P. phalangioides*

30 randomly chosen flies (approx. balanced male/female ratio) from a maximally 7-day old culture were added to one fly culture tube pre-labeled with SPED (see section 2.2.3). Several tubes with SPED1 or SPED3 were prepared for one experiment depending on the amount of flies needed. After 3 hours 5 flies of each culture tube were instantly killed by freezing to serve as positive control, for normalization purposes between different culture tubes and to estimate the initial SPED content in the flies. The remaining flies were allocated to plastic beakers containing one spider specimen each (10 flies per beaker). After letting the spiders catch their prey overnight (16 h), the spiders together with the remaining alive flies were killed by freezing at -20 °C for 15 min. By visually examining how many flies were wrapped in spider silk it was assessed how many flies had been caught. The caught flies were analyzed by qPCR to evaluate the remaining amount of SPED. A total of 45 single spiders with an average weight of 17 mg (stand. dev. = 7 mg) were analyzed. The sex was determined from 27 specimens resulting in 18 females and 9 males.

2.2.8 Flower preference experiment

The flowers of a white and red purple color variant of *Argyranthemum frutescens* (marguerite daisy, Coop, Switzerland) were either labeled with SPED1 (white flowers) or SPED3 (red flowers). 20 flower heads of each plant were labeled by evenly spreading 30 µl of a 10 mg/mL particle water suspension over the whole central area of each flower head. The remaining non-labeled flower heads were cut off. The plants were placed in a small plastic green house (100 x 100 x 50 cm) and 17 *Lucilia caesar* adult flies (randomly selected from stock culture) were exposed to the flowers for 4 hours at room temperature. The flies were collected with a hand-held vacuum cleaner (Mini Vac FC 6142, Philipps) and killed by freezing at -20 °C for 30 min. The experiment was filmed (Canon Legria HF G25) and the color preference evaluated by counting the number of flies per respective flower once per minute.

2.2.9 SPED extraction

D. melanogaster, *P. phalangioides* and *L. caesar* specimens were homogenized with a bead-beater (Mini-bead beater 1, Biospec Products Inc.) after the addition of two 6.34 mm steel beads (Biospec Products Inc.) and 1.5 mL 1% SDS (Sigma Fine Chemicals) aqueous solution to a 2 mL plastic tube with screw cap (Sarstedt) at 4200 rpm for 20 s. In the case of *T. molitor*, the larvae were frozen at -80 °C for 20 min in steel tubes with rubber caps (Biospec Products Inc.) prior to homogenization at 4200 rpm for 20 s. 1.5 mL 1% SDS aqueous solution was added, thoroughly mixed and the dissolved *T. molitor* homogenate transferred to a plastic tube. The homogenate of the investigated animals was centrifuged at 21500 rpm for 5 min (Microcentrifuge Himac CT15E, VWR Hitachi) and the resulting pellet washed 2-3 times with dH_2O. After removing the supernatant carefully, residual liquid was removed by vacuum-drying the sample (Concentrator plus 5305, Eppendorf) at 45 °C for 1 hour. The dried pellet was resuspended in 100 µl buffered oxide etch (BOE) containing 2.3 wt% ammonium hydrogen difluoride (NH_4FHF, pure, Merck) and 1.9 wt% ammonium fluoride (NH_4F, puriss., Sigma-Aldrich) in dH_2O. After incubating for 10 min, 30 µl of supernatant containing released SPED DNA was transferred onto a dialysis filter (MF-Millipore Membrane, diameter: 13 mm; pore size: 0.025 µm, plain white, Merck Millipore) and dialyzed against 5 mL ultra-pure water (MilliQ) for 30 min.

2.2.10 qPCR

All qPCR measurements were at least done in triplicates. For a list of the primer and DNA template sequences refer to **Table 2.2**. A standard SYBR Green qPCR mixture for one sample

contained 10 µl SYBR Green master mix (LightCycler 480 SYBR Green I Master, Roche), 100 nM of both forward and reverse primer, 1 µl dialyzed sample, filled up to 20 µl with ultra-pure water. For the simultanous analysis of flies labeled with both SPED1 and SPED2 in different ratios (see section 'SPED uptake in *D. melanogaster*'), we designed TaqMan probes specific to SPED1 or SPED2 DNA (**Table 2.2**). Differently tagged TaqMan probes allow the analysis of more than one DNA template in one qPCR run. A standard TaqMan qPCR mixture for one sample contained 4 µl probe master mix (5x HOT FIREPol® Probe qPCR Mix Plus (no ROX), Solis BioDyne), 250 nM of each forward and reverse primer (Microsynth AG, Switzerland), 1 µl dialyzed sample, filled up to 20 µl with ultra-pure water. For all qPCR reactions we used the following reaction conditions (45 cycles): 1) pre-incubation 95 °C, 10 min; 2) denaturation 95 °C, 15 s; 3) annealing 60 °C, 30 s; 4) amplification 72 °C, 30 s. For SYBR Green qPCR a melting curve was implemented. Standard curves for SYBR Green or TaqMan qPCR were prepared by mixing and diluting the respective forward and reverse template DNA oligomers (Microsynth AG, Switzerland) to a concentration of 10, 1, 0.1 and 0.01 nM in ultra-pure water.

2.2.11 Efficiency of the SPED extraction procedure

The particle loss during homogenization and subsequent washing was investigated by adding 12 µg particles to freshly sampled flies (N = 15) or just to ultra-pure water. The first sample was homogenized whereas the second sample was left untreated. qPCR revealed that there is no significant loss of particles due to homogenization and washing treatment or due to the presence of fly homogenate (**Figure 2.2**). The experiment was performed in triplicates (n = 3).

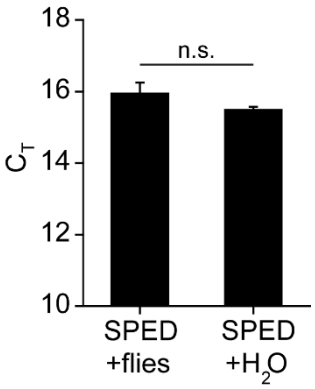

Figure 2.2 *Control of the SPED extraction procedure from flies. SPED were added to flies (N = 15) and homogenized or the same amount of SPED was added to water. Cycle of threshold value (C_T) of qPCR is displayed. n.s. no significant difference, ±SEMs (n = 3).*

2.2.12 Statistical analysis

The SPED load data in flies and mealworms followed a normal distribution. The transfer ratio and normalized particle load in spiders did not follow a normal distribution. These data were therefore analyzed with non-parametric Mann-Whitney and Kruskal-Wallis analysis of variance (≥ 2 levels or factors). For these statistical tests only the assumptions of similar distributions and especially homogeneity of variance (tested with Levene's test), but not a specific distribution such as normal distribution, need to be considered. Statistical analysis was performed with OriginPro 8.6.0G (OriginLab Corp.).

Table 2.2. *DNA sequences of encapsulated oligomers as well as corresponding primers and TaqMan probes used for qPCR analysis. The nucleotide numbers as well as chemical modifications of the respective oligomers are given in brackets.*

SPED#	Template sequences	Primer sequences	Taqman probe
1	5'-ATT CAT GCG ACA GGG GTA AGA CCA TCA GTA GTA GGG ATA GTG CCA AAC CTC ACT CAC CAC TGC CAA TAA GGG GTC CTT ACC TGA AGA ATA AGT GTC AGC CAG TGT AAC CCG AT-3' (113)	**Forward**: 5'-GAC CAT CAG TAG TAG GGA TAG-3' (21) **Reverse**: 5'-CTG GCT GAC ACT TAT TCT TC-3' (20)	5'- (Yakima Yellow)-AAC CTC ACT CAC CAC TGC CAA TAA G-(BHQ1)-3' (25)
2	5'-TTC TCA AAC TCC GAG CGA TTA AGC GTG ACA GCC CCA GGG AAC CCA CAA AAC GTG ATC GCA GTC CAT CCG ATC ATA CAC AGA AAG GAA GGT CCC CAT ACA CC-3' (101)	**Forward**: 5'-GAG CGA TTA AGC GTG ACA-3' (18) **Reverse**: 5'-GGT GTA TGG GGA CCT TCC TT-3' (20)	5'-(FAM)-AAC GTG ATC GCA GTC CAT CC-(BHQ1)-3' (20)
3	5'- TAC CGA TGC TGA ACA AGT CGA TGC AGG CTC CCG TCT TTG AAA AGG GGT AAA CAT ACA AGT GGA TAG ATG ATG GGT AGG GGC CTC CAA TAC ATC CAA CAC TCT ACG CCC-3' (108)	**Forward**: 5'- TAC CGA TGC TGA ACA AGT CG-3' (20) **Reverse**: 5'- GGG CGT AGA GTG TTG GAT GT-3' (20)	5'-(FAM)-CCC CTT TTC AAA GAC GGG AGC CTG C-(BHQ1)-3'

2.3 Results

We synthesized three SPED (1-3) differing in their encapsulated DNA sequence with mean sizes between 116 and 136 nm (**Figure 2.1** and **Table 2.1**). SPED1 particles were additionally tagged with rhodamine allowing the tracking of particles via fluorescence microscopy. We examined the introduction of SPED into a food web by exposing different animals to nutrient medium labeled with SPED. Three hours after transfer of *D. melanogaster* flies to a food medium labeled with $5 \cdot 10^7$ particles per square millimeter, a peak load of $(1.2 \pm 0.2) \cdot 10^5$ SPED1 particles per fly was observed. Subsequently, the particle number declined to $(2.9 \pm 0.8) \cdot 10^4$ after 24 hours and $(3.3 \pm 1.4) \cdot 10^4$ after 48 hours (**Figure 2.3A**). For *T. molitor* larvae exposed to medium labeled with $6 \cdot 10^{10}$ SPED1 per gram we observed an uptake of $(1.9 \pm 0.7) \cdot 10^7$ particles per mealworm after 24 hours (**Figure 2.3C**).

The persistency of SPED in flies and beetle larvae after transfer to a SPED-free environment was examined in a following step. After letting the flies take up SPED from a labeled medium ($7 \cdot 10^8$ particles per square millimeter) for four hours, the number of SPED decreased from $(3.1 \pm 0.1) \cdot 10^6$ before transfer to $(6.2 \pm 1.1) \cdot 10^5$ on day 1, $(2.0 \pm 0.8) \cdot 10^5$ on day 2 and $(2.8 \pm 1.0) \cdot 10^5$ particles per fly on day 7 after transfer to SPED-free medium (**Figure 2.3B**). Similar results were observed with *T. molitor* larvae. After transfer to a tracer-free medium the internal particle load per larva decreased from $(1.7 \pm 0.7) \cdot 10^7$ to $(2.4 \pm 0.8) \cdot 10^6$ after four days. To remove excess particles and medium sticking to the outer surface of the larvae, the animals were washed prior to homogenization. $(1.2 \pm 0.2) \cdot 10^6$ particles were found attached to the outer larva surface after 1 day on SPED-labeled medium and $(4.8 \pm 0.7) \cdot 10^5$ after 4 days on label-free medium (**Figure 2.3D**).

In parallel to qPCR measurements histological sections of flies were prepared to analyze the relative content and anatomical location of the rhodamine-tagged SPED1 by confocal fluorescence microscopy. We observed that the particles accumulated in the gastrointestinal organs of the flies as well as on the outer surface in small crevices of the exoskeleton or in other openings such as tracheae (**Figure 2.4** and **Figure A.1.2**, Appendix). When comparing microscope images from the gut region over the time course of the experiment a decline of the fluorescence signal stemming from the particles in the digestive tract was observable over the first two days. These observations correlated with the data obtained by qPCR analysis. Also after four and seven days on tracer-free medium, particles could be detected in the digestive system (**Figure A.1.2**, Appendix).

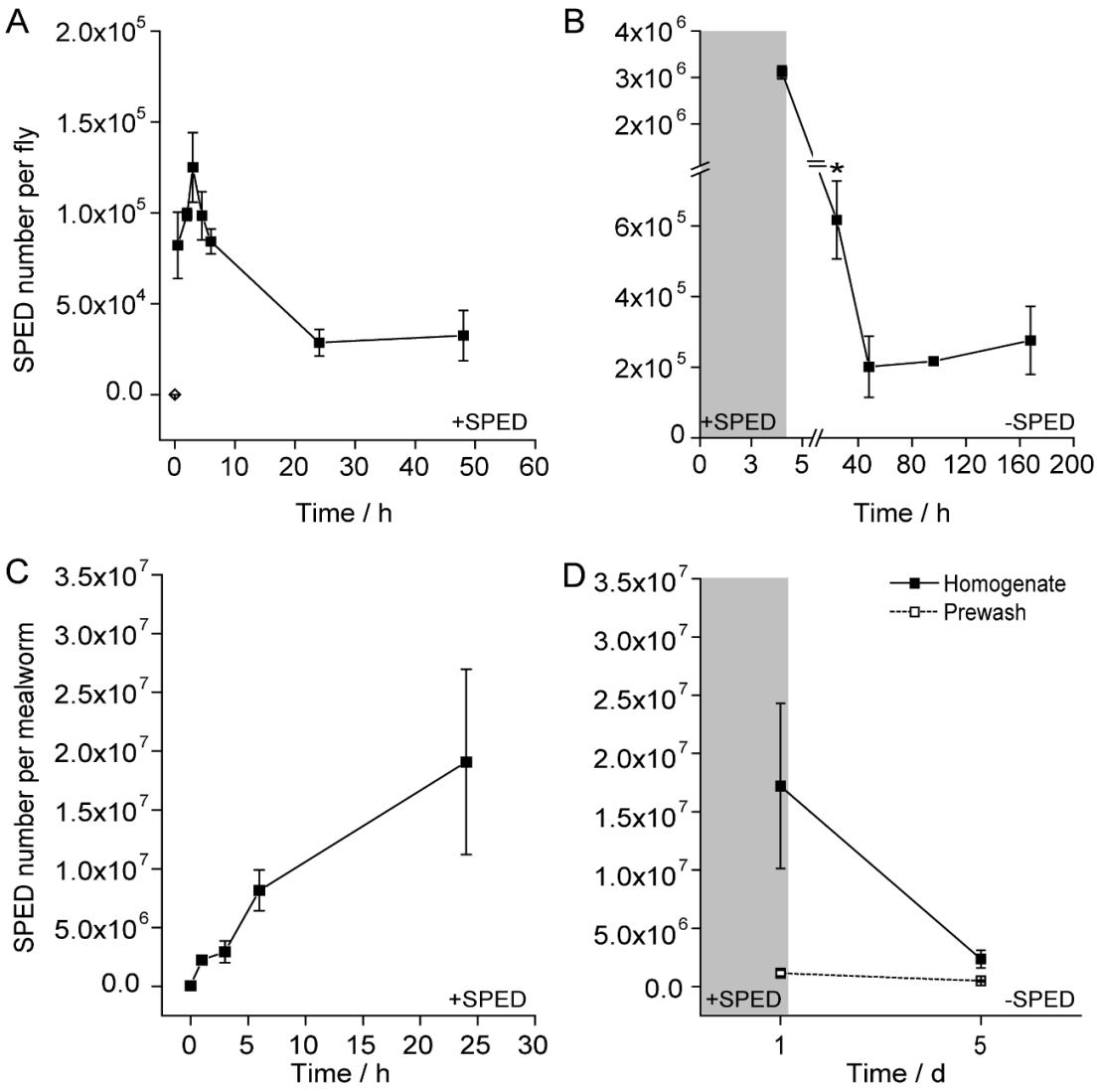

***Figure 2.3**. SPED uptake by adult D. melanogaster flies and T. molitor larvae (mealworm). **(A** and **B)** Kinetics of SPED load per fly over **(A)** the first 2 days on medium labeled with $5 \cdot 10^7$ particles per mm^2 and **(B)** on medium labeled with $7 \cdot 10^8$ particles per mm^2 and subsequent transfer to SPED free medium after t = 4 h. Flies cultivated on non-labeled medium for **(A)** is denoted by diamond shape at t = 0. There is a significant difference between the tracer load after t = 4 h and 24 h (analysis of variance, F = 8.297, *P<0.02). Average of 15 flies, ±SEMs (n = 3). **(C** and **D)** Kinetics of SPED load in T. molitor larvae over 1 day on SPED labeled medium and **(D)** after transfer to a SPED free medium after t = 1 d. The SPED load in the homogenate or in the preliminary washing step with BOE is denoted by a straight or dotted line respectively. ±SEMs (N = 5).*

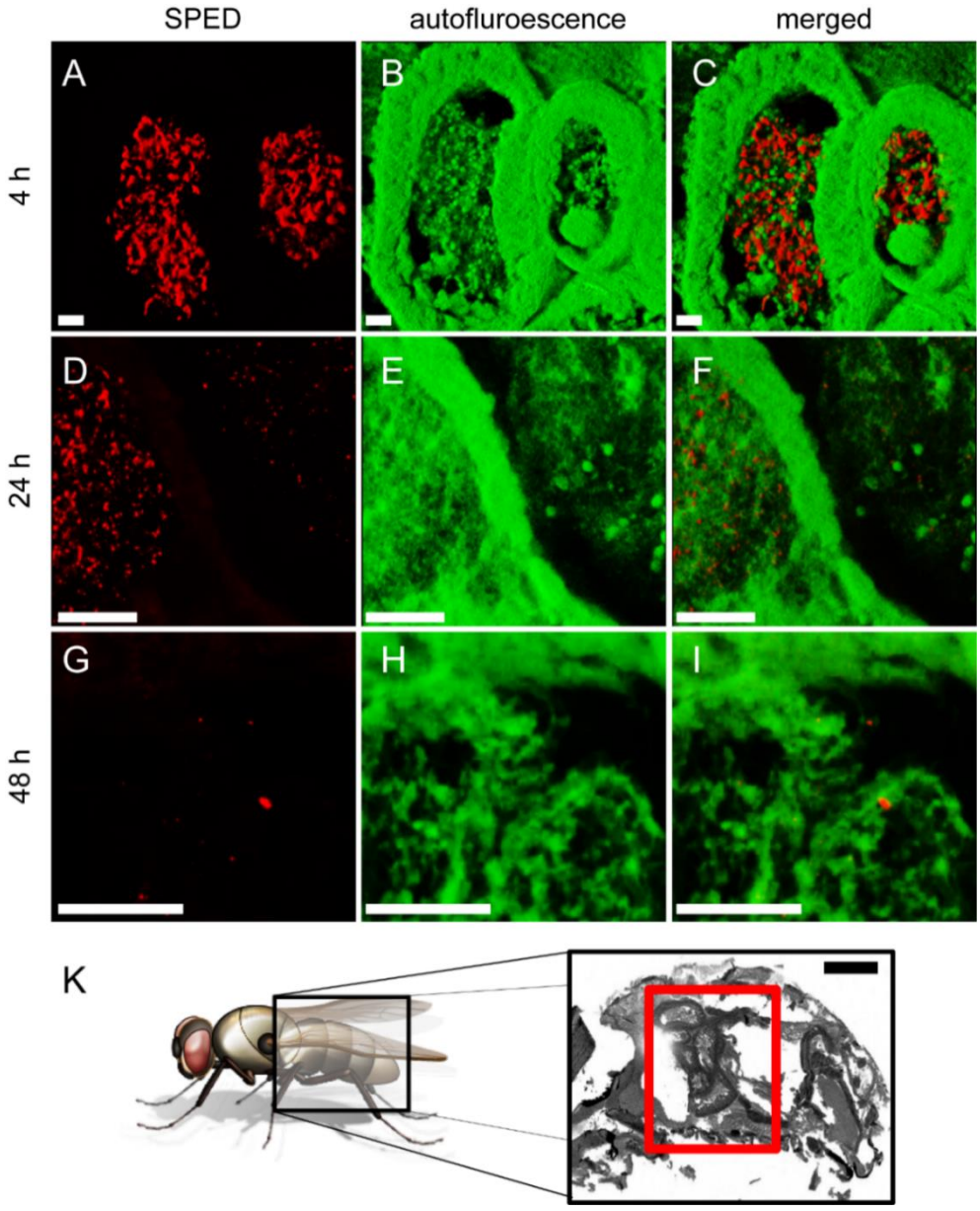

Figure 2.4. *Confocal fluorescence microscopy images of digestive tubes of D. melanogaster. Images were made after letting the flies feed for t = 4 h* ***(A – C)*** *on SPED labeled medium and after transfer to SPED free medium for* ***(D – F)*** *t = 24 h and* ***(G – I)*** *48 h. Scale bars, 20* µm. ***(K)*** *illustrates the abdominal gut region (red square) from where the microscopy images A – I was taken from. Scale bar, 250* µm.

SPED with different DNA labels were produced. The uptake efficiency from food to flies was not different for SPED1 or SPED2 respectively (**Figure A1.3,** Appendix). When SPED1 and SPED2, each containing different DNA tags, were fed to flies in the ratios 1:1, 1:5, 5:1 (SPED1:SPED2), the measured particle ratio in the flies normalized to the ratio of 1:1 after 4 hours (100 %) stayed the same over at least two days, even though the flies had been transferred to a tracer-free environment after 4 hours (**Figure 2.5**). This indicates that the

relative ratio of differently labeled food was preserved over time, although the absolute particle number decreased.

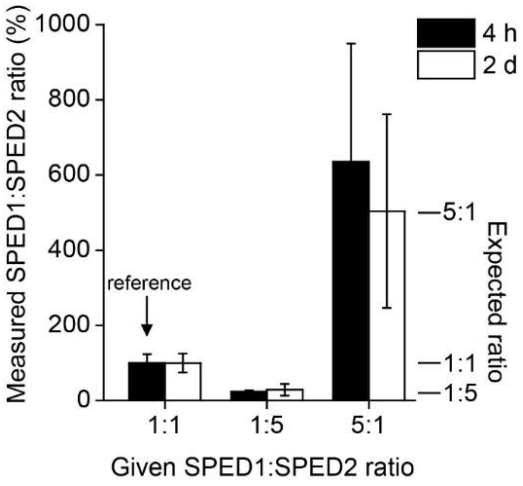

Figure 2.5. *Ratios of SPED1:SPED2 in flies after 4 hours on labeled medium with given ratios of 1:1, 1:5 and 5:1 and after 2 days on SPED-free medium. The expected ratios are given as bars on the right side of the figure. The initial ratios were normalized to the 1:1 ratio after t = 4 h (reference). Average of 5 flies. ±SEMs (n =3).*

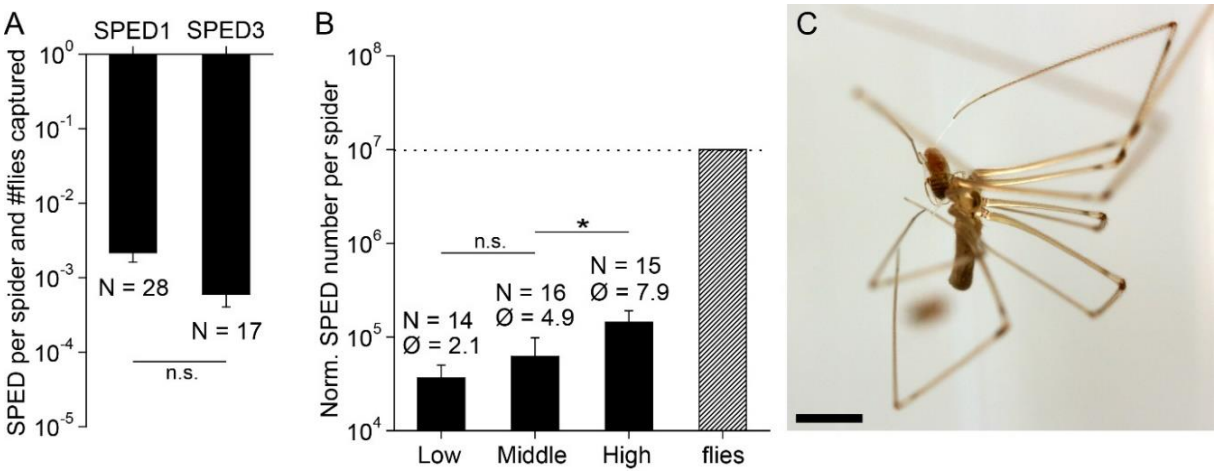

Figure 2.6. *Animal-to-animal transfer of SPED to P. phalangioides.* ***(A)*** *Transfer ratio of SPED from D. melanogaster to P. phalangioides. Data were obtained by dividing the particle load of the spiders by the initial particle load of their prey.* ***(B)*** *The SPED load per spider correlates with the number of flies captured per spider. 'Low' = 1 - 3 flies, 'Middle' = 4 – 6 flies, 'High' = 7 – 8 flies captured, 'flies' = average content of SPED in the fed flies used for normalization. There is a significant difference between the groups 'Middle' and 'High' (Kruskal-Wallis ANOVA, X^2 = 9.025, *P<0.005). Data were normalized to the average SPED load of eaten flies. 'Ø' average number of flies caught per group, n.s. no significant difference, ±SEMs.* ***(C)*** *A P. phalangioides spider eating a caught D. melanogaster fly. Scale bar, 5 mm.*

In order to test whether SPED can be transferred to another trophic level *D. melanogaster* flies previously cultured on SPED-labeled medium were fed to the polyphagous house-spider *Pholcus phalangioides* (Araneae). To estimate the efficiency of particle transfer from flies to spiders we calculated the percentage of SPED found in a spider compared to the total SPED amount in the captured flies estimated from their initial SPED content at the beginning of the experiment. After letting the spiders catch *Drosophila* flies labeled with SPED1 or SPED3 overnight, we recovered 0.2 ± 0.1 % of SPED1 and 0.06 ± 0.02 % of SPED3 in the spiders (**Figure 2.6A**). We compared the number of captured flies and the SPED amounts obtained from the spiders. The latter were normalized to the respective fly SPED load to adjust for variances between different batches of labeled flies. Spiders that caught 7 to 8 flies contained $(1.4 \pm 0.5) \cdot 10^5$ particles per spider, which was significantly more than spiders that caught 4 to 6 or 1 to 3 flies with $(6.2 \pm 3.6) \cdot 10^4$ or $(3.6 \pm 1.4) \cdot 10^4$, respectively (**Figure 2.6B**).

We chose one aspect of the pollination syndrome hypothesis,[76] the color preference of pollinators, as investigative object for an experiment under conditions resembling those in the field. Adult specimens of the green bottle fly species *Lucilia caesar* were exposed to white and red-purple color variants of the marguerite daisy *Argyranthemum frutescens* labeled with SPED1 or SPED3 respectively for four hours. We showed a significant preference for the white flower variant from qPCR analysis with thirteen out of seventeen flies containing more SPED1 than SPED3 (**Figure 2.7A**). These results were confirmed by visual analysis of the fly behavior (**Figure 2.7B**). The frequency of flies sitting on white-colored marguerite flowers peaked at 3.9 (SD = 1.3) flies per flower compared to 1.4 (SD = 0.7) flies on red-purple-colored flowers.

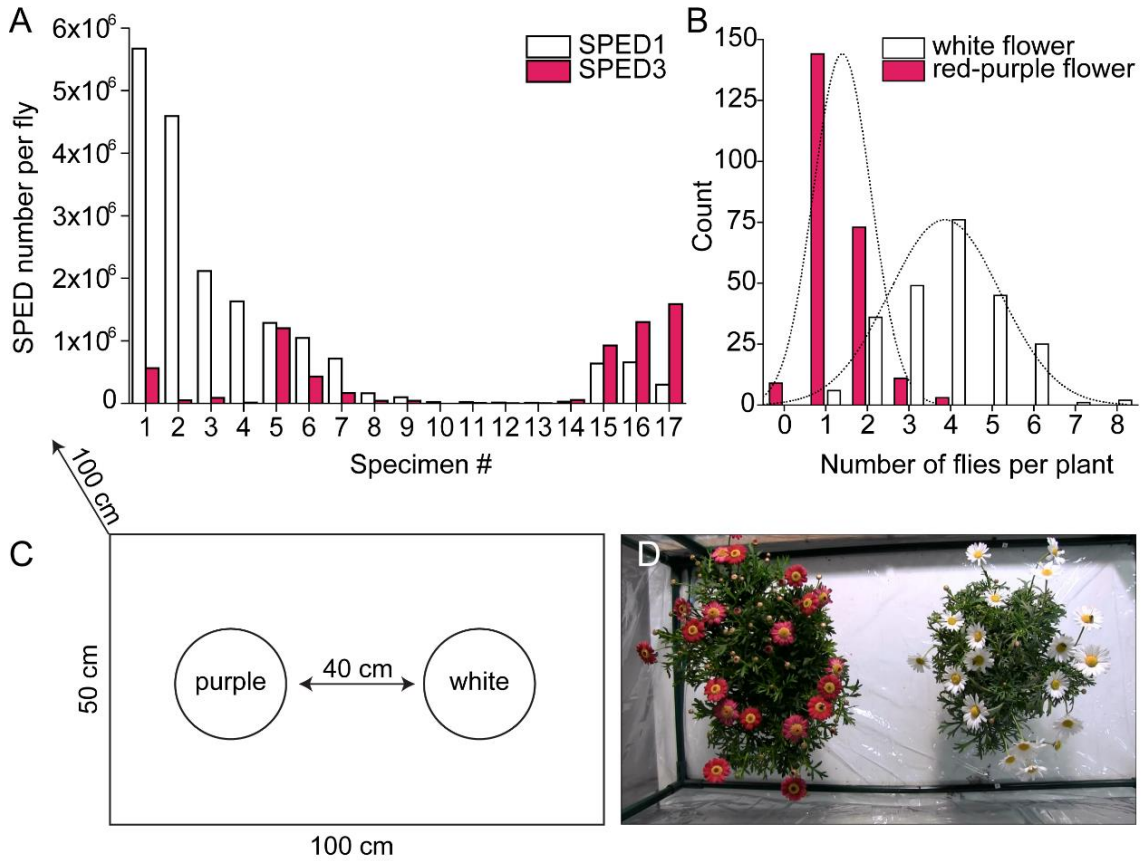

Figure 2.7. *Flower color preference of the green bottle fly* Lucilia caesar. ***(A)*** *SPED content determined by qPCR after exposure of flies (N = 17) to flower color variants of* Argyranthemum frutescens *(SPED1: white flowers; SPED3: red-purple).* ***(B)*** *Observed distributions of the number of flies present on the white or red-purple flower variant over the full duration of the experiment. The number of flies was counted by eye once every minute (Total count: 240).* ***(C)*** *Scheme and* ***(D)*** *image of the experimental setup. The plants were placed in a 50x100x100 cm plastic green house.*

2.4 Discussion

To investigate the uptake and transfer of SPED from one trophic level to another we applied the tracers to the food source of a simple arthropod food chain. As simplification we used a nutrient medium in place of a primary producer. As primary consumers, the fly *Drosophila melanogaster* and the beetle *Tenebrio molitor* were implemented. As secondary consumer we chose the spider *Pholcus phalangioides* that readily feeds on *Drosophila*. We observed that SPED were readily taken up via the oral route when offered as part of a liquid (*D. melanogaster*) or solid (*T. molitor*) nutrient medium and remained in the tested animals over several days. Differently labeled SPED in the same individual remained at a constant ratio over time and are taken up equally well by the tested animals. This was expected since the SPED differ only in the DNA sequence, but not in their surface or material properties.

After assessing the uptake of extrinsically labeled food we investigated the transfer of SPED from labeled living prey to one of their possible predators, in our case from *D. melanogaster* to the spider *P. phalangioides*. This spider species eats its prey by repeatedly regurgitating a droplet of digestive fluid from the stomach and saliva glands onto its prey (Fig 5C). After a short incubation time it sucks the droplet containing dissolved prey tissue back into the stomach.[77] The spiders took up SPED with a transfer rate of around 0.1 % compared to the total number of SPED the captured flies contained at the beginning of the experiment. Interestingly, we found that the caught flies contained up to 50 - 70 % less SPED than at the beginning of the experiment (**Figure 2.8**). Four effects could have influenced the transfer rate of SPED to *P. phalangioides*: First, *P. phalangioides* as many other spider species possesses a special filter device called the 'rostral plate', with which it is able to filter out particles larger than 1 µm.[77] Larger aggregates of SPED particles are thus filtered out. Second, spiders often only partially consume their prey after capturing and consequently not all particles are transferred. Third, the exoskeleton of the prey remains mainly intact during the feeding process. Therefore, SPED sticking to the outside of the fly's exoskeleton will presumably not be taken up. Finally, the flies had probably already lost SPED before being captured, what could have been expected when looking at the SPED uptake and loss kinetics observed for *D. melanogaster* (**Figure 2.3A, B**). Nevertheless, we observed a positive correlation between the number of flies captured and the amount of SPED extracted from the spiders. A quantitative analysis of the number of prey captured and eaten by a spider is therefore possible.

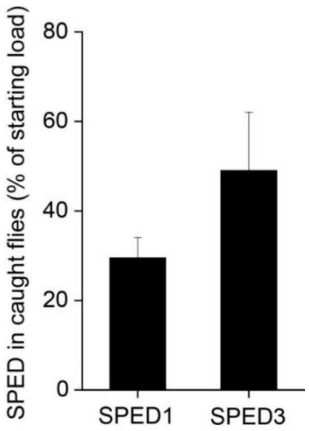

Figure 2.8. *Analysis of the proportion of SPED load remaining in flies caught by P. phalangioides compared to the SPED load of flies at the beginning of feeding. Measurements were made from single flies. ±SEMs (N = 8).*

We also applied SPED to an experimental situation typical for field research and performed a small-scale experiment in a miniature greenhouse investigating the flower color preference of pollinating flies. According to the pollination syndrome hypothesis,[76] flies rather prefer white to yellowish flower colors compared to purple and blue, the favorite colors of bees.[78] Adult green bottle flies (*Lucilia* spp.) are known to feed on nectar and pollen and are used in agricultural applications.[79] We exposed green bottle flies to red-purple and white flowers of the marguerite daisy for four hours. Since we used two types of SPED to label the differently colored flowers, we were able to quantify the preference of each individual fly to one of the two flower colors. From the SPED analysis it could be concluded that the green bottle flies indeed favored the white over the red-purple colored flowers. Visual observations of the frequency of flower visits supported these results although, unlike the SPED data, they did not provide information about the number of times each of the flies actually fed on pollen and nectar. For this analysis it would have been necessary to visually label and monitor each fly over the full experimental time length. SPED thus also offer the possibility to quantitatively analyze complex ecological mechanisms such as insect-mediated pollination and are applicable in an experiment typical for field research.

In the present study we have shown that SPED are useful ecological tools and allow an accurate and quantitative determination of various prey sources in parallel. So far, a limitation shared by all methods of diet analysis such as DNA barcoding has been the ability to accurately quantify different food sources in the diet of an animal, mostly due to biases occurring during the extraction, amplification and sequencing procedure.[57] Since SPED are inert particles, they can be efficiently extracted from homogenized tissue and concentrated by centrifugation, which additionally improves their limit of detection. The DNA labels of SPED can be selected to have similar amplification properties ensuring an optimal qPCR analysis and sequencing is not necessary when doing qPCR. SPED are therefore able to circumvent most of the biases usually

occurring in quantitative diet analysis. Since SPED are non-degradable under standard biological conditions and remain in the digestive organs of an animal over a prolonged time period they can be followed over several trophic levels similar to stable isotopes. In contrast to SPED, food-derived DNA is less stable, as was shown e.g. in the study of Hohlweg and Doerfler (2001) with gene fragments from plant leaves fed to mice, which could be only recovered up to 49 hours from the intestine by PCR amplification.[80] Additionally, SPED also include other information than simply the exact spatial and temporal entry point of food web tracers. When compared to other extrinsic tracers such as isotopes or fluorescent labels, SPED are highly variable and flexibly applicable: (i) The DNA label can be easily varied to produce an enormous number of differently labeled SPED which do not interfere with each other and allow the same system to be studied in multiple ways by applying differently-labeled SPED. (ii) The physical properties (e.g. size) can be adjusted when necessary, e.g. to label microorganisms. (iii) The silica surface of SPED is amenable to various chemical modifications that permit adaptation to special environments such as aquatic- or microenvironments.[81] Additionally, the extraction of SPED and quantitative analysis of its DNA label requires only standard laboratory equipment such as a homogenizer and a qPCR thermocycler that is available in most laboratories working in a bio-molecular research field.

It remains to be shown how SPED perform in large-scale field experiments. Based on their huge variability, accurate traceability and physico-chemical properties, it is possible to flexibly adapt SPED to a huge spectrum of field applications, e.g. to investigate the impact of human-caused environmental changes on ecosystems. Overall, SPED represent an efficient ecological tool for performing accurate quantitative research, which complements the methodological resources for food web analysis.

3. Ultrasensitive quantification of pesticide contamination and drift using silica particles with encapsulated DNA

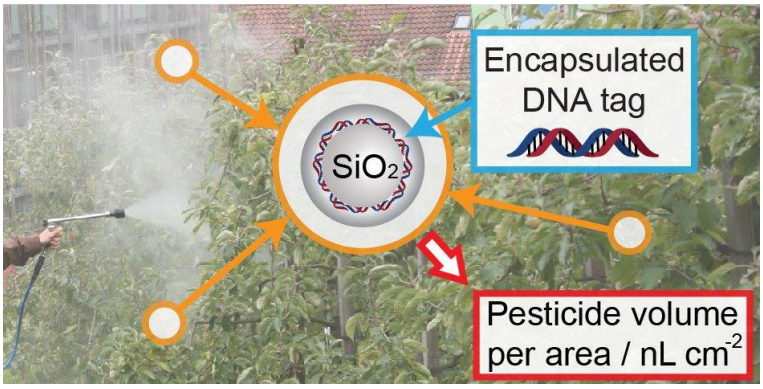

Published in parts as:

Carlos A. Mora, Hans-Jakob Schärer, Thomas Oberhänsli, Mathias Ludwig, Robert Stettler, Philipp R. Stoessel, Robert N. Grass, Wendelin J. Stark,

Environmental Science & Technology Letters **2016**, 3, 19–23.

3.1 Introduction

Pesticides are applied in large quantities (~2.5 million tons) worldwide.[82] Besides undeniable benefits,[83] some pesticides also pose risks to human health and to the environment.[84, 85] For some agricultural practices, contamination with certain pesticides needs to be reduced or completely avoided. One prominent example is organic farming that does not rely on synthetic pesticides.[86] As a consequence, there is a need to develop tools that are able to universally quantify trace amounts of pesticides that allow the evaluation of contamination, drift, and persistence on non-treated areas or in the environment.

Methods for quantifying pesticides are based on either analytical chemistry or tagging techniques. Analytical methods for pesticide analysis include gas chromatography-mass spectrometry (GC-MS),[87, 88] liquid chromatography-MS,[89, 90] single particle aerosol-MS,[91] and diverse biosensor assays.[92, 93] For tagging, fluorescent tracers such as uranine, pyranine or tinopal CBS-X have been employed.[94-96]

Reported lowest limits of detection (LLOD) for GC- or LC- coupled MS methods are in the range of 0.1 – 500 ppb (micrograms per liter).[88-90] Mass spectrometry analysis allows direct identification and analysis of a target compound. However, disadvantages include compound-dependent sampling methods, tedious sample preparation, and complicated and expensive equipment that limits the number of experimental samples. Fluorescent tracers can be detected down to 1 – 200 ppt (ng L^{-1}) in pure water under optimal analytical conditions.[97, 98] They are attractive in terms of cost and simplicity of analysis; however, accurate quantification can be achieved only in a limited linear concentration range, and multiplexing or reproduction of an experiment at the same location can only be done with another fluorophore that has other excitation and emission spectra and different chemical properties. Additionally, matrix effects, e.g., naturally fluorescing chemicals and/or pesticides or natural organic matter from the sampling site, can significantly increase the LLOD.[98] It has been shown that large amounts of a fluorescent tracer [2.0 - 2.5 % (w/v)] are required for the extraction of such a tracer from soil surfaces.[94]

Compared to analytical chemistry methods, tagging techniques are cheaper and easier to implement when it comes to assessing pesticide drift and deposition. To overcome the mentioned deficits of fluorescent tracers, we applied the recently developed silica particles with encapsulated DNA (SPED) as a tagging agent.[41, 42] SPED consist of short deoxyribonucleic acid

(DNA) oligomers having a length of ~100 base pairs that are incorporated into a chemically inert spherical silica matrix and are thus protected from degradation even under irradiation and harsh radical or heat treatments (**Figure 3.1A**). Particle sizes are usually between 100 and 250 nm. Under suitable chemical conditions, the DNA label can be selectively released from the silica and amplified with matching primers and probes using real-time polymerase chain reaction (qPCR), a widely used and ultra-sensitive technique for DNA analysis (**Figure 3.1B**).[72]

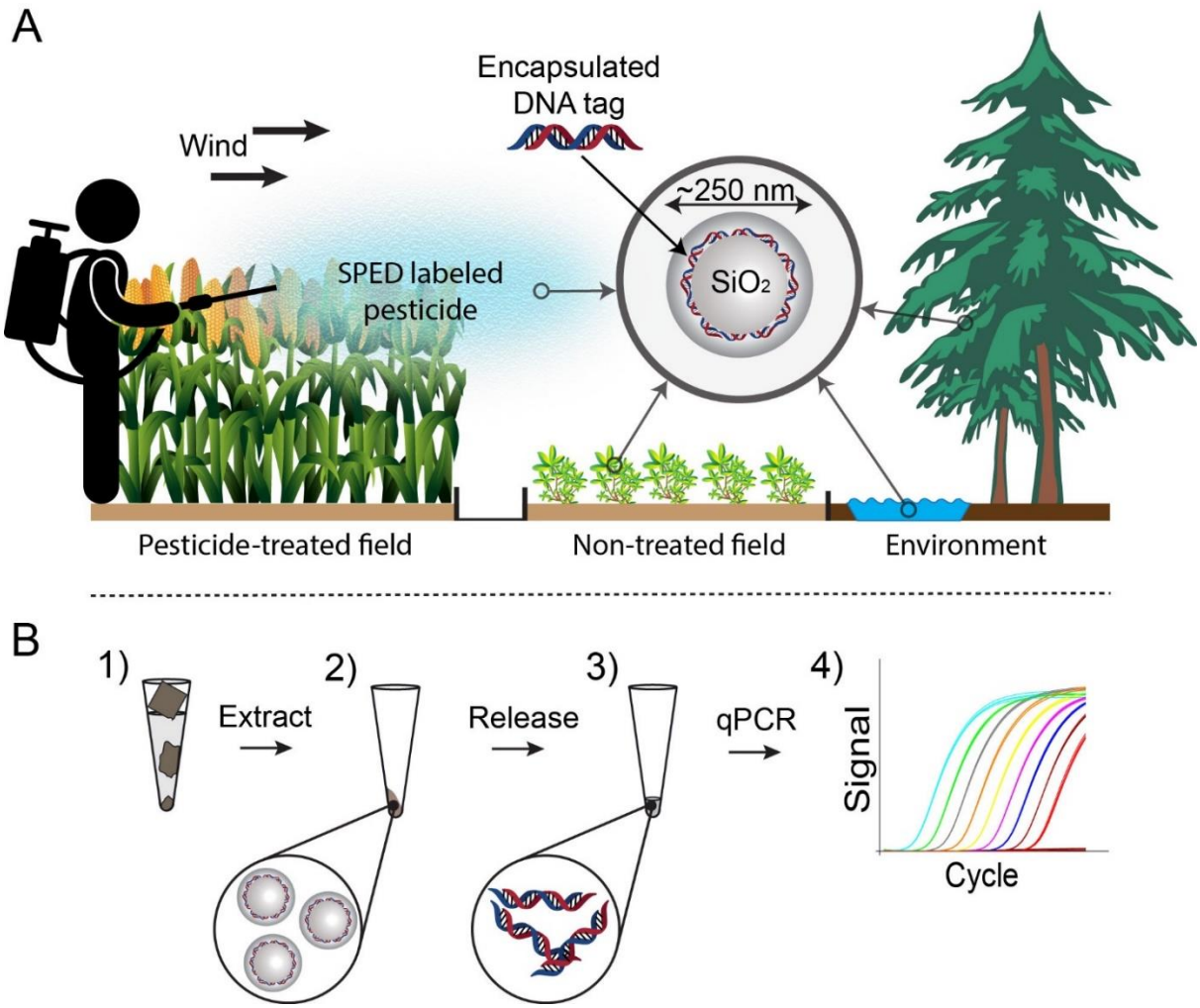

Figure 3.1. *Pesticide tracing with silica particles with encapsulated DNA (SPED). (A) A SPED-labeled pesticide is sprayed over the field and can be sampled from other treated or non-treated fields, from the air and in the environment. SPED contain DNA as tracer tag and have a size of ~250 nm. (B) Sample preparation and quantification of SPED. (1) Samples from the environment are collected and processed if necessary (e.g., by temperature or ultrasound treatments). (2) SPED are upconcentrated by centrifugation and (3) dissolved in buffered oxide etch to release the DNA tag. (4) Quantification of the DNA tag is achieved by quantitative PCR.*

Silica nano- and microcolloids are considered non-toxic and are applied in different industries such as the metal, paper, and food industry (E551) as binders, desiccants, fillers and anti-caking agents.[73-75] Most recent applications of SPED include tracing of ecological networks,[99] food labeling,[44] labeling of wastewater and activated sludge,[43] oil products,[46] and cellular particle uptake analysis.[100] Under optimal conditions, SPED have a LLOD of 1 ppt (i.e.,~ 1 ng of SPED per liter)[101] and LLODs in the sub-parts per billion range upon their extraction from environmental samples.[43, 44]

In this study, we applied SPED for the first time as a pesticide tagging agent, which allowed us to accurately trace and quantify drift and deposition of pesticides in the environment (**Figure 3.1**). For this purpose, we assessed the stability, storage, and recovery of SPED in aqueous suspensions of widely used organic and inorganic pesticides. In field applications, we sprayed a SPED-labeled test liquid in an obstacle-free field setting and in an apple orchard to evaluate the feasibility of using SPED to quantify the amount of sprayed pesticides at different distances and heights. Following extraction of SPED from field samplers, the specific DNA code therein was quantified via quantitative polymerase chain reaction (qPCR) and correlated to the volume of labeled test liquid. Thereby it was possible to visualize the distribution of test liquid in the field. The aim of the experiments was to demonstrate the ability of SPED to serve as a generally applicable, highly versatile, and ultra-sensitive tagging agent for pesticides.

3.2 Experimental

3.2.1 SPED synthesis and characterization

SPED were synthesized and characterized according to the method of Paunescu et al.[42] 50 mg silica particles (sicastar®-redF, 100 nm, Micromod Partikeltechnologie GmbH, Germany) in 1 mL ethanol were functionalized with 10 µL *N*-trimethoxylsilylpropyl-*N,N,N*-trimethylammonium chloride (TMAPS; 50% in MeOH, ABCR GmBH) overnight. For a single batch reaction, 70 µL (=3.5 mg) of TMAPS-functionalized SiO_2 particles were mixed with 1 mL dH_2O and 20 µL of respective pre-annealed double stranded DNA (25 µM, Microsynth AG, Switzerland).[42] To enhance environmental compatibility, we used DNA tags that were derived from the genome of loblolly pine (*Pinus taeda*) from a genome region with no biological function. The DNA sequence was taken from *Pinus taeda* genome (accession no. AC241282.1, bases 59074-59193, length: 120 bases): (forward strand) 5'-TCCCCTTCCTTTGATTCCTTTTGTGATTCTTTAATAAGAGAACAAGAAAAACTCTT ACACCTTAGTCTTCTTAATCTTGGAAACTCGTCTAAGAAAGCCTTAACTGCCCAAC AACAACCA-3', (reverse strand) 5'-TGGTTGTTGTTGGGCAGTTAAGGCTTT CTTAGACGAGTTTCCAAGATTAAGAAGACTAAGGTGTAAGAGTTTTTCTTGTTCTC TTATTAAAGAATCACAAAAGGAATCAAAGGAAGGGGA-3'. To remove excess DNA molecules, the particles were washed 3x with dH_2O (21'500 g, 2 min) and re-suspended in 0.5 mL dH_2O. After stirring with 1.2 µL TMAPS and 1.2 µL tetraethyl orthosilicate (TEOS, ≥ 99 %, Sigma-Aldrich) for 4 hours at room temperature, additional 8 µL TEOS were added and the mixture stirred for 4 days at RT (1000 rpm, Thermomixer, Eppendorf). In total, 10 SPED batches were produced. Nanoparticle size distribution was determined by sedimentation analysis of a SPED dispersion in dH_2O with a concentration of 1 mg/mL at 3000 rpm for 400 x 10s (LUMisizer, LUM GmbH). A density of 2200 kg m^{-3} and a refractive index of 1.458 was assumed for SPED. The particle concentration was determined by dry mass measurement of the particles. For that, 100 µL of the final particle suspension was transferred to a pre-weighed Eppendorf tube, and then vacuum-dried at 30 °C for 12 hrs (Concentrator plus, Eppendorf). The particle DNA load was determined by fluorometric quantitation (Qubit, dsDNA HS assay, Life Technologies Corp.) after dissolving a known amount of particles in buffered oxide etch (BOE) containing 2.3 wt% ammonium hydrogen difluoride (NH_4FHF, pure, Merck) and 1.9 wt% ammonium fluoride (NH_4F, puriss., Sigma-Aldrich) in dH_2O. The SPED had an average hydrodynamic diameter of 266 ± 68 nm when dispersed in water (**Figure 3.2**) and a DNA load of 6.5 ± 0.4 µg of dsDNA per mg of particles.

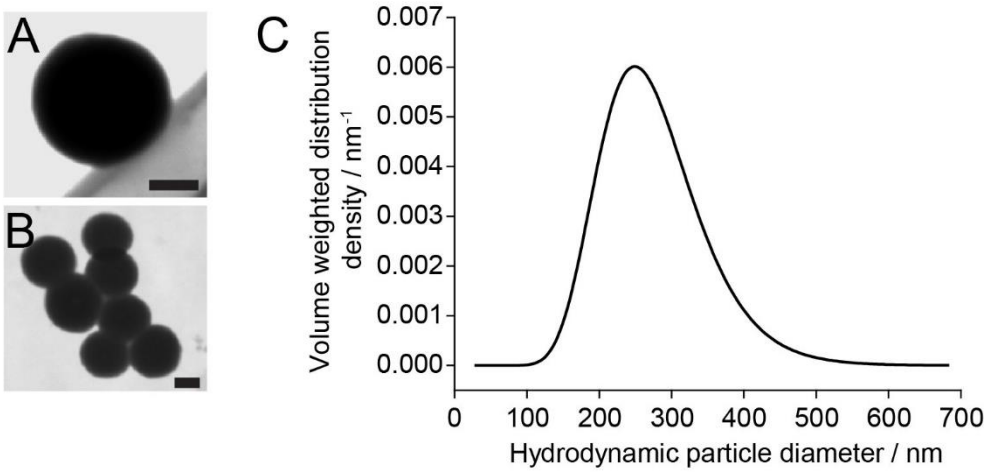

Figure 3.2*. SPED characterization. (A), (B) Scanning transmission elelectron microscopy (STEM) images of SPED, scale bar = 50 nm (C) Average particle size distribution of SPED particles (log-normal, mean ± standard deviation = 266 ± 68 nm) in water was measured by sedimentation analysis.*

3.2.2 Stability and storage in pesticides

Different pesticide solutions and/or suspensions of the pesticides pyrethrine, glyphosate, $Cu(OH)_2$, and sulfur were prepared in dH_2O according to the manufacturer's specifications (see **Table 3.1** for more information). SPED (50 µg, 5 ppm) were added to 10 mL of prepared aqueous pesticide solutions and/or suspensions and to 10 mL of dH_2O as a recovery control. Samples were analyzed after 0, 1, 2, 7, 21, and 76 days. A sample of 0.1 mL was taken and centrifuged at 21'500 g for 5 min. The samples from organic pesticide suspensions were washed 2x with 1 mL dH_2O. Since copper and sulfur ions would inhibit qPCR, they had to be removed from samples of pesticide suspensions containing these ions. Copper containing samples were washed 1x with 1 mL ammonium hydroxide (25% aq., NH_4OH, Sigma Aldrich). Sulfur containing samples were washed 1x with 1 mL ethanol (>99.8%, Fluka) and 1x with 1 mL of a 4:1 mixture of toluol (>99.7%, Fluka) and ethanol. The samples were then washed 2x with 1 mL dH_2O. The resulting pellet was vacuum-dried at 30 °C for 12 h (Concentrator plus, Eppendorf).

3.2.3 SPED-labeled test liquid

A SPED-labeled test liquid was prepared for all further experiments by dispersing 28.8 mg of SPED in 5 L of tap H_2O, resulting in a concentration of 5.8 ppm (milligrams per liter) SPED.

***Table 3.1**. Pesticides used for storage and recovery experiments of SPED.*

Name	Company	Contents (product label)	Type	w/v% final conc. in dH_2O (pH)
Bio Schädlingsfrei AF	Bayer	pyrethrine (0.05 g/L), rape oil (8.25 g/L)	insecticide	ready to use (7)
Microperl	Burri Agricide	61.45% $CuOH_2$, 7% aromatic sulfonate polymer, 19% SiO_2	fungicide	1% (9)
Netzschwefel	Andermatt Biocontrol	80% sulfur, 20% aromatic sulfonate and SiO_2	fungicide	2% (7)
Roundup LB Plus	Monsanto	41.5% glyphosate isopropylamine, 16% surfactant, 42.5% H_2O	herbicide	10% (5)
Negative control	-	dH_2O	-	- (7)

3.2.4 Sampling methods

Two different kinds of droplet samplers were employed: Petri dishes (16 mm x 137 mm, Greiner Bio-One) for horizontal ground sampling at h = 0 m and gauze samplers for vertical sampling at heights of 1.0 and 1.8 m.[96] For the gauze samplers 10 cm x 10 cm gauze (double-layered, 1 mm x 1 mm mesh size, cellulose, Flawa) was unfolded and attached to a 1 cm thick segment of a plastic tube with a 10 cm diameter using cable fixer. To assess optimal recovery from both sampler types, volumes of 10, 100, and 1000 µL of the SPED-labeled test liquid were applied in a lab-scale experiment onto either gauze samplers, Petri dish samplers, or directly to Eppendorf tubes. The latter served as a recovery reference. SPED from samplers were extracted and quantified by qPCR**.** Gauze sampler: The gauze was removed from the plastic frame and transferred to a 50 mL Falcon type plastic tube. 20 mL of an aqueous 1 w/v% sodium dodecyl sulfate (SDS) solution was added. The gauze was washed well in the solution by shaking (300 rpm, 10 min, Unimax 2010, Heidolph) and was then removed from the tube and squeezed carefully to retain most of the liquid. Petri dish sampler: 5 mL of an aqueous 1 w/v% sodium dodecyl sulfate (SDS) solution was added and the dish inner surface was washed several times by pipetting up and down. The washing solution was then transferred to a 15 mL plastic tube and centrifuged at 11'000 g for 15 min. The pellets containing the SPED were then transferred to a 2 mL tube, washed 2x with 1 mL ultra-pure water (21'500 g, 3 min) and finally vacuum-dried at 30 °C for 1 h (Concentrator plus, Eppendorf). For recovery experiments from samplers, a reference amount of SPED-labeled test liquid was directly centrifuged in an Eppendorf tube and vacuum-dried without further washings. The obtained SPED pellet was subsequently

dissolved in 50 µL buffered oxide etch (BOE, 2.3 wt% NH_4FHF, 1.9 wt% NH_4F in dH_2O) and diluted 1:100 in ultra-pure water for qPCR analysis.

3.2.5 TaqMan qPCR and standard curves

A single TaqMan quantitative real-time PCR reaction had a total volume of 12.5 µL and contained 6.25 µl probe master mix (2x TaqMan Universal PCR Master Mix, Life Technologies), 450 nM (final concentration) of each forward and reverse primer, 125 nM TaqMan probe, 1.5 mM $MgCl_2$, 2.5 µl sample, filled up to 12.5 µl with ultra-pure water. The following DNA oligomers were used (Microsynth AG, Switzerland): Forward primer: 5'-CCTTCCTTTGATTCCTTTTGTGATTC-3', Reverse primer: 5'-TGGTTGTTGTTGGGCAG TTAAG-3', Taqman probe: 5'-FAM-TAGTCTTCTTAATCTTGGAAACTCGTCT-BHQ1-3'. For all qPCR reactions we used the following reaction conditions: 1) pre-incubation 50 °C, 2 min, 2) 95 °C, 10 min; 3) denaturation 95 °C, 15 s; 4) annealing and amplification 58 °C, 60 s. Steps 3) and 4) were repeated in 50 cycles. To deduce the amount of SPED-labeled test liquid from qPCR data a standard curve was established (**Figure A.2.1**, Appendix). Standard curves for TaqMan qPCR were prepared by using 100, 10, 1, and 0.1 µl, respectively, of an aqueous pesticide surrogate suspension containing 5.8 ppm SPED.

3.2.6 Field experiments

The experimental site was situated in Frick, Switzerland (geographical coordinates 47°31'03.5"N 8°01'34.7"E). For both field experiments a Yamaho-nozzle handheld sprayer (WJR2525, Honda) with a Yamaho 20-10 nozzle was used. After the field experiments, the samplers were let dry for 30 min. Afterwards they were carefully collected and stored separately in sealed plastic bags until further processing.

Obstacle-free field experiment

In an obstacle-free meadow, gauze samplers were attached to wooden poles 3, 9, and 15 m from to the point of application at heights of 1.0 and 1.8 m height. Petri dish samplers were positioned 3, 9, and 15 m in front of the poles on the ground. The sprayer and samplers were aligned to wind direction, and the SPED-labeled test liquid was sprayed at a constant rate. 2.9 L SPED-labeled test liquid were sprayed at a spray flow rate of 2.0 L min^{-1} in wind direction. The spraying height was ~ 1 m above ground. The average wind velocity was 1.7 m s^{-1} (AN200, Extech Instruments).

Field experiment in apple orchard

The apple orchard had an area of 25 m x 17.5 m and was divided into 24 equally sized plots distributed in an 8 x 3 matrix. Each plot contained five apple trees planted in row. The average apple tree height was ~ 2 m. Spray drift was evaluated in all directions up to a distance of 13 m and at three different heights. A total of 76 samplers were symmetrically distributed over the whole field as follows: 20 vertical gauze samplers attached to apple trees at a height of 1.0 m height and 26 samplers at a height of 1.8 m facing toward the application site. Thirty horizontal petri dish samplers were positioned on the ground 50 cm in front of the tree lines facing towards the application site. SPED-labeled test liquid was sprayed on one single plot in the orchard center. This plot was sprayed from all sides by walking continuously around it in t = 57 s with 1.9 L surrogate suspension at a spraying height between 1.0 – 1.8 m, a spraying angle of 60-130° compared to a vertical axis, a nozzle distance of 30 cm from the plants, and a spray flow rate of 2.0 L min^{-1}. The average wind velocity was 1.6 m s^{-1} with a downwind direction of ~240°.

3.2.7 Contour plots

3D coordinates (x, y, z) in distance to the point of origin (x = 0 m, y = 0 m, z = 0 m) were assigned to each sampler measurement according to their position in the field. To generate contour plots that optimally visualize the measured pesticide load per area, the cycle of threshold values obtained by qPCR were converted to their reciprocal values. For each height (z = 0m, 1m and 1.8 m) a rainbow-colored 2D contour plot was then created using OriginPro 9.1.0 (OriginLab Coorporation). A lowest threshold was set according to the determined LLOQ of around 1 nL cm^{-2} (an average of the LLOQ of 1.3 nL cm^{-2} for gauze samplers and 0.7 nL cm^{-2} for petri dish samplers). In order to determine the longitudinal pesticide distribution at different sampling heights (**Figure A.2.2**, Apppendix), grayscale (black to white gradient) 2D contour plots were generated with the same datasets as for the colored 2D contour plots. The longitudinal plot profile along the plot y-axis was determined using the 'Plot profile' function of ImageJ 1.49u.[102]

3.2.8 Calculation of the potential number of SPED DNA labels

The encapsulated DNA oligonucleotide tag with a sequence length of about 100 nucleotides is detected and quantified by TaqMan qPCR. Three sequence sections confer specificity: The (1) forward and (2) reverse primer sequences and the (3) TaqMan probe sequence. Each section has an average length of 20 nucleotides. All three specific sequence sections together have a

sequence length of 60 nucleotides. For each position in the sequence, one of four different nucleotides (adenine, cytosine, guanine and thymine) can be used and the sequence can only be 'read' in one direction (5'->3'). The number of different possible combinations is thus $4^{60} \approx 1 \cdot 10^{36}$ (short scale: one undecillion).

3.2.9 Replicability and statistical analysis

Storage and recovery experiments as well as qPCR standard curve were performed in independent triplicates. All qPCR reactions were additionally conducted in technical duplicates. Statistical tests were performed using one-way analysis-of-variance (Origin 9.1.0, OriginLab Coorperation).

3.3 Results and Discussion

The stability and storage of SPED in solutions and/or suspensions of different commercially available organic (glyphosate, and pyrethrine) and inorganic pesticides (copper hydroxide, and sulfur) were tested over more than 10 weeks (**Figure 3.3**, and **Table 3.1**). SPED remained stable over the course of 76 days and could be recovered without loss in comparison to storage in deionized water, except for $Cu(OH)_2$, for which only ~10 % SPED could be recovered after 21 and 76 days. The lower long-term stability may be due to the elevated alkalinity of the aqueous $Cu(OH)_2$ suspension (pH 9) that is known to increase the degree of dissolution of amorphous silica,[103] but this remains to be further investigated. Different strategies could be applied to make SPED more stable for the long term in alkaline (or acidic) solutions, e.g., coating with polyethylene glycol.[104] Because the stability and recovery of SPED from different types of pesticides or pure water were reasonably similar, and we wanted to show the general applicability of our method, we used a SPED-labeled test liquid containing 5.8 ppm (milligrams per liter) SPED in water for all further experiments. At such a low concentration, the presence of SPED does not significantly alter the physico-chemical properties (e.g., viscosity, and droplet contact angle) of the fluid in which they are suspended.[105, 106] Thus, the tag does not influence the properties of the material to be tagged, which is one of the prerequisites of an ideal tagging agent.

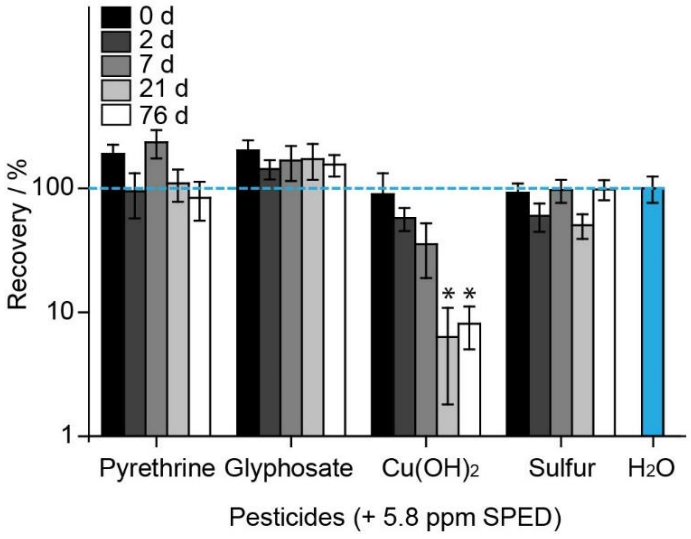

Figure 3.3. *Storage and recovery of SPED from pesticide suspensions. SPED were added to various organic and inorganic pesticides at a concentration of 5 ppm. Data show the stability over time and normalized recovery of SPED from water. The principal pesticide components are indicated. For more information about the used pesticides, see Table 1. *P<0.05, one-way analysis of variance (ANOVA), compared to t = 0 days (n = 3).*

On the basis of a qPCR standard curve (**Figure A.2.1**, Appendix), a lower limit of quantification (LLOQ) of 0.1 µL of SPED-labeled test liquid was determined corresponding to 1.3 nL cm^{-2} for gauze samplers and 0.7 nL cm^{-2} for Petri dish samplers. The performance of the employed droplet samplers was investigated in a lab-scale experiment prior to field tests (**Figure 3.4**). Around 85 – 91 % of SPED could be recovered from both sampler types upon application of a load of 1000 µL of a SPED-labeled suspension per sampler corresponding to 7 µL cm^{-2} for Petri dish samplers and 13 µL cm^{-2} for gauze samplers. Recovery from Petri dish samplers remained similar for loadings of 100 and 10 µL, whereas recovery from gauze samplers dropped to 33 ± 11 and 23 ± 9 % for 100 and 10 µL loadings, respectively. Because of the high surface per area ratio, gauze is an excellent absorptive material which is necessary to efficiently catch airborne droplets but makes it more difficult to wash off small amounts of SPED. Data from gauze samplers thus probably underestimate the actual amount of labeled test liquid for low sampler loadings, but because field results ranged over 3 – 5 orders of magnitude, this did not impair the interpretation of data in our experiments. The choice of samplers is also not restricted to those used in this proof-of-principle study, and SPED recovery may be enhanced even by using other sampling types (e.g., gel-coated plates, and air sampling devices) or by using magnetic SPED that have been successfully employed in a previous study.[46]

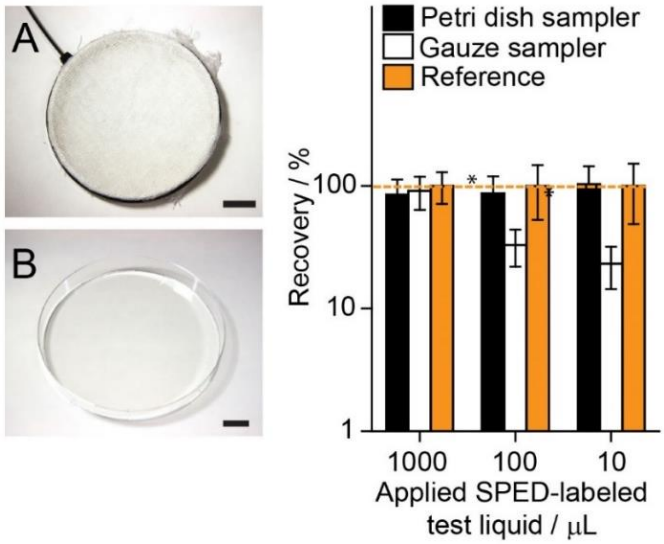

***Figure 3.4**. Field samplers and SPED recovery. (A) Gauze sampler: Vertical hanging sampler covered by a double-layer of cellulose gauze, Ø 10 cm, scale bar = 2 cm. (D) Petri dish sampler: Horizontal ground sampler, Ø 13.7 cm, scale bar = 2 cm. (C) Recovery of SPED from petri dish samplers and gauze samplers for different pesticide surrogate loadings (5.8 ppm SPED) normalized to the actual reference amount of SPED in the same volume. *P<0.05, one-way ANOVA, compared to reference, n = 3.*

In an obstacle-free field trial we assessed the drift of SPED-labeled test liquid when directly sprayed in wind direction (**Figure 3.5A, B**). The volume per area decreased from 160 µL cm^{-2} in 3 m distance down to 5 µL cm^{-2} in 15 m distance at 1.8 m height (vertically) and from 101 µL cm^{-2} in 6 m to 0.6 µL cm^{-2} in 15 m distance on ground level (horizontally). With no obstacles in the way, sprayed droplets were carried by the wind, i.e. by advective forces, over larger distances without falling to the ground which could explain the lower amounts found on the ground compared to 1.0 – 1.8 m height.

A field trial with obstacles was performed by applying the SPED-labeled test liquid onto apple trees in an apple orchard (**Figure 3.5C, D**). By displaying the measured amounts of the SPED-labeled test liquid from each sampler as contour plots over the whole field, we revealed a clear drift in the dependence of the wind direction. Overall, the measured amount of SPED-labeled test liquid was on the same order of magnitude as the volume of liquid sprayed on the apple orchard (**Figure A.2.3**, Appendix). Ground deposition measured by horizontal samplers at h = 0.0 m was relatively high (up to 52 µL cm^{-2}) on the downwind side of the central plot and rapidly decreased after one plant tree row. At heights of 1.0 and 1.8 m, the amount of test liquid volume per vertical area decreased slower than horizontally on the ground with increasing distance from the application site and traces of test liquid could be detected up to four tree rows (13 m) away (5 and 4 nL cm^{-2}, respectively), see also **Figure A.2.2**, Appendix. The observed difference between horizontal ground deposition and vertical deposition at 1.0 and 1.8 m can be explained by the fact that, in contrast to the obstacle-free field experiment, the ~ 2 m high apple tree rows were standing almost perpendicular to the wind direction and created a relatively wind-free zone close to the ground between the rows. This impeded drift and increased ground deposition of off-target droplets, i.e., droplets that do not end up on the intended plant surface. Only off-target droplets that were sprayed high enough to be able to enter the wind stream were transported over the next rows. There may be other mechanisms involved, but their investigation goes beyond the scope of this study. However, we can conclude, that SPED are a suitable tagging agent for uncovering the distribution of sprayed liquids down to 1 nL cm^{-2} in the field and for investigating their drift behavior in different experimental setups.

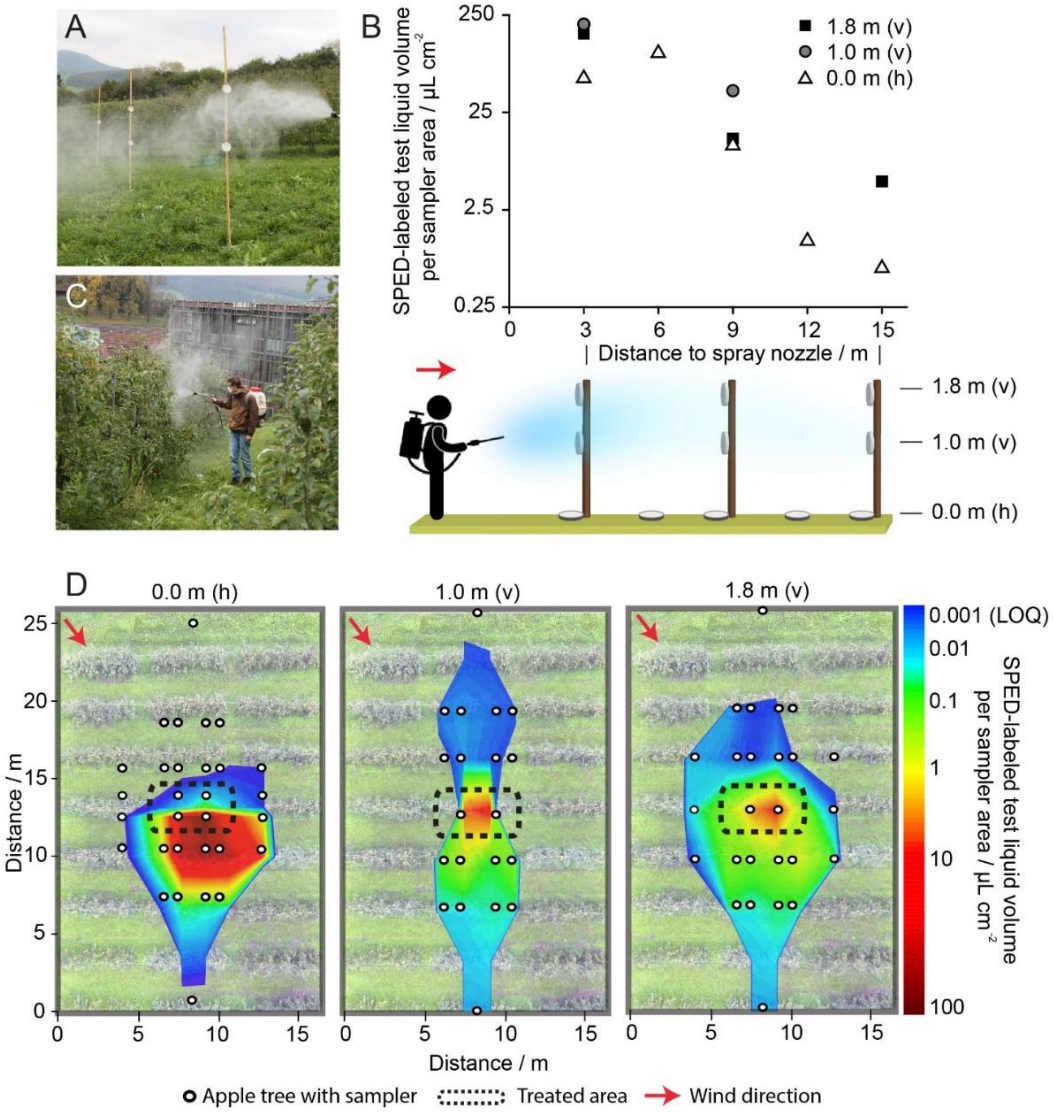

***Figure 3.5**. Analysis of the drift of the SPED-labeled test liquid when sprayed in an obstacle-free field setup (A and B) and in an apple orchard (C and D). (A) Vertically (v) hanging gauze samplers (Ø10.0 cm) were attached to a wooden pole at heights of 1.0 and 1.8 m. Horizontal (h) Petri dish samplers (Ø13.7 cm) were positioned on the ground. (B) The diagram shows the logarithmized amounts of pesticide volume per area for different distances and heights. The scheme below illustrates the setup of the obstacle-free field experiment. (C) In an apple orchard, the SPED-labeled test liquid was applied to a central sample plot. (D) Contour plots of pesticide distribution at three different sampling heights underlaid by a bird's eye view image of the apple orchard. The contour plots show the color-coded volume of the SPED-labeled test liquid per area interpolated between different sampling sites. At a height of 0.0 m (left image), 30 horizontal (h) Petri dish samplers, at a height of 1 m, 20 vertical (v) gauze samplers, and at a height of 1.8 m, 26 vertical gauze samplers were employed. Sampler positions in the field are indicated by filled circles. The treated area is framed by a dashed box. The wind direction is indicated by a red arrow.*

Because the actual tag is embedded in silica, which is a sufficiently stable material in pesticides and withstands harsh sample extraction and washing procedures, SPED are less prone to matrix effects than fluorescent tags. The synthesis of SPED and quantitative analysis of its DNA label require only standard laboratory equipment and a qPCR thermocycler that is available in most biomolecular laboratories.[42] The material costs are ~ 0.06 USD per liter of a liquid to be labeled,[44] when employed in the concentration range used in this study (5.8 ppm of SPED). One of the advantages of SPED is the possibility of generating an almost unlimited number (~1 x 10^{36}) of different labels, i.e., SPED with different DNA tags, allowing the tracing of many pesticides or other environmentally applied substances in parallel without cross-interference of the individual SPED tags (**Figure 3.6**). SPED could be also used as a unique chemical barcode for pesticides and other environmentally applied chemicals, helping, e.g., to identify the source of a contaminating pesticide. Eventually, there are many possibilities for modifying the chemical or physical properties of SPED, for example, by surface functionalization or by incorporation of a magnetic core, that allow the adaptation of SPED to different experimental conditions and to optimize stability and recovery of SPED.

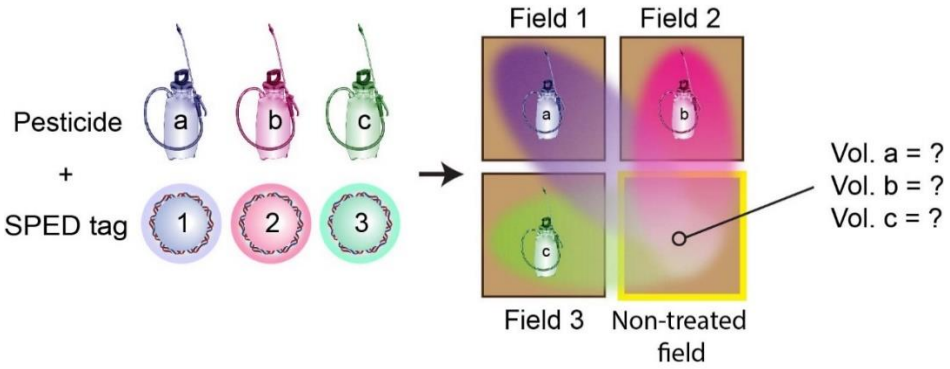

Figure 3.6. *Multiplexing approach for pesticide tracing. Since an extremely high number of different SPED labels are achievable, large scale multiplexing experiments become feasible. E.g. it could be easily evaluated how much of a certain SPED-labeled pesticide was deposited on a non-treated field.*

Although silica particles in the applied size and concentration range as well as the encapsulated DNA oligonucleotides are environmentally non-hazardous according to current understanding, regulatory issues regarding a potential large-scale environmental application of SPED need to be addressed. Overall, the use of SPED improves and simplifies pesticide drift assessments for agricultural or environmental protection purposes, thus facilitating the use of new agricultural techniques and decreasing pesticide-related safety risks.

4. Programmable living material containing reporter microorganisms permits quantitative detection of oligosaccharides

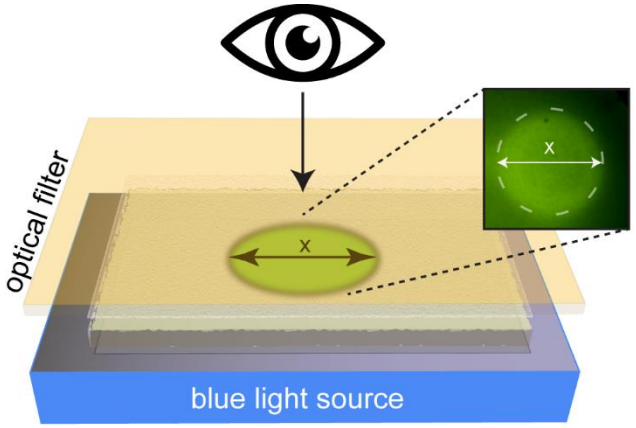

Published in parts as:

Carlos A. Mora, Antoine F. Herzog, Renzo A. Raso, Wendelin J. Stark,
Biomaterials **2015**, 61, 1-9.

4.1 Introduction

In the past few years the spectrum of applications for stimuli-responsive materials has broadened significantly ranging from materials that heal themselves, regulate environmental conditions, defend themselves against microorganisms or protect from vandalism to biomedical devices including drug delivery, tissue replacement or diagnostics.[107-112] Particularly in biomedicine, the increasing understanding of many diseases on a molecular basis has led to a need for novel diagnostic tools that are preferably easy-to-use and inexpensive. For example, food intolerances and allergies affect up to 20 % of the population.[113, 114] Thus, from a consumer's perspective, it would be of great advantage to have tools that allow a facile analysis of diet constituents in order to avoid adverse food reactions.

Recently, stimuli-responsive materials containing living organisms have been reported.[50, 51] By enclosing microorganisms into a sandwich consisting of a solid bottom and a porous top polymer sheet, the organisms could not escape but were still able to interact with the outer environment by absorbing nutrients or by producing antibiotics. Many microorganisms offer a broad range of possibilities for sensor-related applications, since they can be relatively easily genetically manipulated, cultivated and flexibly adapted to produce own or foreign proteins under programmable, external conditions.[115, 116] Another benefit of using living organisms is their capability to perform several complex tasks at once, such as detection, amplification and response to an external stimulus. Additionally, expensive and laborious material synthesis procedures can be avoided due to the fact that living organisms can reproduce themselves. Several microbial whole-cell sensing systems have been developed in the past years that employ different reporting systems (*e.g.* growth rate, oxygen respiration, engineered fluorescence or bioluminescence reporter genes) and implemented in different applications and setups (*e.g.* biochip arrays) to evaluate the toxicity of chemicals or to measure the concentration of environmental pollutants and other chemicals.[117-119]

However, when assessing these applications for their potential usage by non-scientifically trained people outside of a laboratory environment, many of these applications are not easy to handle and require relatively expensive scientific analysis equipment such as spectrophoto-, fluoro- or luminometers. Additionally, ways have to be found to keep living microorganisms alive, functional and protected from contaminating agents over a relevant timespan. According to bio-safety regulations, it must be also assured that genetically modified organisms cannot escape from the sensor device.

Diffusion, a substance-specific physical property, has been used among others in the classical agar diffusion assay, and there in particular to analyze growth inhibiting substances - such as antibiotics[120, 121] or signaling molecules involved in quorum sensing.[122] Another example of diffusion-based analysis is the quantification of antigens by immuno-diffusion.[123] The quantification in agar diffusion assays is based on the fact that the diffusion behavior of a substance correlates to its initial concentration. For instance, to quantify the activity of a bactericidal substance, the area of the clear, bacteria-free "inhibition" zone needs to be measured. It has been shown, that the diameter x of the clear zone depends on the initial (c_0) and critical (c_{crit}) inhibitory antibiotic concentration as well as on bacterial growth. This dependence can be described using the following formula which also includes the diffusion factor D and the critical time for zone development t_{crit}:[121]

$$x^2 \propto D \cdot t_{crit} \cdot \ln(c_0 - c_{crit}) \qquad (1)$$

In this study, we report the development of a sensor material that combines the diffusion behavior of an analyte with an analyte-specific bacterial fluorescence reporter system. The analysis requires only a camera, a blue-light source and a blue-light filter. We incorporated the well-established model bacteria *Escherichia coli,* genetically modified with a fluorescent reporter system, in a matrix of different polymers to create a programmable living material-based analytical sensor (LiMBAS). This material shows an easily quantifiable and specific response when coming into contact with an analyte anywhere on its surface and works at ambient temperature and humidity conditions. We established methods to easily detect and analyze the diffusion behavior of chemical stimuli that have been applied as droplets onto the materials surface using well-known optical techniques such as fluorescence trans-illumination and fluorometry. We programmed the organisms in the material to recognize the sugars lactose, galactose and isopropyl 1-thiogalactopyranoside and evaluated its application as a sensor for measuring lactose and galactose in food products in comparison with other established quantification techniques. We further determined the detection limit and storability of the material.

4.2 Experimental

4.2.1 Organisms and bacterial culture

For overnight cultures the bacteria were grown in 10 mL Lysogeny broth (Difco LB Broth Miller, tryptone 10 g/L, yeast extract 5 g/L, NaCl 10 g/L) supplemented with the appropriate antibiotics in a 50 mL culture tube under constant mixing (250 rpm) at 37 °C (KBF-ICH, Binder). For the material preparation, M9 minimal agar medium was used. M9 minimal medium (1x) contained M9 salts (17.2 g/L $Na_2HPO_4 \cdot 12\ H_2O$, 3 g/L KH_2PO_4, 0.5 g/L NaCl, 1 g/L NH_4Cl), 0.2% glycerol as main carbon source, 0.2% casamino acids (Amresco), 1 mM thiamine hydrochloride (Fisher Bioreagents), 2 mM $MgSO_4$, 0.1 mM $CaCl_2$, filled up to 1 L with ultrapure water. Appropriate amounts of pre-dissolved sterile agarose (electrophoresis grade, Apollo Scientific) were added to the media to reach the desired agar content. All media components had been sterilized by autoclaving or filtering (0.2 µm, Filtropur S, Sarstedt). 25 µg/mL chloramphenicol (Cm, Fisher Bioreagents) and 100 µg/mL ampicillin (Amp, Fisher Bioreagents) were added to all media.

Escherichia coli BL21(DE3) pLysS cells containing the pLysS plasmid (Cm^R) coding for T7 lysozyme, a natural inhibitor of the T7 RNA polymerase allowing for improved transcriptional control, were purchased from Sigma-Aldrich (chem.-competent, Cat No: B3310). The BL21 strain is deficient for two proteases and therefore degradation of heterologous proteins is reduced. The strain genome includes the λ(DE3) prophage containing an inducible T7 RNA polymerase under the control of the *lac*UV5 promoter. The bacteria were transformed with pRSET/EmGFP plasmid (Life Technologies, Amp^R, Cat No: V353-20) following the transformation protocol provided by the manufacturer. pRSET/EmGFP codes for emerald green fluorescent protein (EmGFP) under the control of the T7/lac promoter. A total number of 20 colonies were selected after transformation of pRSET/EmGFP. After culturing them in liquid LB medium at 37 °C overnight, they were re-suspended at an OD_{600} of 0.4 in a volume of 200 μL LB medium containing 0.5 % agarose and filled into 96-well microplate. After incubation for 3 hrs @ 37 °C they were induced with 10 μL 1 M Isopropyl-beta-D-thiogalactopyranoside (IPTG, >99% dioxin-free, Apollo) and incubated at 20 °C overnight. The best fluorescing colony was then selected and used in all further experiments.

4.2.2 Preparation of living materials

The optical density of the bacterial culture grown overnight was measured at λ = 600 nm. The volume of cell suspension for OD_{600} = 0.4 in a volume of 20 mL was centrifuged at 11'000 x g for 1 min and re-suspended in 20 mL M9 minimal agar medium containing 0.5% agarose at 40 – 45 °C. The resulting suspension was poured into a sterile petri dish (polystyrene, 16 x 92 mm, Sarstedt) and let solidify. A nano-porous polycarbonate membrane (400 nm pore size, PCTE, thickness Ø 30 µm, Sterlitech) was placed on top of the agar layer. After incubating at 37 °C for 4 - 5 hours, the material was ready for usage.

4.2.3 Fluorescence imaging and zone analysis

Microplate reader: a well plate of 41 x 32 wells at a diameter of 1 mm had been previously designed as template grid on the microplate reader (TECAN). emGFP fluorescence was measured at excitation = 485 nm, emission = 520 nm at 25 °C. The data from the microplate reader measurements were arranged in an Excel data sheet (Office 2010, Microsoft) so that the fluorescence values of a plate were ordered according to their measurement time point and spatial location. The differences in fluorescence were made visible by conditional formatting (lowest to highest value, blue – white – red) (see **Figure 4.1**). Camera: the biosensor material was placed on a blue-light transilluminator (E-Gel® Safe Imager™ Real-Time Transilluminator, Invitrogen) and covered with a blue-light filter to detect emGFP fluorescence. Images were made with a camera (450D, Canon) or a smartphone (iPhone 4, Apple). Image analysis was done with Photoshop CS5 (12.0.4, Adobe). The zone diameter was measured using the integrated ruler tool of Photoshop.

4.2.4 Diffusion experiments

Serial dilutions of IPTG, lactose (anhydrous, Fluka) and galactose (D-(+), > 99%, Acros) at concentrations of 500, 250, 125, 62.5 and 31.25 mM were prepared in ultra-pure water (18.2 MΩ, Millipore). 1 µL droplets of each dilution were placed on top of the cover membrane so that all dilutions of a specific inducer fitted onto one plate. The material was then incubated at room temperature (25 °C). Fluorescence measurements were performed repeatedly up to 20 hours after induction.

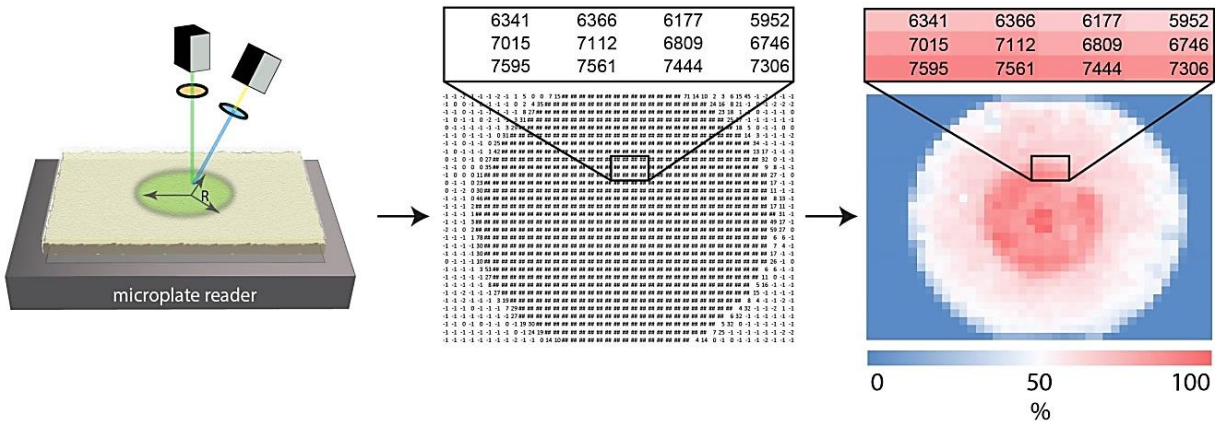

Figure 4.1. *Process of developing an image from microplate reader data. A well plate of 41 x 32 wells at a diameter of 1 mm had been previously designed as template grid on the microplate reader (TECAN). The data from the microplate reader measurements were arranged in an Excel data sheet so that the fluorescence values of a plate were ordered according to their measurement time point and spatial location. The differences in fluorescence were made visible by conditional formatting (lowest to highest value, blue – white – red).*

4.2.5 Detection limit

Serial dilutions of IPTG, lactose and galactose at concentrations of 10, 1, 0.1 and 0.01 mM were prepared in ultra-pure water. 1 µL and 10 µL droplets of each dilution were placed on top of the cover membrane so that all dilutions of a specific inducer fitted onto one plate. Fluorescence measurements were performed after 5 hours (IPTG) and 15.5 hours (Lactose, Galactose) after induction. Light intensity was calculated using ImageJ [102] from inverted, 8-bit fluorescence trans-illuminescence images after optimizing contrast and brightness. The experiment was repeated twice.

4.2.6 Storability

The prepared living material was hermetically sealed using parafilm and then stored in the fridge at 2 – 6 °C for 1, 4, and 7 days. Serial dilutions of IPTG (500, 250, 125, 62.5 and 31.25 mM) were prepared in ultra-pure water. 5 µL droplets of each dilution were placed on top of the cover membrane so that all dilutions of a specific inducer fitted onto one plate. The experiment was repeated twice.

4.2.7 Measurement of Lactose/Galactose concentration in milk/lactose-free milk

Additionally, to serial dilutions of pure lactose and galactose solutions at concentrations of 500, 250, 125, 62.5 and 31.25 mM, 1 µL droplets of milk (3.9% fat, Naturaplan, Coop Switzerland) or lactose-free milk (3.9% fat, FreeForm, Coop Switzerland) were placed on top of the cover

membrane. The material was then incubated at room temperature (25 °C). Fluorescence measurements were performed after 7 and 19 hours after induction. Lactose and Galactose concentrations in the standard concentrations and milk samples were validated by HPLC-MS analysis (Agilent 1100 Series LC/MSD, single Quadrupole, Electro Spray Ionization, flow injection (10 µL, dilution in water of 10^{-4}) with water/MeOH 20/80 isocratic with 0.1% formic acid) and a flourometric lactose/galactose enzymatic assay (MAK011, Sigma-Aldrich).

4.2.8 Cost analysis

Material costs for an assumed 1 dm^2 area, 10 mL agarose (1%) and 10 mL M9 medium (2x) were calculated. Following materials were included in the cost analysis: porous membrane, 2.33 \$ / dm^2 (Sterlitech, PCT0420030, 09.10.2014); agarose (1%), 0.07 \$ / 10 mL (Apollo Scientific, BIA1176, 09.10.2014); M9 minimal medium (2x), 0.08 \$ / 10 mL (Sigma-Aldrich, M6030).

4.3 Results

To create LiMBAS, we mixed pre-cultured *E. coli* containing the *emgfp* reporter gene under the control of the T7/lac promoter at a concentration of $3.2 \cdot 10^8$ colony forming units (cfu) per mL with selective nutrient medium and agar (0.5%) and applied the mixture on a transparent sheet of polystyrene. This resulted in an approximately 3 mm thick 'living layer' (**Figure 4.2**). This layer was covered with a ∅ 30 µm thick porous pre-sterilized polycarbonate membrane with a pore size (∅ 400 nm) small enough to retain the bacteria. The composite material was incubated at 37 °C for 4 to 5 hours. This is enough time for the bacteria to adapt to the new conditions and enter the growth phase during which reporter gene expression is optimal.

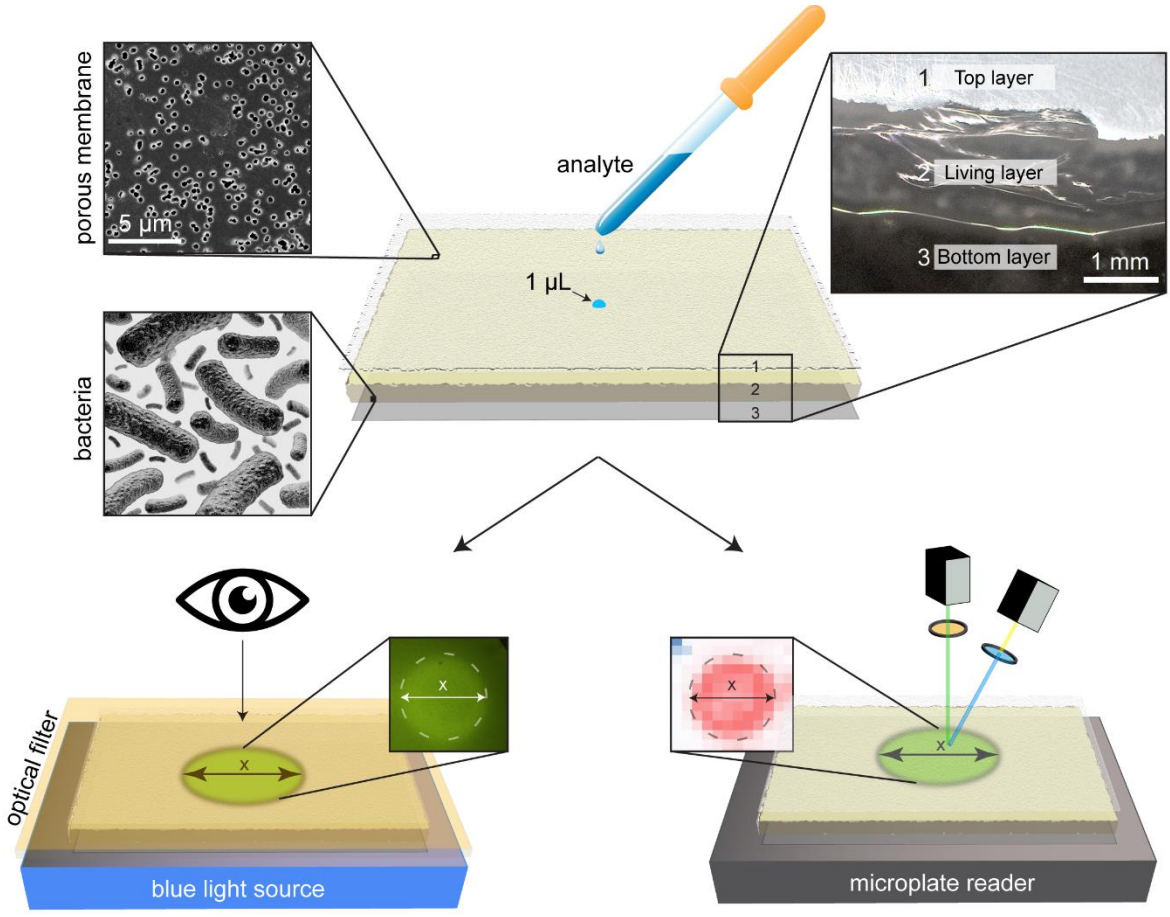

Figure 4.2. *Illustration of the quantification principle. A droplet of analyte (e.g. 1 µL) is applied on top of the porous membrane (1). In the upper left part, a surface electron microscope image of the porous membrane is shown. The analyte diffuses radially through the living layer (2) inducing the bacteria to express fluorescent proteins. The extent x of the fluorescent zone is quantifiable by eye or camera using a blue light source and an optical filter, or alternatively by a fluorescence microplate reader.*

After the initial incubation period, the biomaterial was ready to be used at ambient environmental conditions (25 °C, 50% humidity). To investigate whether the bacteria can be induced when incorporated into the living surface we applied 10 µL or 1 µL droplets of isopropyl β-D-1-thiogalactopyranoside (IPTG), at various concentrations on top of the living surface. IPTG is a well-known, non-hydrolysable inducer for the T7/lac promoter. We initially used a standard microplate reader to visualize the developing fluorescence signals over time by conditionally formatting the obtained fluorescence values from each well with a color scale. But the fluorescence signal could also be directly made visible using a blue-light source and a blue-light optical filter (**Figure 4.2**).

Besides IPTG, the sugars lactose and galactose can also induce the expression of genes under the control of the T7/lac promoter, if the medium does not contain glucose as a major carbon source.[124] Therefore, we replaced glucose with glycerol for our experiments. The inducers diffused radially from the point of application causing a circular fluorescent zone. The border of the circular zone showed strong fluorescence intensities which enabled a clear discrimination of the zone from the background (**Figure 4.3**).

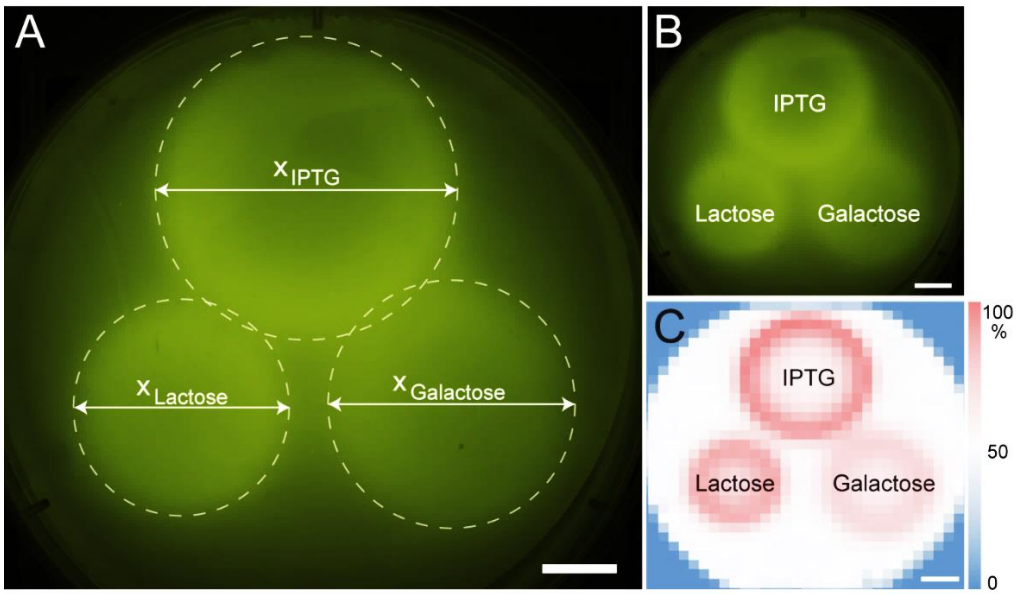

Figure 4.3. *Fluorescent diffusion zones caused by IPTG, lactose and galactose. (A) The extent of the zone (dashed line) was quantified by measuring the zone diameter x. The image was generated using a camera, a blue-light source (LED array) and blue-light filter. Panel (B) shows the same image as in (A) without lines. (C) Fluorescence heat map of the same assay generated with a fluorescence microplate reader (Ex/Em 485/510 nm). A volume of 1 µL at a concentration of 1 M IPTG, galactose and lactose was applied. The images were generated 13 h after induction. Scale bar, 1 cm.*

When using the inducer IPTG, we observed a strong linear correlation between the zone diameter *x* and the logarithm of the initial inducer concentration *log*(*c*) for all time-points measured after the initial inducer application (**Figure 4.4**). There was also a linear correlation between the zone area x^2 and *log*(*c*), but less pronounced as compared to *x* vs. *log*(*c*). The diffusion velocity described by plotting the zone area x^2 versus time behaves linearly in the experimental time range (0-540 min) (**Figure 4.4C**).

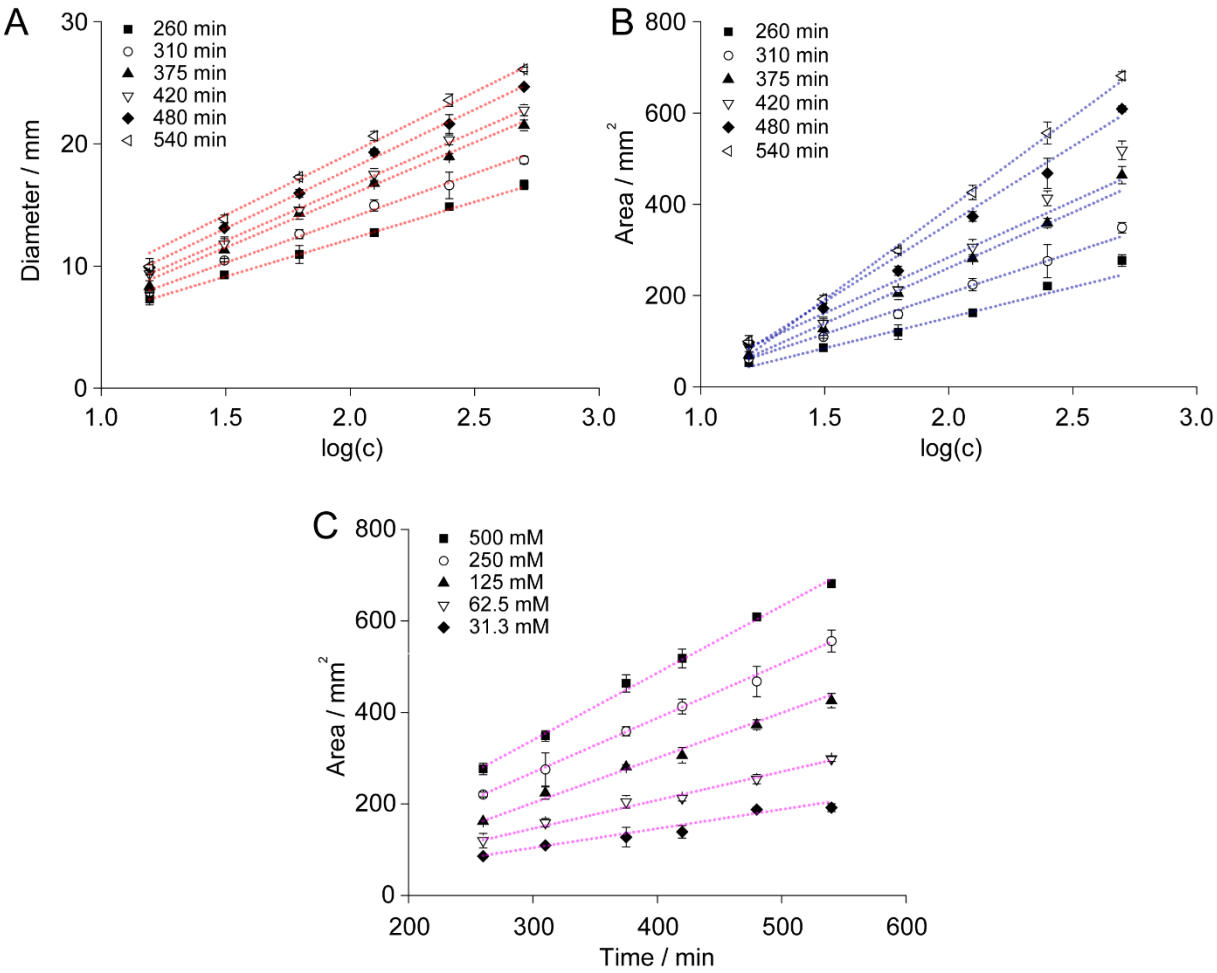

Figure 4.4. *Zone development in response to different concentrations of the inducer IPTG. The semi-logarithmic plots of (A) the fluorescent zone diameter x and (B) area x^2 against the initial concentration c_0 (15.1, 31.3, 62.5, 125, 250 and 500 mM) of IPTG are shown. The data points were fitted to a linear function (red and blue dotted lines), (A) R^2 > 99.1%, (B) R^2 > 97.1%. (C) Linear plot of the fluorescent zone area x^2 against the time after start of the measurement. The data points were fitted to a linear function (magenta dotted line), R^2 > 97.7%.The applied inducer volume was 1 µL. Mean values and standard deviations are displayed (n = 3).*

After characterizing the material's response to IPTG, we compared the performance of the two other inducers galactose and lactose with IPTG. The results show that the slope of the linear correlation between diameter *x* and the logarithmic concentration *log*(*c*) depended much more on the time after induction then on the type of inducer (**Figure 4.5A**). In contrast to that, the *y*-intercept of the respective fitting functions, *i.e.* the zone extent at a given concentration, differed significantly depending on the type of inducer. After seven hours, the zone diameter for IPTG was on average 3.1 ± 0.3 mm larger than the one caused by galactose and 6.9 ± 0.3 mm larger than that of lactose. Besides the zone diameter, the development of fluorescence over time also differed between the three inducers. When measured in the center of the zone, the lag time of fluorescence development was 36 min for IPTG and thus much shorter than for lactose and galactose with 112 and 121 min, respectively (**Figure 4.5B**).

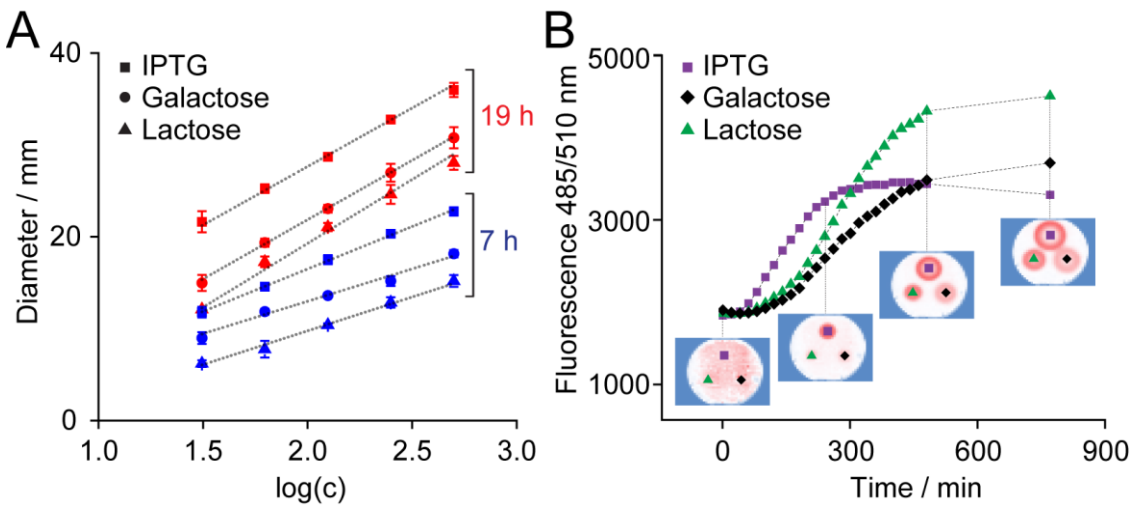

Figure 4.5. *Fluorescence development for lactose, galactose and IPTG. (A) Semi-logarithmic plot of the fluorescent zone diameter x against the initial concentration c_0 of IPTG, lactose and galactose (31.3, 62.5, 125, 250 and 500 mM) after 7 h and 19 h. The data points were fitted to a linear function (dotted line), R^2 > 98.0%. The applied inducer volume was 1 µL. (B) Fluorescence intensity of zone centers for zones induced by IPTG, lactose or galactose at a concentration at a concentration of 1 M (Vol = 1 µL). Fluorescence readings (arbitrary units, Ex 485 nm, Em 510 nm) measured by microplate reader are given (t = 0, 4, 8, and 16 h after induction). Mean values and standard deviations are displayed (n = 3).*

Besides the time of fluorescence development, also the limits of detection differed between IPGT and the two other sugars based on a signal-to-noise ratio of 3:1. For IPTG, concentrations could be detected down to 0.1 mM using a volume of 10 μL (1 mM with 1 μL), which is equivalent to an absolute amount of 1 nmol. Lactose could be detected down to 1 mM (10 nmol) and galactose to 10 mM (100 nmol) (**Figure 4.6**).

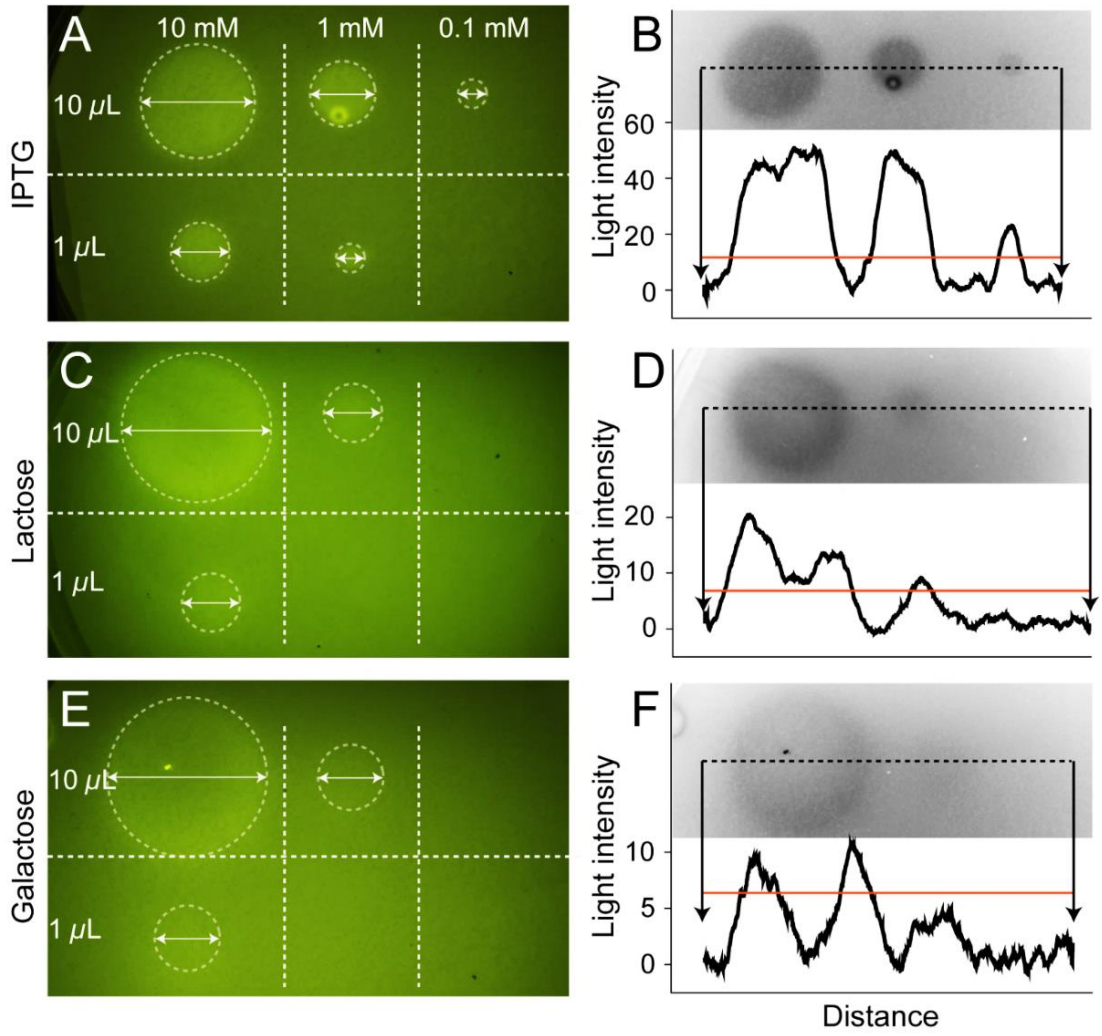

Figure 4.6. *Determination of the limit of detection for IPTG, lactose and galactose. The applied inducer volume was 10 or 1 µL, the applied concentration 10, 1 and 0.1 mM. LiMBAS was measured by blue-light trans-luminescence. (A, C, E) represent non-modified images. Arrows indicate the zone radius. (B, D, F) depict the light intensity of fluorescence zones calculated from an inverted gray-scale image of the upper 10* µL *row of the respective left-side image. The horizontal red line represents a signal-to-noise ratio of 3:1. Pictures were taken after (A, B) 5 h, (C, D) 15.5 h and (E, F) 15.5 h post induction. The bright spot in panels A and B in the diffusion zone of 0.1 mM is caused by an air bubble entrapped in the agar layer.*

For a future application of LiMBAS as a diagnostic tool, we tested the storability of the material at low temperatures. After freshly preparing the material, we stored it hermetically sealed in the fridge at 2 - 6 °C for up to 7 days before applying inducer at different concentrations again at ambient conditions. The material was storable for seven days at least and could be readily used after this period, although the background fluorescence increased over time (**Figure 4.7**).

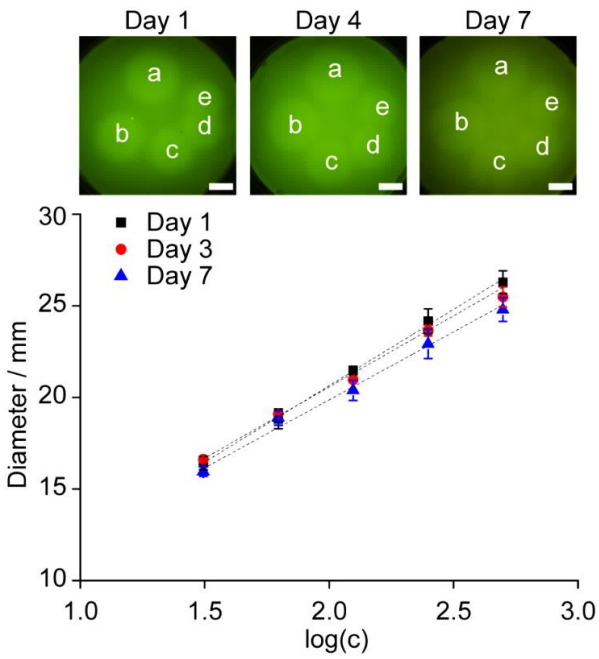

Figure 4.7. *Storability over time. The living material was stored for 1, 4 and 7 days in the fridge at 2 – 6 °C. The applied inducer volume was 5 µL, the applied concentration (a) 500, (b) 250, (c) 125, (d) 62.5 and (e) 31.25 mM. Semi-logarithmic plot of the fluorescent zone diameter x against the applied concentration* c_0 *of IPTG after t = 6 h. The data points were fitted to a linear function (dotted line),* $R^2 > 98.6\%$*. Scale bar = 1 cm. Mean values and standard deviations are displayed (n = 2).*

In a real-world application we used LiMBAS to determine the lactose or galactose content directly from food samples. Lactose was measured from commercially available pasteurized cow's milk. Galactose was measured in lactose-free milk. We used lactose-free milk derived from cow's milk that had been industrially treated with the enzyme lactase. Lactase is a glycosidase (EC 3.2.1.108) and converts the disaccharide lactose to the monosaccharides galactose and glucose. The content of lactose is negligibly small in lactose-free milk and vice-versa the content of free galactose in cow's milk is negligible compared to the amount of lactose [125]. Around the same concentration of galactose in lactose-free milk as lactose in the original cow's milk can thus be expected. We derived the concentrations of lactose in milk or galactose in lactose-free milk by applying a liquid food sample together with five standard solutions of the respective sugars prepared in water at concentrations ranging between 31 and 500 mM onto the sensing material. The incubation time after addition of the milk sample (7 or 19 h) did not have a significant effect on the final concentration (**Figure 4.8**, see also Figure 5). The results obtained from LiMBAS were compared to standard measurement methods for lactose and galactose concentration in milk, high pressure liquid chromatography (HPLC) coupled to a

mass spectrometer (MS) and fluorometric enzymatic assays using the same food and standard samples.

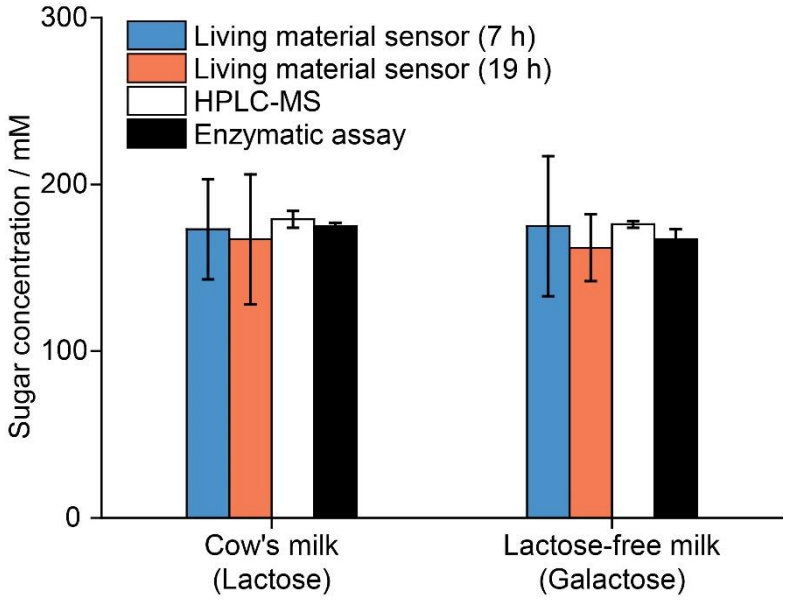

Figure 4.8. *Measured concentration (mM) of lactose in (galactose-free) cow's milk or galactose in lactose-free milk. Measurement was done with LiMBAS after 7 h and 19 h of analyte applicaton (Vol. = 1 µL) and with HPLC-MS and an enzymatic assay. Mean values and standard deviations are displayed (n = 3).*

4.4 Discussion

We showed that the diffusion behavior of a chemical substance can be visualized by a gel-matrix embedded whole-cell microbial reporter system and used to quantify the concentration of the investigated substance. As expected from previous diffusion studies with matrix-embedded microorganisms (Equation 1), the response of the material to the diffusing inducer chemical suggested a semi-logarithmic dependence between the diffusion zone extent and the initial inducer concentration (**Figure 4.4**). However, in contrast to Equation 1, we observed that the correlation between the zone diameter x and the initial concentration c_0 is slightly better ($R^2 > 99.1\%$) than for the area x^2 and c_0 ($R^2 > 97.1\%$). This observation can be explained by the fact that the diffusing layer of our material is around three millimeters thick, thus not completely two-dimensional and additionally covered by a porous membrane, which is deviating from the two-dimensional diffusion behavior approximated by Equation 1. Concerning the diffusion velocity during the first few hours after induction, not x but x^2 was dependent on time, which can be expected for a two-dimensional diffusion (**Figure 4.4**).

LiMBAS with *E. coli* works at ambient temperatures (~25 °C) which reduces the required equipment but slows down the production of reporter proteins by the bacteria, which have an optimal growth temperature at 37 °C.[126] The necessary time for signal development could thus be optimized by increasing the incubation temperature which has to be addressed in future studies. Nevertheless, using a blue-light transilluminator, the development of clear distinguishable fluorescent zones took between 2 hours for IPTG to 5 hours for lactose or galactose. The duration to develop a detectable response signal after exposure to an inducer differed for the tested substances. The lag time for fluorescence development was around three times higher for galactose and lactose than for IPTG. This difference is based on the fact that IPTG is capable to directly and irreversibly deactivate the lac repressor. The sugars lactose and galactose need to undergo further transformation steps to the IPTG-analogue allolactose which naturally and reversibly inhibits the lac repressor.[127]

Analogous to the time of development, the necessary amount of inducer to give a detectable fluorescence signal with an S/N ratio ≥ 3 was one order of magnitude lower for IPTG compared to lactose or galactose (**Figure 4.6**). For higher concentrations of IPTG, lactose or galactose, the S/N ratio increased further (data not shown).

In a realistic application, we tested LiMBAS for its ability to detect lactose directly from cow's milk and galactose from lactose-free milk - without previous dilution, which is necessary for methods such as HPLC-MS or enzymatic assays. We chose milk for our proof-of-principle

experiment since it is a widely used food product and a source of several common food disorders including lactose intolerance, allergies as well as galactosaemia, a genetic disorder of the human metabolism of galactose with potentially lethal outcome if untreated.[128] We observed that the time point of relative zone extent measurement (either 7 h or 19 h) does not have an influence on the measured analyte concentration. Thus, analysis could be done over a range of several hours after sample application.

We compared the results of our material to measurements obtained using a commercially available fluorometric enzymatic assay and HPLC-MS. The standard deviation of our assay was around one order of magnitude higher in comparison to the other methods with the same number of replicates (n = 3) (**Figure 4.8**). One possible factor contributing to a higher variation is the semi-logarithmic relationship of zone extent and concentration. Both HPLC-MS (signal intensity) and enzymatic assay (light/fluorescence intensity) are based on a linear correlation.

However, our material has several advantages compared to established diagnostic techniques: firstly, the handling of our diagnostic assay requires little technical knowledge and does not need complex and expensive devices. The user only needs to apply the liquid containing the analyte and standard solutions onto the membrane. After incubation at ambient conditions over a time course of a few hours, the living material has to be placed above a blue-light source and covered by a blue-light filter. As blue-light source an array of blue-light LED lamps is already enough to serve as a blue-light source.

Analysis can be done for instance by taking a picture with the camera of a smartphone, which could then automatically be analyzed by a smartphone application programmed to measure the zone extent and to calculate the resulting analyte concentration from a standard curve (**Figure 4.9**). In contrast to enzymatic assays, there is no need for a colori- or fluorometric quantitative analysis using a spectrophoto- or fluorometer.

Secondly, our material has a size-selective porous top membrane, which prevents contamination of the environment and the living layer by bacteria and decreases dehydration of the living layer. For our experiments we used a top membrane with an average pore size of 400 nm, but also smaller pores could be used to retain smaller bacteria and to lower the risk of contamination with bacteriophages. Genetically modified microorganisms could be used outside of a protected laboratory environment. In any case, these organisms should not be capable of surviving outside of LiMBAS. Mandell *et al.* (2014) recently demonstrated that genetically modified *E. coli* bacteria can be made incapable of surviving in or adapting to a

natural environment by rendering the microorganims auxotrophic for certain artificially modified metabolites such as amino acids.[129] Such bacteria could be also used in LiMBAS. Nevertheless, the material's environmental safety and in particular its safe disposal need more in-depth investigation and testing.

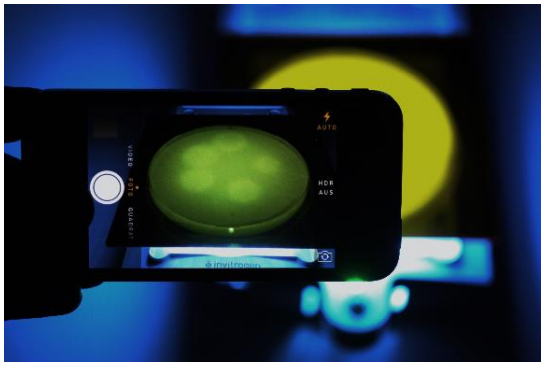

Figure 4.9. *Taking an image of LiMBAS using a smartphone and a blue-light source with optical filter.*

Furthermore, our material is storable at fridge temperatures (2 – 8 °C) in a ready-to-use fashion without losing its functionality prior to a potential 'home' application. From literature it is known that a temperature of 5 °C reduces the growth and metabolism of *E. coli* to almost zero [130]. We showed that the prepared material is usable for at least seven days when stored in the fridge. However, for a final application as a real-world product, the time to manufacture, ship and purchase the material would have to be considered and the storage time would have to be prolonged to around at least one month. This could be done by optimizing the material preparation procedure, storing temperature and chemical composition of the living layer medium.

Considering the costs, the raw materials sum up to around 2.50 $ per biosensor unit (assuming an area of 1 dm^2 per unit), of which more than 90% can be attributed to the porous top membrane. Moreover, microorganisms such as *E. coli* can easily be propagated and numerous tools are available for genetic modification.

For this proof-of-principle study we programmed our bacterial reporter system by combining the well-established lac promoter with a highly fluorescent version of the traditional reporter gene for the green fluorescent protein. Many bacterial reporter systems with various promoters and reporter genes have been developed in the past years. Besides that, the technique to introduce new reporter systems *via* promoter-less reporter vectors is already well-established and commercially available [131]. **Table 4.1** gives a selection of various chemical compounds that can be quantitatively reported by genetically engineered microorganisms. Besides others, the bioluminescence reporter systems such as the lux reporter would also be applicable with

LiMBAS and, compared to fluorescence reporter systems not even need an external light source. Furthermore, the sensitivity of the living surface can be enhanced by using multiple promoter systems – each coupled to different fluorescence or bioluminescence reporter genes. Consequently, different substances could be detected and quantified in a simple or multiplex approach.

Table 4.1. *Examples of substances detectable by microorganisms.*

Microorganism	**Reportable chemical**	**Reporter system**	**References**
Escherichia coli	Chromated copper arsenate	lux	[132]
	Nitrate	gfp, ice	[133]
	Diverse toxins	lux	[134]
Pseudomonas spp.	Naphtalene	lux	[135]
	Benzene,Toluene, Ethylbenzene, Xylene	lux	[136]
Ralstonia eutropha	Polychlorinated biphenyls	lux	[137]

Overall, taking the mentioned advantages such as easy handling, use of well-established materials, potential out-of-lab application, low costs and high flexibility of adaptation into consideration, LiMBAS can clearly be advantageous compared to other diagnostic techniques such as HPLC-MS, enzymatic assays or also other whole-cell based assays. LiMBAS as biomaterial offers the possibility to safely use engineered microorganisms outside of a laboratory environment without the need for culturing or complicated analysis. The quantification principle of combining diffusion behavior with matrix-embedded microbial whole cell reporter systems could be applied to develop a variety of diagnosis tools for the analysis of food, blood or environmental constituents, which can be used in domestic or outdoor applications.

5. Conclusion and Outlook

The here presented work describes advanced, novel strategies for quantitative analysis based on bioinspired materials, i.e., fossilized DNA particles and living materials. Lab-scale and in some cases also small field-scale studies were performed showing promising results. However, the presented analytical tools and strategies still need to be tested under large-scale conditions as well as in other experimental settings in order to evaluate the robustness of the presented methods. In the following sections, the principal findings of this thesis are concluded and current investigations as well as potential directions for future research are discussed in addition to those already mentioned in the previous chapters.

5.1 Monitoring of ecological relationships with SPED

It was demonstrated in Chapter 2 that silica particles with encapsulated DNA (SPED) combine attributes of two common techniques of ecological relationship analysis: DNA barcoding and stable isotope analysis. SPED allow for unique labeling, quantification via qPCR and exact backtracking to the tracer source. This improves and simplifies the analysis and monitoring of ecological networks.

So far, it was shown that SPED may work in a food chain of arthropods. Future studies will aim at investigating whether the SPED method can be expanded to other ecological food webs, over how many trophic levels (i.e., organism-to-organism transfers) SPED can be used, and how robust and quantitative the method performs in a true field setting. Although we have demonstrated that SPED can persist over longer time periods (at least seven days) in the investigated animals (*D. melanogaster* and *T. molitor*), the persistence of SPED within the digestive organs needs to be prolonged and better regulated to achieve a monitoring over several trophic levels and longer time periods (weeks to months). This could be achieved by adapting the particle size and/or surface functionalization of SPED with chemical groups that protect the particles better from the harsh digestive environments and slow down their passage through the digestive system of the tagged animals. Of course, it has to be ensured that the modified SPED remain non-toxic.

It has been recently shown in our group that unicellular microorganisms such as *Paramecium caudatum* can be labeled with SPED.[45] SPED could be thus used in particular to elucidate and monitor the trophic interactions of protozoan aquatic microorganism (e.g., photo- or zooplankton) with other microorganism and macroorganisms (e.g., fish) of higher trophic levels, which is usually difficult to assess by conventional means. But also terrestrial ecosystems are a potential field of application, and therefore, studies are under way, that aim to

use SPED as quantitative tool to assess the spreading mechanism and possible control measures of the fruit crop pest *Drosophila suzukii* (spotted-wing fly) in the field.

5.2 Tracing anthropogenic substances in the environment

A slightly different strategy of using SPED was shown in Chapter 3. The labeling of environmentally applied, potentially harmful anthropogenic substances with SPED leads to ultrasensitive quantitative substance distributions. Additionally, an almost unlimited number of different and non-interfering tracers for environmental studies that investigate, e.g., the safety and behavior of the anthropogenic substance in the environment, can be created.

Future experiments would include studies in real-world applications such as pesticide drift studies evaluating the effect of different spraying conditions (e.g., spray nozzle type, and spraying angle), obstacles (e.g., fences, hedges, and trees), and other important factors. The samplers used in the presented studies would need to be optimized, so that the accuracy of analysis can be even more improved (this has been discussed in detail in Chapter 3.3).

For this application and in general for the work with SPED it would be of advantage to have an even faster quantification method at hand than qPCR. A new method based on qPCR and the so-called digital PCR is currently developed in our lab, which aims at decreasing the time of analysis, and is coupled to a mobile smartphone-based analysis platform.

5.3 Developing living material sensors to create a biosensor platform

The proof-of-principle study presented in Chapter 4 successfully demonstrated the feasibility of creating a quantitative programmable and easy-to-use biosensor based on living material containing genetically modified reporter organisms. This living materials based analytical sensor (LiMBAS) requires only minimal equipment because it relies on a straightforward quantification strategy, i.e., visualizing the diffusion of the analyte within the material. Thus, there is no need for a relatively expensive spectrophotometer evaluating the emission light intensity. A normal camera equipped with a simple light source, e.g., a smartphone camera, is sufficient. The only additional requirement would be a light filter in the respective ranges of the excitation and emission wavelengths of the fluorescent reporter molecules that are produced by the material-incorporated microorganisms in response to the analyte.

A few challenges need to be tackled until LiMBAS is ready for market introduction: First, the current time of analysis of a few hours is too long. This could be solved by changing the

incubation conditions, e.g. using a higher temperature, or by employing time-optimized reporter gene constructs such as faster folding reporter proteins. Another possibility would be the use of more sensitive light sensors to detect fluorescence more efficient and thus earlier.

Second, the sensor design has to be optimized, i) to improve readout accuracy and replicability, ii) to enable a better integration of the sensor transducer and data processing elements and thus simplify the handling, iii) to enhance storability, and iv) to increase biosafety. Instead of the previous 2D diffusion design, a linear diffusion design on a plate with narrow channels filled with hydrogel containing the sensor microorganisms was designed and tested (see **Figure 5.1**).

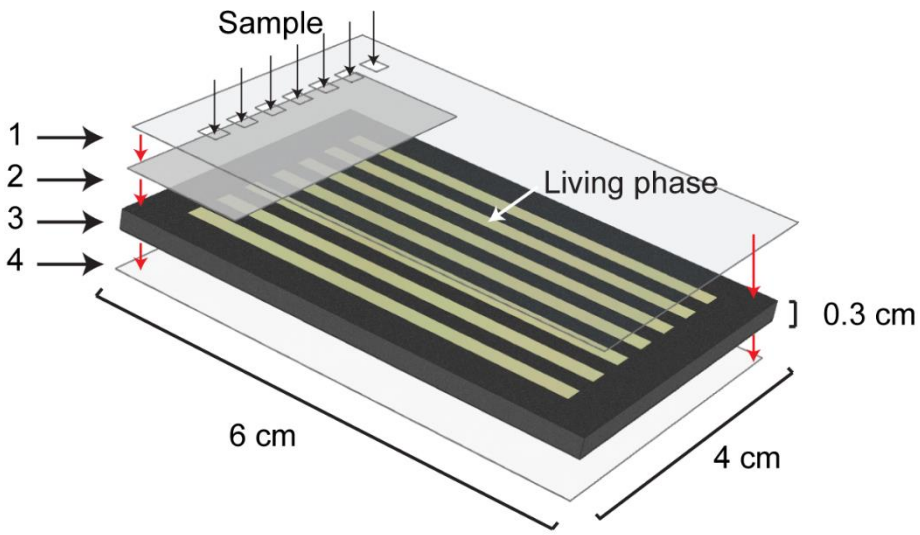

Figure 5.1. *First prototype of a modified LiMBAS sensor based on a linear diffusion design. (A) Schematic setup: To increase biosafety and to lower water evaporation, the sensor is covered by (1) a non-porous polymer layer with holes for sample application, followed by a (2) porous membrane covering only the sample application area, (3) a 3D-printed flat plate with channels filled with reporter microorganisms in hydrogel (living phase), and enclosed by (4) a bottom polymer membrane.*

The final goal is to further decrease the size of the sensor to a smaller format which can then be read out by an add-on gadget (transducer element) of a programmable digital device such as a smartphone. Storability of the sensor could be increased by exchanging the currently used 'living layer' hydrogel material, agarose, with a material that has a similar biocompatibility but shows a higher material stability so that it can be better dried and rehydrated and/or stored at temperatures below freezing point. Biosafety could be increased by using membranes with smaller pore size, and by limiting the area of possible exchange with the environment. Additionally, as mentioned in Chapter 4.4, microorganisms that are inherently safe, e.g., that can only survive with artificial amino acids, could be employed.

Third, the sensor capabilities have to be broadened so that it can serve as a multi-analytes biosensor platform able to detect different analytes separately or simultaneously, e.g., by using different reporter genes. The oligosaccharides lactose or galactose are disease-relevant molecules, but various laboratory to point-of-care methods already exist to assess them. Interesting analytes could be medically or environmentally relevant substances for which corresponding natural bioreceptors exist, but which are difficult or costly to detect by conventional means, such as allergens, hormones and other disease-relevant biomarkers and toxins.

Appendix

A.1 Supplementary data for Chapter 2

A.1.1 Reference images for confocal fluorescence microscopy.

Silica particles containing a fluorescent rhodamine-derivative (Ex: 569 nm, Em: 585 nm) were purchased (sicastar®-redF, 100 nm and 1 µm, Micromod Partikeltechnologie GmbH, Germany) (**Figure A1.1**).

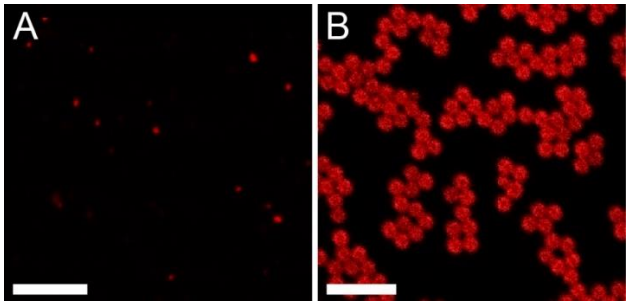

Figure A.1.1. *SPED characteristics.* ***(A*** *and* ***B)*** *Confocal fluorescence microscopy images of (A) fluorescent SPED1 (SiO_2-rhodamine) particles and (B) 1 µm SiO_2-rhodamine particles used as positive control for histological experiments in D. melanogaster. The particles were detected at Ex = 561 nm/Em = 605(30) nm. Scale bars, 5 µm.*

A.1.2 Additional confocal fluorescence microscopy images.

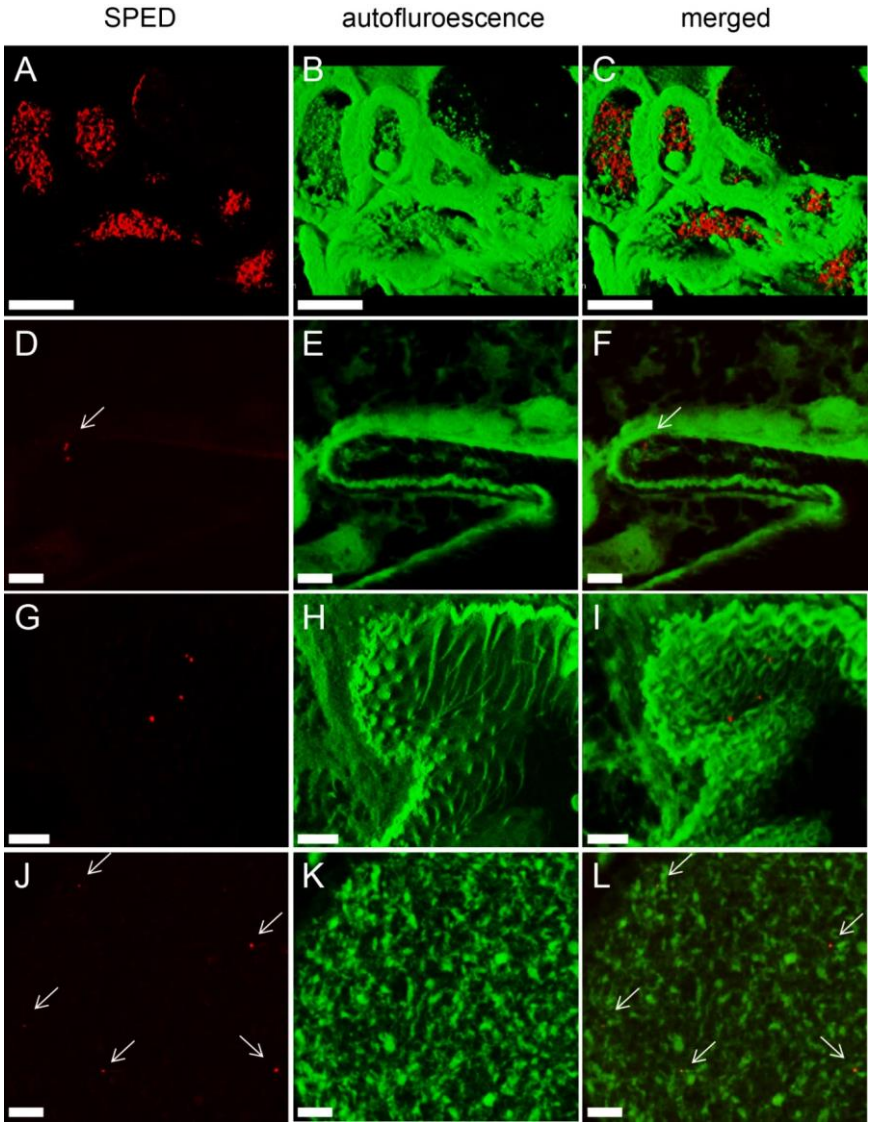

Figure A.1.2. *Additional confocal microscopy images of the gut and exoskeletal region of D. melanogaster fed with fluorescent SPED1 particles. Rhodamine-labeled particles were detected at Ex = 561 nm/Em = 605(30) nm (red color). Biological structures were visualized by autofluorescence at Ex = 405 nm/Em = 447(32) (green color). All images display histological sections (d = 12 µm) of D. melanogaster cultured on medium containing SPED1 (c = 6 x 10^8 mm^{-2}) or sicastar®-redF 1 µm particles embedded in paraffin.* ***(A-C)*** *Overview of the digestive tract of a D. melanogaster fly immediately after feeding for t = 4 h on labeled medium. This image is the same as shown in Fig. 2C a-c but with a lower zoom factor. Scale bars, 100 µm.* ***(D-F)*** *These images shows SPED1 particles on the bottom exoskeleton crevice (indicated with a white arrow) and* ***(G-H)*** *in a trachea opening of a fly after transfer for t = 4 d to a SPED-free medium.* ***(J-K)*** *Cross-section of a digestive tube of a fly after transfer for t = 7 d to a SPED-free medium. Particles are indicated by a white arrow. Scale bars, 10 µm.*

A.1.3 Uptake comparison of differently labelled SPED

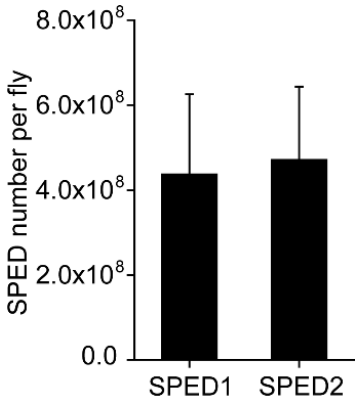

Figure A.1.3. *Uptake comparison of differently labeled SPED for single D. melanogaster flies. Measurements were made from single flies. The difference between SPED1 and SPED2 is not significant, tested with analysis of variance and Mann-Whitney test. ±SEMs (N = 9).*

A.1.4 Validation of fluorescent particle uptake

For validation purposes we first fed the bigger 1 µm particles to *D. melanogaster* flies by applying 100 µL of a 5 mg/mL particle suspension to nutrient medium and allowing the flies to feed for 4 hours. Afterwards, we verified their presence and location in the fly before assessing the one order of magnitude smaller SPED1 particles (100 nm). We could clearly identify the bigger particles in the digestive tract of the flies (**Figure A.1.4A-C**). Images of flies containing no SPED were made to adjust the background fluorescence (**Figure A.1.4D-F**).

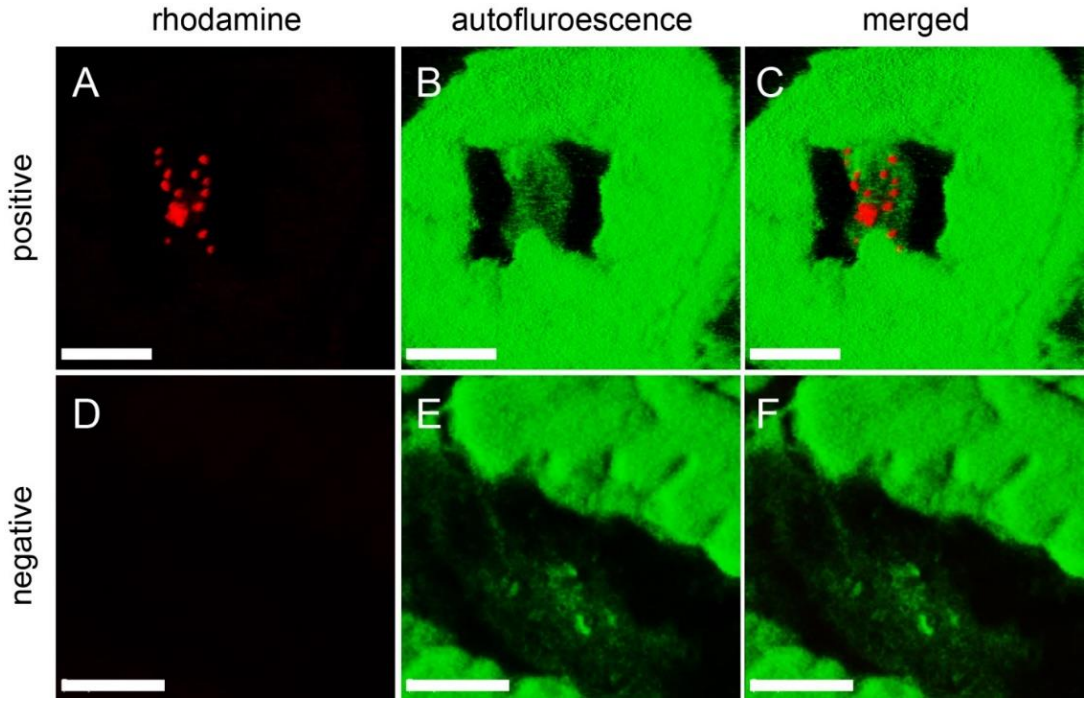

Figure A.1.4. *Reference images of Drosophila fed with larger fluorescent particles and negative control. Rhodamine-labeled particles were detected at Ex = 561 nm/Em = 605(30) nm (red color). Biological structures were visualized by auto-fluorescence (AF) at Ex = 405 nm/Em = 447(32) (green color).* ***(A-C)*** *Images of a digestive tube of a fly fed with non-functionalized sicastar®-redF particles (size = 1 µm) for 4 hours.* ***(D-F)*** *Images of a digestive tube of a fly that has not come into contact with SPED particles. Scale bars, 20 µm.*

A.1.5 Non-template qPCR controls

Non-template qPCR controls for the DNA labels of SPED2 and SPED3 showed no amplification. Only for the SPED1 DNA label in 7 out of 9 cases amplification could be detected corresponding to $4 \cdot 10^3$ particles on average, which is probably due to contamination. (**Figure A.1.5**). This observed NTC amplification had no influence on the main results shown.

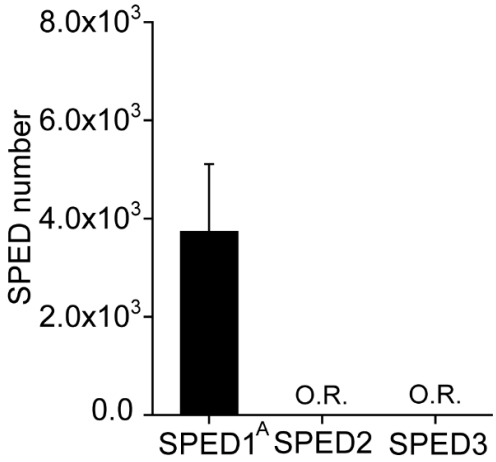

Figure A.1.5. *Limit of detection of qPCR quantitation (No Template Control, NTC). The average and SEM in brackets (n = 3) is displayed.* [A] *Average of seven out of nine independent qPCR analyses, i.e. in two cases NTC did not amplify at all. O.R.: Out of Range, i.e. NTC did not amplify below* $C_t = 45$.

A.2 Supplementary data for Chapter 3

A.2.1 qPCR standard curve

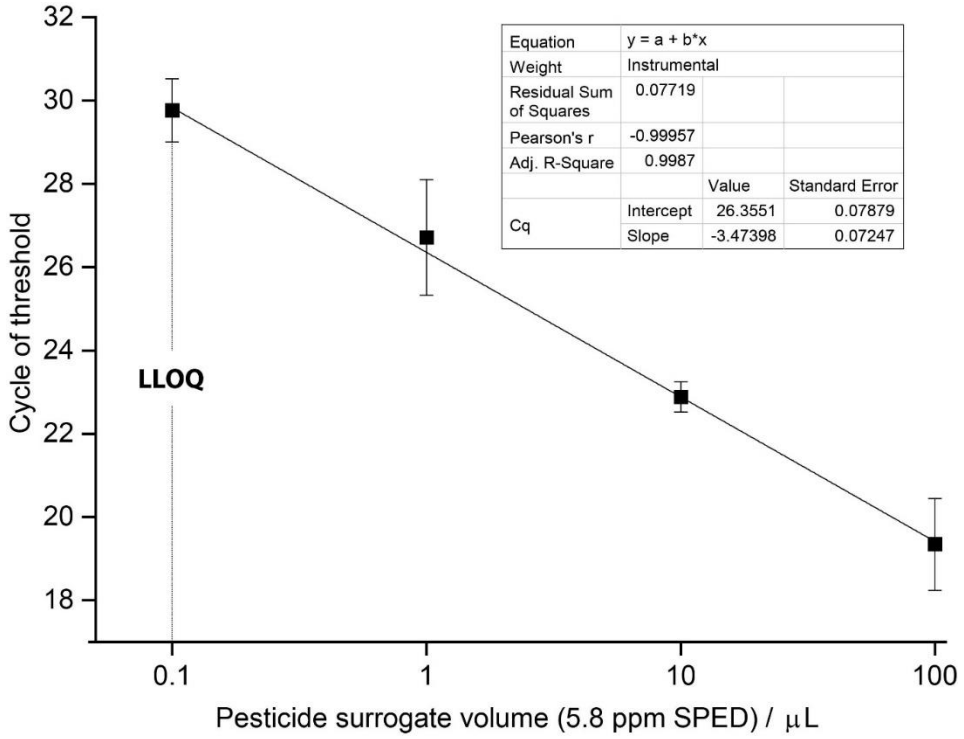

Figure A.2.1. *Standard curve for converting cycle threshold to pesticide volume. The lower limit of quantification (LLOQ) was determined as the lowest amount of pesticide surrogate volume that is covered by the standard curve, n = 3.*

A.2.2 Pesticide distribution profile

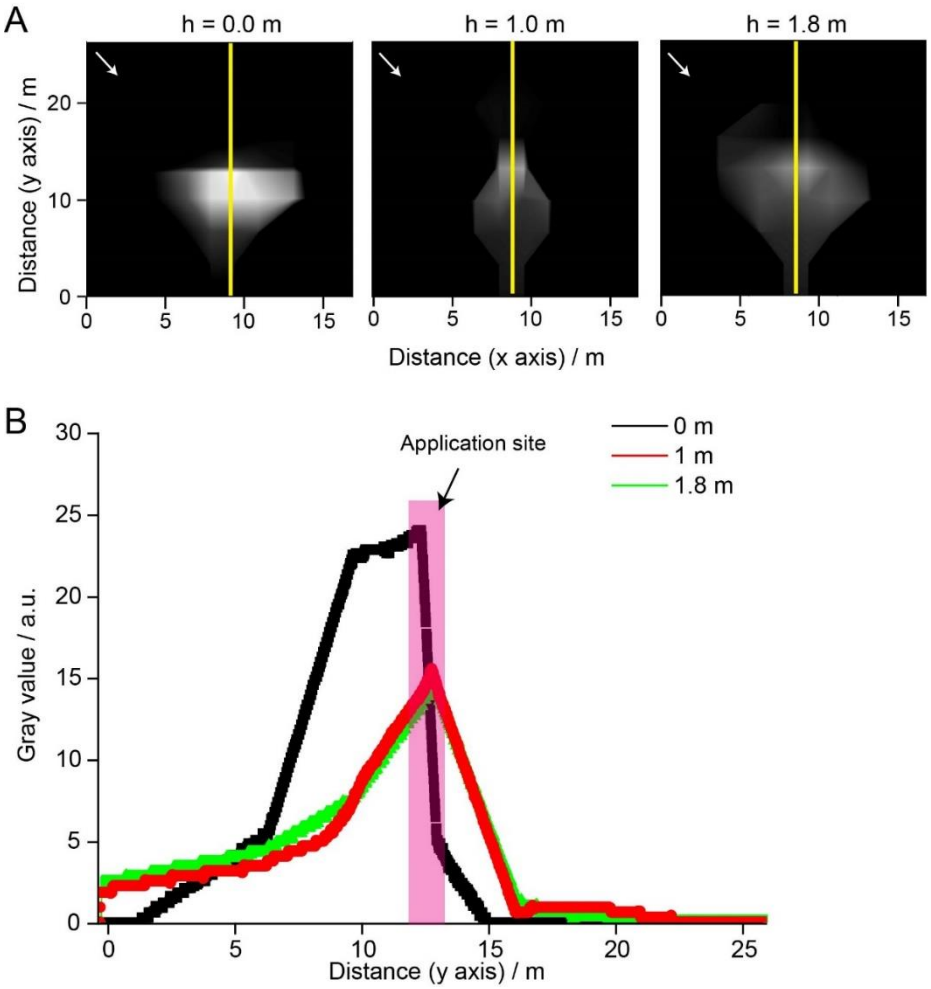

Figure A.2.2. *Longitudinal pesticide distribution profile at different sampling heights. (A) Contour plots of Figure 3 were converted to gray scale images. The gray value increases with a higher pesticide load per area. A gray value profile was created along the yellow line. The white arrows depict the wind direction. (B) The gray value profile was plotted against the y-axis of the contour plots. The pink area depicts the range of pesticide application, the grey areas depict the range, where no sampling was done.*

A.2.3 Calculation of (recovered) deposited volume

We approximately calculated the volume of SPED-labeled test liquid deposited on (horizontal) ground level. For simplification we defined a 'high deposition' area having a ground deposition > 1 µL cm^{-2}, since lower amounts are negligible for an approximate calculation (**Figure A.2.3**). This 'high deposition' area comprised approximately 20 m^2 with an average deposition of ca. 20 µL cm^{-2}. This resulted in a ground deposition of ca. 4 L, which is in the same order of magnitude as the sprayed volume (1.9 L). This value is not exact, due to interpolation and a complex environment. More data points per area in a controlled environment need to be taken to determine an exact mass balance.

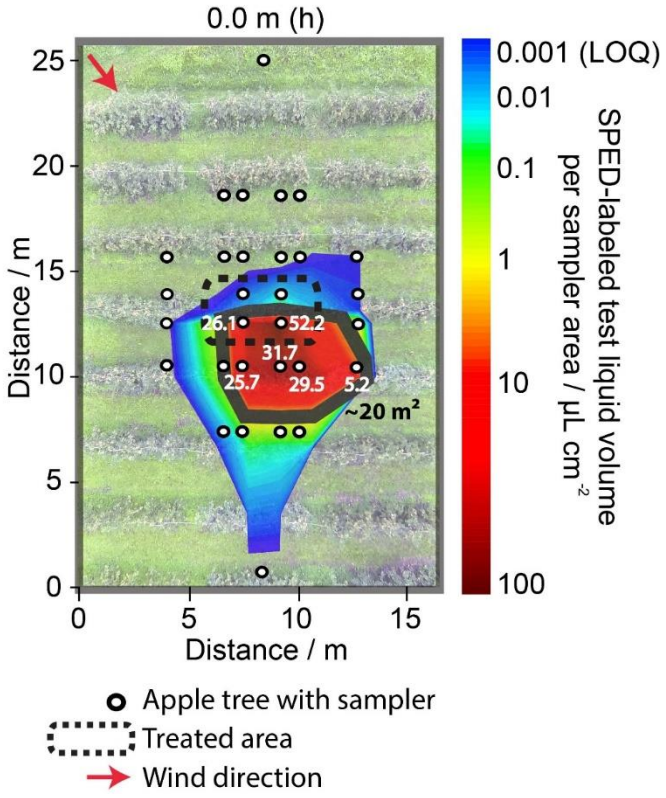

Figure A.2.3. *Calculation of (recovered) deposited volume on ground level, i.e. mass balance. A 'high deposition' area (~20 m^2) with > 1 µL cm^{-2} was defined. The measured volumes per sampler (µL cm^{-2}) are directly indicated in the graph. The average deposition over the whole 'high-deposition' area was approximately 20 µL cm^{-2}.*

References

1. Currie, L. A. Nomenclature in evaluation of analytical methods including detection and quantification capabilities (IUPAC Recommendations 1995). *Pure and Applied Chemistry* **1995**, 67, 1699.

2. Trullols, E.; Ruisánchez, I.; Rius, F. X. Validation of qualitative analytical methods. *TrAC Trends in Analytical Chemistry* **2004**, 23, 137-145.

3. Skoog, D. A.; Holler, F. J.; Crouch, S. R. *Principles of instrumental analysis*. 6th ed ed.; Thomson, Brooks/Cole: Belmont, CA, **2007**.

4. Giustarini, D.; Rossi, R.; Milzani, A.; Dalle-Donne, I. Nitrite and nitrate measurement by Griess reagent in human plasma: Evaluation of interferences and standardization. *Methods in Enzymology* **2008**, 440, 361-380.

5. Engvall, E.; Perlmann, P. Enzyme-linked immunosorbent assay (ELISA) quantitative assay of immunoglobulin G. *Immunochemistry* **1971**, 8, 871-874.

6. Bartle, K. D.; Myers, P. History of gas chromatography. *TrAC Trends in Analytical Chemistry* **2002**, 21, 547-557.

7. Tonyushkina, K.; Nichols, J. H. Glucose meters: A review of technical challenges to obtaining accurate results. *Journal of Diabetes Science and Technology* **2009**, 3, 971-980.

8. Voet, D.; Voet, J. G.; Pratt, C. W. *Fundamentals of Biochemistry*. 2nd ed.; John Wiley & Sons, Inc.: Hoboken, USA, **2006**.

9. Nealon, C. M.; Musa, M. M.; Patel, J. M.; Phillips, R. S. Controlling substrate specificity and stereospecificity of alcohol dehydrogenases. *ACS Catalysis* **2015**, 5, 2100-2114.

10. Goddard, J.-P.; Reymond, J.-L. Recent advances in enzyme assays. *Trends in Biotechnology* **2004**, 22, 363-370.

11. Guilbault, G. G. Use of enzymes in analytical chemistry. *Analytical Chemistry* **1968**, 40, 459-471.

12. Bartholomew, B. A rapid method for the assay of nitrate in urine using the nitrate reductase enzyme of Escherichia coli. *Food and Chemical Toxicology* **1984**, 22, 541-543.

13. Kindt, T. J.; Goldsby, R. A.; Osborne, B. A.; Kuby, J. Kuby Immunology. In *Kuby Immunology*, 6th ed. ed.; W.H. Freeman and Company: New York, USA, **2007**.

14. Milstein, C. The hybridoma revolution: an offshoot of basic research. *BioEssays* **1999**, 21, 966-973.

15. Diaz-Amigo, C. Antibody-Based detection methods: From theory to practice. In *Molecular biological and immunological techniques and applications for food chemists*, Popping, B.; Diaz-Amigo, C.; Hoenicke, K., Eds. John Wiley & Sons, Inc.: Hoboken, USA, **2009**; 221-245.

16. Thomas, P. S. Hybridization of denatured RNA and small DNA fragments transferred to nitrocellulose. *Proceedings of the National Academy of Sciences of the United States of America* **1980**, 77, 5201-5205.

17. Southern, E. M. Detection of specific sequences among DNA fragments separated by gel electrophoresis. *Journal of Molecular Biology* **1975**, 98, 503-517.

18. Schena, M.; Shalon, D.; Davis, R. W.; Brown, P. O. Quantitative monitoring of gene expression patterns with a complementary DNA microarray. *Science* **1995**, 270, 467-470.

19. Kuzuya, A.; Watanabe, R.; Yamanaka, Y.; Tamaki, T.; Kaino, M.; Ohya, Y. Nanomechanical DNA origami pH sensors. *Sensors* **2014**, 14, 19329-35.

20. Bell, N. A. W.; Engst, C. R.; Ablay, M.; Divitini, G.; Ducati, C.; Liedl, T.; Keyser, U. F. DNA origami nanopores. *Nano Letters* **2012**, 12, 512-517.

21. Melkko, S.; Scheuermann, J.; Dumelin, C. E.; Neri, D. Encoded self-assembling chemical libraries. *Nature Biotech* **2004**, 22, 568-574.

22. Paunescu, D.; Stark, W. J.; Grass, R. N. Particles with an identity: Tracking and tracing in commodity products. *Powder Technology* **2016**, 291, 344-350.

23. Sabir, H. I.; Torgersen, J.; Haldorsen, S.; Aleström, P. DNA tracers with information capacity and high detection sensitivity tested in groundwater studies. *Hydrogeology Journal* **2002**, 7, 264-272.

24. Foppen, J. W.; Orup, C.; Adell, R.; Poulalion, V.; Uhlenbrook, S. Using multiple artificial DNA tracers in hydrology. *Hydrological Processes* **2011**, 25, 3101-3106.

25. Eustaquio, T.; Leary, J. F. Nanobarcoding: detecting nanoparticles in biological samples using in situ polymerase chain reaction. *International Journal of Nanomedicine* **2012**, 7, 5625-5639.

26. Tateishi-Karimata, H.; Sugimoto, N. Structure, stability and behaviour of nucleic acids in ionic liquids. *Nucleic Acids Research* **2014**, 42, 8831–8844.

27. Sharma, V.; Narayanan, A.; Rengachari, T.; Temes, G. C.; Chaplen, F.; Moon, U. K. A low-cost, portable generic biotoxicity assay for environmental monitoring applications. *Biosensors and Bioelectronics* **2005**, 20, 2218-2227.

28. Naylor, L. H. Reporter gene technology: the future looks bright. *Biochemical Pharmacology* **1999**, 58, 749-757.

29. Phyu, Y. L.; Warne, M. S. J.; Lim, R. P. Effect of river water, sediment and time on the toxicity and bioavailability of molinate to the marine bacterium *Vibrio fischeri* (Microtox). *Water Research* **2005**, 39, 2738-2746.

30. Védrine, C.; Leclerc, J.-C.; Durrieu, C.; Tran-Minh, C. Optical whole-cell biosensor using Chlorella vulgaris designed for monitoring herbicides. *Biosensors and Bioelectronics* **2003**, 18, 457-463.

31. Hernandez Espitia, C. A.; Osma, J. F. Whole cell biosensors. In *Biosensors: Recent advances and mathematical challenges*, Osma, J. F.; Stoytcheva, M., Eds. OmniaScience Monographs: **2014**; 51-96.

32. Lindahl, T.; Nyberg, B. Rate of depurination of native deoxyribonucleic acid. *Biochemistry* **1972**, 11, 3610-3618.

33. Bonnet, J.; Colotte, M.; Coudy, D.; Couallier, V.; Portier, J.; Morin, B.; Tuffet, S. Chain and conformation stability of solid-state DNA: implications for room temperature storage. *Nucleic Acids Research* **2010**, 38, 1531-1546.

34. Evans, R. K.; Xu, Z.; Bohannon, K. E.; Wang, B.; Bruner, M. W.; Volkin, D. B. Evaluation of degradation pathways for plasmid DNA in pharmaceutical formulations via accelerated stability studies. *Journal of Pharmaceutical Sciences* **2000**, 89, 76-87.

35. Buchanan, J. T.; Simpson, A. J.; Aziz, R. K.; Liu, G. Y.; Kristian, S. A.; Kotb, M.; Feramisco, J.; Nizet, V. DNase expression allows the pathogen group A *Streptococcus* to escape killing in neutrophil extracellular traps. *Current Biology* **2006**, 16, 396-400.

36. Lindahl, T.; Andersson, A. Rate of chain breakage at apurinic sites in double-stranded deoxyribonucleic acid. *Biochemistry* **1972**, 11, 3618-3623.

37. Suzuki, T.; Ohsumi, S.; Makino, K. Mechanistic studies on depurination and apurinic site chain breakage in oligodeoxyribonucleotides. *Nucleic Acids Research* **1994**, 22, 4997-5003.

38. Kuluncsics, Z.; Perdiz, D.; Brulay, E.; Muel, B.; Sage, E. Wavelength dependence of ultraviolet-induced DNA damage distribution: Involvement of direct or indirect mechanisms and possible artefacts. *Journal of Photochemistry and Photobiology B* **1999**, 49, 71-80.

39. Lindahl, T. Instability and decay of the primary structure of DNA. *Nature* **1993**, 362, 709-715.

40. Stöber, W.; Fink, A.; Bohn, E. Controlled growth of monodisperse silica spheres in the micron size range. *Journal of Colloid and Interface Science* **1968**, 26, 62-69.

41. Paunescu, D.; Fuhrer, R.; Grass, R. N. Protection and deprotection of DNA - high-temperature stability of nucleic acid barcodes for polymer labeling. *Angewandte Chemie - International Edition* **2013**, 52, 4269-4272.

42. Paunescu, D.; Puddu, M.; Soellner, J. O. B.; Stoessel, P. R.; Grass, R. N. Reversible DNA encapsulation in silica to produce ROS-resistant and heat-resistant synthetic DNA 'fossils'. *Nature Protocols* **2013**, 8, 2440-2448.

43. Grass, R. N.; Schälchli, J.; Paunescu, D.; Soellner, J. O. B.; Kaegi, R.; Stark, W. J. Tracking trace amounts of submicrometer silica particles in wastewaters and activated sludge using silica-encapsulated DNA barcodes. *Environmental Science & Technology Letters* **2014**, 1, 484-489.

44. Bloch, M. S.; Paunescu, D.; Stoessel, P. R.; Mora, C. A.; Stark, W. J.; Grass, R. N. Labeling milk along its production chain with DNA encapsulated in silica. *Journal of Agricultural and Food Chemistry* **2014**, 62, 10615-10620.

45. Mikutis, G.; Mora, C. A.; Puddu, M.; Paunescu, D.; Grass, R. N.; Stark, W. J. DNA-based sensor particles enable measuring light intensity in single cells. *Advanced Materials* **2016**, 14, 2765–2770.

46. Puddu, M.; Paunescu, D.; Stark, W. J.; Grass, R. N. Magnetically recoverable, thermostable, hydrophobic DNA/silica encapsulates and their application as invisible oil tags. *ACS Nano* **2014**, 8, 2677-2685.

47. Paunescu, D.; Mora, C. A.; Puddu, M.; Krumeich, F.; Grass, R. N. DNA protection against ultraviolet irradiation by encapsulation in a multilayered SiO2/TiO2 assembly. *Journal of Materials Chemistry B* **2014**, 2, 8504-8509.

48. Grass, R. N.; Heckel, R.; Puddu, M.; Paunescu, D.; Stark, W. J. Robust chemical preservation of digital information on DNA in silica with error-correcting codes. *Angewandte Chemie International Edition* **2015**, 54, 2552-2555.

49. Lyngberg, O. K.; Stemke, D. J.; Schottel, J. L.; Flickinger, M. C. A single-use luciferase-based mercury biosensor using *Escherichia coli* HB101 immobilized in a latex copolymer film. *Journal of Industrial Microbiology and Biotechnology* **1999**, 23, 668-676.

50. Gerber, L. C.; Koehler, F. M.; Grass, R. N.; Stark, W. J. Incorporating microorganisms into polymer layers provides bioinspired functional living materials. *Proceedings of the National Academy of Sciences* **2012**, 109, 90-94.

51. Gerber, L. C.; Koehler, F. M.; Grass, R. N.; Stark, W. J. Incorporation of penicillin-producing fungi into living materials to provide chemically active and antibiotic-releasing surfaces. *Angewandte Chemie - International Edition* **2012**, 51, 11293-11296.

52. Pimm, S. L. Food webs. In *Food webs*, Usher, M. B.; Rosenzweig, M. L., Eds. Springer Netherlands: **1982**; 1-11.

53. Sheppard, S. K.; Harwood, J. D. Advances in molecular ecology: tracking trophic links through predator-prey food-webs. *Functional Ecology* **2005**, 19, 751-762.

54. Montoya, J. M.; Pimm, S. L.; Solé, R. V. Ecological networks and their fragility. *Nature* **2006**, 442, 259-264.

55. Corse, E.; Costedoat, C.; Chappaz, R.; Pech, N.; Martin, J.-F.; Gilles, A. A PCR-based method for diet analysis in freshwater organisms using 18S rDNA barcoding on faeces. *Molecular Ecology Resources* **2010**, 10, 96-108.

56. King, R. A.; Read, D. S.; Traugott, M.; Symondson, W. O. C. Molecular analysis of predation: a review of best practice for DNA-based approaches. *Molecular Ecology* **2008**, 17, 947-963.

57. Pompanon, F.; Deagle, B. E.; Symondson, W. O. C.; Brown, D. S.; Jarman, S. N.; Taberlet, P. Who is eating what: diet assessment using next generation sequencing. *Molecular Ecology* **2012**, 21, 1931-1950.

58. Boreham, P. F. L.; Ohiagu, C. E. The use of serology in evaluating invertebrate prey-predator relationships : a review. *Bulletin of Entomological Research* **1978**, 68, 171-194.

59. Hebert, C. E.; Arts, M. T.; Weseloh, D. V. C. Ecological tracers can quantify food web structure and change. *Environmental Science & Technology* **2006**, 40, 5618-5623.

60. DeNiro, M. J.; Epstein, S. Influence of diet on the distribution of carbon isotopes in animals. *Geochimica et Cosmochimica Acta* **1978**, 42, 495-506.

61. DeNiro, M. J.; Epstein, S. Influence of diet on the distribution of nitrogen isotopes in animals. *Geochimica et Cosmochimica Acta* **1981**, 45, 341-351.

62. Peterson, B. J.; Howarth, R. W.; Garrit, R. H. Multiple stable isotopes used to trace the flow of organic matter in estuarine food webs. *Science* **1985**, 227, 1361-1363.

63. Minagawa, M.; Wada, E. Stepwise enrichment of 15N along food chains: Further evidence and the relation between δ15N and animal age. *Geochimica et Cosmochimica Acta* **1984**, 48, 1135-1140.

64. Cabana, G.; Rasmussen, J. B. Modelling food chain structure and contaminant bioaccumulation using stable nitrogen isotopes. *Nature* **1994**, 372, 255-257.

65. Smith, D. F.; Bulleid, N. C.; Campbell, R.; Higgins, H. W.; Rowe, F.; Tranter, D. J.; Tranter, H. Marine food-web analysis: An experimental study of demersal zooplankton using isotopically labelled prey species. *Marine Biology* **1979**, 54, 49-59.

66. Epstein, S.; Rossel, J. Methodology of in situ grazing experiments: evaluation of a new vital dye for preparation of fluorescently labeled bacteria. *Marine Ecology Progress Series* **1995**, 128, 143-150.

67. McManus, G. B.; Okubo, A. On the use of surrogate food particles to measure protistan ingestion. *Limnology and Oceanography* **1991**, 36, 613-617.

68. Carreon-Martinez, L.; Heath, D. D. Revolution in food web analysis and trophic ecology: diet analysis by DNA and stable isotope analysis. *Molecular Ecology* **2010**, 19, 25-27.

69. Hesslein, R. H.; Hallard, K. A.; Ramlal, P. Replacement of sulfur, carbon, and nitrogen in tissue of growing broad whitefish (*Coregonus nasus*) in response to a change in diet traced by $\delta^{34}S$, $\delta^{13}C$, and $\delta^{15}N$. *Canadian Journal of Fisheries and Aquatic Sciences* **1993**, 50, 2071-2076.

70. Sakano, H.; Fujiwara, E.; Nohara, S.; Ueda, H. Estimation of nitrogen stable isotope turnover rate of *Oncorhynchus nerka*. *Environmental Biology of Fishes* **2005**, 72, 13-18.

71. Maruyama, A.; Yamada, Y.; Rusuwa, B.; Yuma, M. Change in stable nitrogen isotope ratio in the muscle tissue of a migratory goby, *Rhinogobius sp.*, in a natural setting. *Canadian Journal of Fisheries and Aquatic Sciences* **2001**, 58, 2125-2128.

72. VanGuilder, H. D.; Vrana, K. E.; Freeman, W. M. Twenty-five years of quantitative PCR for gene expression analysis. *Biotechniques* **2008**, 44, 619-26.

73. Flörke, O. W.; Graetsch, H. A.; Brunk, F.; Benda, L.; Paschen, S.; Bergna, H. E.; Roberts, W. O.; Welsh, W. A.; Libanati, C.; Ettlinger, M.; Kerner, D.; Maier, M.; Meon, W.; Schmoll, R.; Gies, H.; Schiffmann, D. Silica. In *Ullmann's Encyclopedia of Industrial Chemistry*, Wiley-VCH: **2000**; 442-507.

74. Brunner, T. J.; Wick, P.; Manser, P.; Spohn, P.; Grass, R. N.; Limbach, L. K.; Bruinink, A.; Stark, W. J. In vitro cytotoxicity of oxide nanoparticles: comparison to asbestos, silica, and the effect of particle solubility. *Environmental Science & Technology* **2006**, 40, 4374-4381.

75. Zhang, H.; Dunphy, D. R.; Jiang, X.; Meng, H.; Sun, B.; Tarn, D.; Xue, M.; Wang, X.; Lin, S.; Ji, Z.; Li, R.; Garcia, F. L.; Yang, J.; Kirk, M. L.; Xia, T.; Zink, J. I.; Nel, A.; Brinker,

C. J. Processing pathway dependence of amorphous silica nanoparticle toxicity: colloidal vs pyrolytic. *Journal of the American Chemical Society* **2012**, 134, 15790-15804.

76. Faegri, K.; Pijl, L. v. d. *The principles of pollination ecology*. 3rd ed.; Pergamon Press: Amsterdam, **1979**.

77. Foelix, R. F. *Biology of spiders*. 3rd ed.; Oxford University Press: Oxford, **2011**.

78. Arnold, S. J.; Savolainen, V.; Chittka, L. Flower colours along an alpine altitude gradient, seen through the eyes of fly and bee pollinators. *Arthropod-Plant Interactions* **2009**, 3, 27-43.

79. Rader, R.; Howlett, B. G.; Cunningham, S. A.; Westcott, D. A.; Newstrom-Lloyd, L. E.; Walker, M. K.; Teulon, D. A. J.; Edwards, W. Alternative pollinator taxa are equally efficient but not as effective as the honeybee in a mass flowering crop. *Journal of Applied Ecology* **2009**, 46, 1080-1087.

80. Hohlweg, U.; Doerfler, W. On the fate of plant or other foreign genes upon the uptake in food or after intramuscular injection in mice. *Molecular Genetics and Genomics* **2001**, 265, 225-233.

81. Vansant, E. F.; Vrancken, K. C.; Voort, P. v. d. *Characterization and chemical modification of the silica surface*. Elsevier: Amsterdam, **1995**.

82. Alavanja, M. C. R. Pesticides Use and Exposure Extensive Worldwide. *Reviews on Environmental Health* **2009**, 24, 303-309.

83. Cooper, J.; Dobson, H. The benefits of pesticides to mankind and the environment. *Crop Protection* **2007**, 26, 1337-1348.

84. Guyton, K. Z.; Loomis, D.; Grosse, Y.; El Ghissassi, F.; Benbrahim-Tallaa, L.; Guha, N.; Scoccianti, C.; Mattock, H.; Straif, K. Carcinogenicity of tetrachlorvinphos, parathion, malathion, diazinon, and glyphosate. *The Lancet Oncology* **2015**, 16, 490-491.

85. Hallmann, C. A.; Foppen, R. P. B.; van Turnhout, C. A. M.; de Kroon, H.; Jongejans, E. Declines in insectivorous birds are associated with high neonicotinoid concentrations. *Nature* **2014**, 511, 341-343.

86. Browne, A. W.; Harris, P. J. C.; Hofny-Collins, A. H.; Pasiecznik, N.; Wallace, R. R. Organic production and ethical trade: definition, practice and links. *Food Policy* **2000**, 25, 69-89.

87. Ahrens, L.; Daneshvar, A.; Lau, A. E.; Kreuger, J. Characterization of five passive sampling devices for monitoring of pesticides in water. *Journal of Chromatography A* **2015**, 1405, 1-11.

88. Briand, O.; Bertrand, F.; Seux, R.; Millet, M. Comparison of different sampling techniques for the evaluation of pesticide spray drift in apple orchards. *Science of The Total Environment* **2002**, 288, 199-213.

89. Bonmatin, J. M.; Marchand, P. A.; Charvet, R.; Moineau, I.; Bengsch, E. R.; Colin, M. E. Quantification of imidacloprid uptake in maize crops. *Journal of Agricultural and Food Chemistry* **2005**, 53, 5336-5341.

90. Raina, R.; Sun, L. Trace level determination of selected organophosphorus pesticides and their degradation products in environmental air samples by liquid chromatography-positive ion electrospray tandem mass spectrometry. *Journal of Environmental Science and Health, Part B* **2008**, 43, 323-332.

91. Barker, Z.; Venkatchalam, V.; Martin, A. N.; Farquar, G. R.; Frank, M. Detecting trace pesticides in real time using single particle aerosol mass spectrometry. *Analytica Chimica Acta* **2010**, 661, 188-194.

92. Viveros, L.; Paliwal, S.; McCrae, D.; Wild, J.; Simonian, A. A fluorescence-based biosensor for the detection of organophosphate pesticides and chemical warfare agents. *Sensors and Actuators, B: Chemical* **2006**, 115, 150-157.

93. Wang, J.; Chen, D.; Xu, Y.; Liu, W. Label-free immunosensor based on micromachined bulk acoustic resonator for the detection of trace pesticide residues. *Sensors and Actuators B: Chemical* **2014**, 190, 378-383.

94. Barber, J. A. S.; Parkin, C. S. Fluorescent tracer technique for measuring the quantity of pesticide deposited to soil following spray applications. *Crop Protection* **2003**, 22, 15-21.

95. MacIntyre-Allen, J. K.; Tolman, J. H.; Scott-Dupree, C. D.; Harris, C. R. Confirmation by fluorescent tracer of coverage of onion leaves for control of onion thrips using selected nozzles, surfactants and spray volumes. *Crop Protection* **2007**, 26, 1625-1633.

96. Staffa, C.; Fent, G.; Seitz, F.; Kubiak, R. Spray Drift application of Plant Protection Products: Semi-outdoor experiments to investigate transport and non-target plant deposition. In *59. Deutsche Pflanzenschutztagung "Forschen-Wissen-Pflanzen schützen: Ernährung sichern!", 23.-26. September 2014* Julius-Kühn-Archiv: Freiburg, **2014**; Vol. 447.

97. Field, M.; Wilhelm, R.; Quinlan, J.; Aley, T. An assessment of the potential adverse properties of fluorescent tracer dyes used for groundwater tracing. *Environmental Monitoring and Assessment* **1995**, 38, 75-96.

98. Goldscheider, N.; Meiman, J.; Pronk, M.; Smart, C. Tracer tests in karst hydrogeology and speleology. *International Journal of Speleology* **2008**, 37, 27-40.

99. Mora, C. A.; Paunescu, D.; Grass, R. N.; Stark, W. J. Silica particles with encapsulated DNA as trophic tracers. *Molecular Ecology Resources* **2015**, 15, 231-241.

100. Hoop, M.; Paunescu, D.; Stoessel, P. R.; Eichenseher, F.; Stark, W. J.; Grass, R. N. PCR quantification of SiO2 particle uptake in cells in the ppb and ppm range via silica encapsulated DNA barcodes. *Chemical Communications* **2014**, 50, 10707-10709.

101. Paunescu, D.; Mora, C. A.; Querci, L.; Heckel, R.; Puddu, M.; Hattendorf, B.; Günther, D.; Grass, R. N. Detecting and number counting of single engineered nanoparticles by digital particle polymerase chain reaction. *ACS Nano* **2015**, 9, 9564-72.

102. Schneider, C. A.; Rasband, W. S.; Eliceiri, K. W. NIH Image to ImageJ: 25 years of image analysis. *Nature Methods* **2012**, 9, 671-675.

103. Alexander, G. B.; Heston, W. M.; Iler, R. K. The solubility of amorphous silica in water. *The Journal of Physical Chemistry* **1954**, 58, 453-455.

104. Hu, X.; Gao, X. Silica−polymer dual layer-encapsulated quantum dots with remarkable stability. *ACS Nano* **2010**, 4, 6080-6086.

105. Mondragon, R.; Julia, J. E.; Barba, A.; Jarque, J. C. Characterization of silica–water nanofluids dispersed with an ultrasound probe: A study of their physical properties and stability. *Powder Technology* **2012**, 224, 138-146.

106. Al-Anssari, S.; Barifcani, A.; Wang, S.; Maxim, L.; Iglauer, S. Wettability alteration of oil-wet carbonate by silica nanofluid. *Journal of Colloid and Interface Science* **2016**, 461, 435-442.

107. Stuart, M. A. C.; Huck, W. T. S.; Genzer, J.; Muller, M.; Ober, C.; Stamm, M.; Sukhorukov, G. B.; Szleifer, I.; Tsukruk, V. V.; Urban, M.; Winnik, F.; Zauscher, S.; Luzinov, I.; Minko, S. Emerging applications of stimuli-responsive polymer materials. *Nature Materials* **2010**, 9, 101-113.

108. Hager, M. D.; Greil, P.; Leyens, C.; van der Zwaag, S.; Schubert, U. S. Self-healing materials. *Advanced Materials* **2010**, 22, 5424-5430.

109. Rotzetter, A. C. C.; Schumacher, C. M.; Bubenhofer, S. B.; Grass, R. N.; Gerber, L. C.; Zeltner, M.; Stark, W. J. Thermoresponsive polymer induced sweating surfaces as an efficient way to passively cool buildings. *Advanced Materials* **2012**, 24, 5352-5356.

110. Loher, S.; Schneider, O. D.; Maienfisch, T.; Bokorny, S.; Stark, W. J. Micro-organism-triggered release of silver nanoparticles from biodegradable oxide carriers allows preparation of self-sterilizing polymer surfaces. *Small* **2008**, 4, 824-832.

111. Halter, J. G.; Cohrs, N. H.; Hild, N.; Paunescu, D.; Grass, R. N.; Stark, W. J. Self-defending anti-vandalism surfaces based on mechanically triggered mixing of reactants in polymer foils. *Journal of Materials Chemistry A* **2014**, 2, 8425-8430.

112. Langer, R.; Tirrell, D. A. Designing materials for biology and medicine. *Nature* **2004**, 428, 487-492.

113. Nelson, M.; Ogden, J. An exploration of food intolerance in the primary care setting: The general practitioner's experience. *Social Science & Medicine* **2008**, 67, 1038-1045.

114. Sicherer, S. H.; Sampson, H. A. Food allergy. *Journal of Allergy and Clinical Immunology* **2006**, 117, 470-475.

115. Yanyan, L.; Yingchun, Z.; Yu, Y. Processing of Biosensing Materials and Biosensors. In *Biomaterials Fabrication and Processing Handbook*, CRC Press: **2008**; 401-453.

116. Vo-Dinh, T.; Cullum, B. Biosensors and biochips: advances in biological and medical diagnostics. *Fresenius' Journal of Analytical Chemistry* **2000**, 366, 540-551.

117. Belkin, S. Microbial whole-cell sensing systems of environmental pollutants. *Current Opinion in Microbiology* **2003**, 6, 206-212.

118. Yagi, K. Applications of whole-cell bacterial sensors in biotechnology and environmental science. *Applied Microbiology and Biotechnology* **2007**, 73, 1251-1258.

119. Belkin, S.; Alhadrami, H. A. *Whole cell sensing systems II applications*. Springer Verlag: Berlin, **2010**.

120. Bonev, B.; Hooper, J.; Parisot, J. Principles of assessing bacterial susceptibility to antibiotics using the agar diffusion method. *Journal of Antimicrobial Chemotherapy* **2008**, 61, 1295-1301.

121. Finn, R. K. Theory of agar diffusion methods for bioassay. *Analytical Chemistry* **1959**, 31, 975-977.

122. Tahrioui, A.; Schwab, M.; Quesada, E.; Llamas, I. Quorum sensing in some representative species of halomonadaceae. *Life* **2013**, 3, 260-275.

123. Mancini, G.; Carbonara, A. O.; Heremans, J. F. Immunochemical quantitation of antigens by single radial immunodiffusion. *Immunochemistry* **1965**, 2, 235-54.

124. De León, A.; Breceda, G.; Barba de la Rosa, A.; Jiménez-Bremont, J.; López-Revilla, R. Galactose induces the expression of penicillin acylase under control of the lac promoter in recombinant Escherichia coli. *Biotechnology Letters* **2003**, 25, 1397-1402.

125. Olano, A.; Calvo, M. M.; Corzo, N. Changes in the carbohydrate fraction of milk during heating processes. *Food Chemistry* **1989**, 31, 259-265.

126. Farewell, A.; Neidhardt, F. C. Effect of temperature on *in vivo* protein synthetic capacity in *Escherichia coli*. *Journal of Bacteriology* **1998**, 180, 4704-4710.

127. Daber, R.; Stayrook, S.; Rosenberg, A.; Lewis, M. Structural analysis of lac repressor bound to allosteric effectors. *Journal of Molecular Biology* **2007**, 370, 609-619.

128. Portnoi, P. A.; MacDonald, A. Determination of the lactose and galactose content of cheese for use in the galactosaemia diet. *Journal of Human Nutrition and Dietetics* **2009**, 22, 400-408.

129. Mandell, D. J.; Lajoie, M. J.; Mee, M. T.; Takeuchi, R.; Kuznetsov, G.; Norville, J. E.; Gregg, C. J.; Stoddard, B. L.; Church, G. M. Biocontainment of genetically modified organisms by synthetic protein design. *Nature* **2015**, 518, 55-60.

130. Broeze, R. J.; Solomon, C. J.; Pope, D. H. Effects of low temperature on in vivo and in vitro protein synthesis in Escherichia coli and Pseudomonas fluorescens. *Journal of Bacteriology* **1978**, 134, 861-874.

131. Farinha, M. A.; Kropinski, A. M. Construction of broad-host-range plasmid vectors for easy visible selection and analysis of promoters. *Journal of Bacteriology* **1990**, 172, 3496-3499.

132. Cai, J.; DuBow, M. S. Use of a luminescent bacterial biosensor for biomonitoring and characterization of arsenic toxicity of chromated copper arsenate (CCA). *Biodegradation* **1997**, 8, 105-111.

133. DeAngelis, K. M.; Ji, P.; Firestone, M. K.; Lindow, S. E. Two novel bacterial biosensors for detection of nitrate availability in the rhizosphere. *Applied and Environmental Microbiology* **2005**, 71, 8537-8547.

134. Ben-Israel, O.; Ben-Israel, H.; Ulitzur, S. Identification and quantification of toxic chemicals by use of *Escherichia coli* carrying lux genes fused to stress promoters. *Applied and Environmental Microbiology* **1998**, 64, 4346-4352.

135. King, J. M. H.; DiGrazia, P. M.; Applegate, B.; Burlage, R.; Sanseverino, J.; Dunbar, P.; Larimer, F.; Sayler, G. S. Rapid, sensitive bioluminescent reporter technology for naphthalene exposure and biodegradation. *Science* **1990**, 249, 778-781.

136. Applegate, B. M.; Kehrmeyer, S. R.; Sayler, G. S. A chromosomally based tod-luxCDABE whole-cell reporter for benzene, toluene, ethybenzene, and xylene (BTEX) sensing. *Applied and Environmental Microbiology* **1998**, 64, 2730-2735.

137. Layton, A. C.; Muccini, M.; Ghosh, M. M.; Sayler, G. S. Construction of a bioluminescent reporter strain to detect polychlorinated biphenyls. *Applied and Environmental Microbiology* **1998**, 64, 5023-5026.

Curriculum Vitae

Carlos Andrea Mora

Functional Materials Laboratory
Institute for Chemical and Bioengineering
Department of Chemistry and Applied Biosciences
ETH Zurich, HCI E105
8093 Zurich
Switzerland
Phone: +41 44 632 30 54
Email: carlos.mora@chem.ethz.ch

Private Address:
Carlos A. Mora
Bergacker 22
8046 Zürich
Switzerland

Born: July 27th, 1987 in Zurich (CH)
Citizen of Switzerland
Languages: German (native), English (fluent), French (basic), Italian (basic)

Education

07/2012 – current **PhD studies** in Chemical- and Bioengineering at the *Functional Materials Laboratory*, Prof. Wendelin J. Stark, at the Institute for Chemical and Bioengineering, **ETH Zurich** (CH).

Dissertation: Advanced sensing and quantification strategies using DNA and living cell based materials, Prof. Dr. W.J. Stark, ETH Zurich.

9/2010 – 3/2012 **Master studies** in Biology (Microbiology, Immunology), **ETH Zurich** (CH).

Master thesis: *Optimization of Methanol Dehydrogenases for Establishing Methanol Metabolism in Escherichia coli*, Prof. Dr. J. Vorholt, ETH Zurich.

Research project: *The role of the Dot/Icm type IV secretion system in Legionella pneumophila specific CD4 T-cell responses*, Prof. Dr. A. Oxenius, ETH Zurich.

9/2007 – 6/2010 **Bachelor studies** in Biology, **ETH Zurich** (CH).

8/2006 **High-school diploma** (Swiss Matura), **Kantonsschule Wiedikon**, Zürich (CH).

Refereed Journal Articles

12. C. Hofer, R.N. Grass, M. Zeltner, C.A. Mora, F. Krumeich, W.J. Stark, Hollow carbon nanobubbles: synthesis, chemical functionalization and container-type behavior in water, *Angewandte Chemie International Edition* **2016**, (in print).

11. C.A. Mora[*], J.G. Halter[*], C. Adler, A. Hund, H. Anders, K. Yu, W.J. Stark, Application of the *Prunus* spp. cyanide seed defense system onto wheat: Reduced insect feeding and field growth tests, *Journal of Agricultural and Food Chemistry* **2016**, 64, 3501–3507. [*]shared first-author

10. G. Mikutis, C.A. Mora, M. Puddu, D. Paunescu, R.N. Grass, W.J. Stark, DNA-based Sensor Particles Enable Measuring Light Intensity in Single Cells, *Advanced Materials* **2016,** 14, 2765–2770.

9. C. A. Mora, H.-J. Schärer, T. Oberhänsli, M. Ludwig, R. Stettler, P. R. Stoessel, R. N. Grass, W. J. Stark, Ultrasensitive Quantification of Pesticide Contamination and Drift Using Silica Particles with Encapsulated DNA, *Environmental Science & Technology Letters* **2016**, 3, 19–23.

8. D. Paunescu, C. A. Mora, L. Querci, R. Heckel, M. Puddu, B. Hattendorf, D. Günther, R. N. Grass, Detecting and Number Counting of Single Engineered Nanoparticles by Digital Particle Polymerase Chain Reaction, *ACS Nano* **2015**, 9, 9564–9572.

7. C. A. Mora, A. F. Herzog, R. A. Raso, W. J. Stark, Programmable living material containing reporter microorganisms permits quantitative detection of oligosaccharides. *Biomaterials* **2015**, 61, 1-9.

6. C. A. Mora, D. Paunescu, R. N. Grass, W. J. Stark, Silica Particles with Encapsulated DNA as Trophic Tracers, *Molecular Ecology Resources* **2015**, 15, 231-241.

5. M. S. Bloch, D. Paunescu, P. R. Stoessel, C. A. Mora, W. J. Stark, R. N. Grass, Labeling milk along its production chain with DNA encapsulated in silica, *Journal of Agricultural Food Chemistry* **2014**, 62, 10615-10620.

4. A. M. Ochsner, J. E. N. Müller, C. A. Mora, J. A. Vorholt, *In vitro* activation of NAD-dependent alcohol dehydrogenases by Nudix hydrolases is more widespread than assumed. *Febs Letters* **2014**, 588, 2993-2999.

3. J. G. Halter, W. D. Chen, N. Hild, C. A. Mora, P. R. Stoessel, F. M. Koehler, R. N. Grass, W. J. Stark, Induced cyanogenesis from hydroxynitrile lyase and mandelonitrile on wheat with polylactic acid multilayer-coating produces self-defending seeds. *Journal of Materials Chemistry A* **2014**, 2, 853-858.

2. D. Paunescu, C. A. Mora, M. Puddu, F. Krumeich, R. N. Grass, DNA protection against ultraviolet irradiation by encapsulation in a multilayered SiO_2/TiO_2 assembly, *Journal of Materials Chemistry B* **2014**, 2, 8504-8509.

1. A. C. C. Rotzetter, C. R. Kellenberger, C. M. Schumacher, C. A. Mora, R. N. Grass, M. Loepfe, N. A. Luechinger, W. J. Stark, Combining phosphate and bacteria removal on chemically active filter membranes allows prolonged storage of drinking water. *Advanced Materials* **2013**, 25, 6057-6063.

Conference Presentations and Proceedings

2. C. A. Mora, A. F. Herzog, R. A. Raso, W. J. Stark, Programmable living material containing reporter microorganisms permits quantitative detection of disease-relevant molecules (oral presentation), **MRS Fall Meeting**, Boston, Massachusetts, USA, December 3, 2015

1. C. A. Mora, D. Paunescu, R. N. Grass, W. J. Stark, Silica particles with encapsulated DNA as ecological sensors - Tracing nanoparticles in the sub-pbb range (poster presentation), **MRS Fall Meeting**, Boston, Massachusetts, USA, December 1, 2014

Student supervision

6. Olivier Gröninger (Research project, 09/2015 – 12/2015): Development of a programmable 3D-printed lab-on-a-chip biosensor.

5. Andri Mani (Master thesis, 05/2015 – 09/2015): Uptake quantification of different surface functionalized silica particles into A549 human epithelial cells.

4. Antoine F. Herzog (Master thesis, 10/2014 – 03/2015): In vivo intracellular metabolite reduction with an exogenous platinum nanocatalyst under hydrogen-containing atmosphere.

3. Célia Mignan (Research project, 05/2014 – 06/2014): Magnetic separation of histidine-tagged proteins with novel cobalt-based nanoparticles.

2. Madeleine S. Bloch (Master thesis, 09/2013 – 02/2014): Labeling food products with silica/DNA nanoparticles.

1. Antoine F. Herzog (Research project, 03/2013 – 05/2013): Feasibility study of a living surface having the ability to inducibly express emerald green fluorescent protein.

Teaching experience

02/2013 – 12/2014	Lecture assistant (exam preparation/correction, once per semester) – Lecture 'Chemical engineering', Functional Materials Laboratory, ETH Zurich
02/2013 – 05/2014	Course assistant (weekly course, one semester per year) - Laboratory course 'Basic chemistry for UWIS', Institute for Chemical- and Bioengineering, ETH Zurich
01/2013 – 02/2015	Course assistant (daily course, three weeks per year) - Laboratory course 'Basic chemistry for AGRL, HEST', Institute for Chemical- and Bioengineering, ETH Zurich
09/2010 – 12/2011	Teaching assistant (weekly exercises, 1 hour) – Lecture 'Statistics/Mathematics IV for BIOL, PHARM, AGRL, UWIS', Department of Mathematics, ETH Zurich
04/2010 – 05/2011	Course assistant (weekly course) – Laboratory course 'Fundamentals of Biology I', Institute of Biochemistry, ETH Zurich
09/2009 – 12/2009	Teaching assistant (weekly exercises, 2 hours) – Lecture 'Mathematics I for BIOL, PHARM', Department of Mathematics, ETH Zurich
05/2009 – 07/2010	Tutor – Mathematics, Physics, Biology, Chemistry, Lernbüro, Zurich

Varia

- Co-founder and vice-president of the student think tank reatch (research and technology in Switzerland/CH) (founded in May 2014). reatch aims at bringing together young scientists and students from all scientific disciplines to critically discuss scientific and technological concepts that could have an influence on society and to propagate and popularize those concepts to the public.

- Member of the Swiss Study Foundation (Schweizerische Studienstiftung) since 2008. The Swiss Study Foundation is supporting excellent students and postgraduates at universities and technical colleges who due to their personality, creativity and intellectual skills are in a position to contribute to science, business, culture and politics.